August 2014

AMULSAR GOLD PROJECT

Groundwater Modelling Study

Submitted to:
Lydian International Ltd
Ground Floor
Charles House
Charles Street
St Helier
JE2 4SF
Channel Islands, UK

Report Number. 14514150095.506/B.2

Distribution:

Lydian International Ltd - 1 copy (pdf)
Golder Associates (UK) Ltd - 1 copy

REPORT

Golder Associates

Table of Contents

TABLES

FIGURES

APPENDICES

1.0 TERMS OF REFERENCE

Golder Associates (UK) Ltd (Golder) has been commissioned by Lydian International Ltd (Lydian) to complete surface water and groundwater components of an Environmental and Social Impact Assessment (ESIA) for the Amulsar Project. The Amulsar Project is a proposed open pit gold mine development located in southeastern Armenia. As part of this work, a three dimensional (3-D) groundwater flow model has been constructed to improve understanding of the hydrogeological setting of the proposed mine and associated infrastructure, and to facilitate estimation of groundwater inflow to the pit following construction. This report is intended to be read in conjunction with and as an addendum to the ESIA.

The assistance of Lydian and their Armenian based subsidiary Geoteam Closed Joint Stock Company (Geoteam), in provision of baseline data for this study is gratefully acknowledged.

2.0 BACKGROUND

The proposed development associated with the Amulsar Project is described in Chapter 3 of the ESIA. The proposed development includes the Tigranes-Artavazdes and Erato open pits, a barren rock storage facility (BRSF), a heap leach facility (HLF), a crusher, a processing plant and other necessary supporting infrastructure.

The hydrogeological conceptual model is described in Chapter 4.8 of the ESIA. Description of the model input parameters in this report is confined to those inputs which are not described in the hydrogeological conceptual model, and to a description of the implementation of the conceptual model in the numerical model, where necessary.

The primary features of the hydrogeological conceptual model for Amulsar and the surrounding area are summarised as follows:

- An isolated mountain ridge (Amulsar Mountain) forming part of the topographic boundary of three river catchments, the Arpa River to the northwest, the Vorotan River to the east and the Darb River to the southwest;
- Groundwater recharge being greatest at higher elevations where precipitation (and snow accumulation) is highest and soils are thin or absent promoting infiltration. Groundwater discharges to local springs on Amulsar Mountain and as baseflow to incised Arpa, Darb and Vorotan River valleys and their tributaries;
- Groundwater recharge predominantly arising from high infiltration rates in April, May and June during and following the spring snow melt;
- Predominantly topographically-driven groundwater flow, resulting in groundwater flow from the water table below Amulsar Mountain ridge west and northwest toward the Arpa River, east toward the Vorotan River and southwest toward the Darb River;
- Five hydrogeological units:
  - Colluvium overlying bedrock throughout the project area at thicknesses varying between less than 1 m and up to 20 m;
  - The silicified Upper Volcano-sedimentary Sequence (VC) hosting the ore body and outcropping along the mountain ridge and on the eastern flank of Amulsar Mountain. This unit has moderate permeability and minimal primary porosity; porosity and permeability associated with secondary fracture porosity;

  - The argillically altered andesites of the Lower Volcano-sedimentary Sequence (Lower Volcanic Andesites, LVA) occurring in layered 'panels' beneath, within and below the highly faulted ore bodies, and outcropping to the west and north of Amulsar Mountain. Although the extent of alteration varies, this unit predominantly comprises an amorphous low permeability clay in the mountain area with high total porosity and low effective (drainable) porosity;
  - The unaltered Lower Volcano-sedimentary sequence (LV), outcropping at lower elevations surrounding Amulsar Mountain. The LV as a whole is indicated, based on outcrop extent, to be at least 1,300 m in thickness and in the Amulsar Project area predominantly comprises low to moderately permeable fractured andesites with some interbedded tuffs and sedimentary sequences; and
  - The Cenozoic Basalt Flows, overlying the LV on plains to the east, west and south of Amulsar Mountain, and extending northwest from the scoria cone which forms the peak north of the BRSF. The basalts have been proven at up to 120 m in thickness. The basalts are intensely fractured and relatively permeable.

- Low vertical permeability in the areas of outcrop of the argillically altered andesite on Amulsar Mountain, promoting groundwater discharge as springs at high elevations, particularly immediately to the west of the mountain ridge, and in valleys to the north and northeast of the ridge in the vicinity of the proposed BRSF;
- Intense faulting and juxtaposed 'panels' of argillically altered andesite sustaining localised areas of perched saturated conditions in comparatively higher permeability fractured rocks in the VC surrounding the Amulsar ridge;
- Low permeability argillically-altered andesite forming the base of the VC/LVA sequence that hosts the ore body;
- More permeable unaltered rocks of the LV, also incorporating a greater proportion of sedimentary and volcano-sedimentary rocks, at lower elevations;
- Groundwater discharge to the Spandaryan-Kechut tunnel which passes at approximately 2,000 masl to the west of Amulsar Mountain connecting the Spandaryan Reservoir to the south of the project area with the Kechut Reservoir in the north of the project area; and
- Flowing artesian conditions and groundwater discharge at the base of the valley immediately east of the BRSF, where discharge to surface water is restricted by alluvial clays.

The Amulsar mine pits will be developed sequentially commencing with the Tigranes pit; excavation of the Artavazdes pit will commence three months later. These two starter pits will merge to form the Tigranes-Artavazdes pit by the end of the first year of operation. Mining in Erato will begin three years following commencement of mining in Artavazdes. Backfilling of the Tigranes-Artavazdes pit will begin six months after commencement of mining in Erato and will reach its full extent 12 months prior to the end of the operational period. There will not be any period in the mine life when both pits are open to their full extent: the Tigranes-Artavazdes will be backfilled with barren rock from the Erato pit as this pit develops.

3.0 MODELLING OBJECTIVES

The objectives of the modelling study are:

- To evaluate the hydrogeological regime underlying the pits and associated infrastructure (the HLF and BRSF); and
- To determine the potential groundwater-related impacts associated with mine operations and closure/post closure.

This report describes the operational and post-closure groundwater quantity impacts derived from the groundwater model. Quality impacts are described in other technical studies incorporated in the ESIA.

4.0 MODEL INPUTS

4.1 Topography

Topography in the project area has been mapped within the license area as a digital elevation model on a 10 m grid and over a wider area as a digital elevation model (DEM) on a 30 m grid. The smaller scale DEM has been used as the basis for the modelling study, as it covers the entire model domain. The topography of the project vicinity is illustrated in Figure 1.

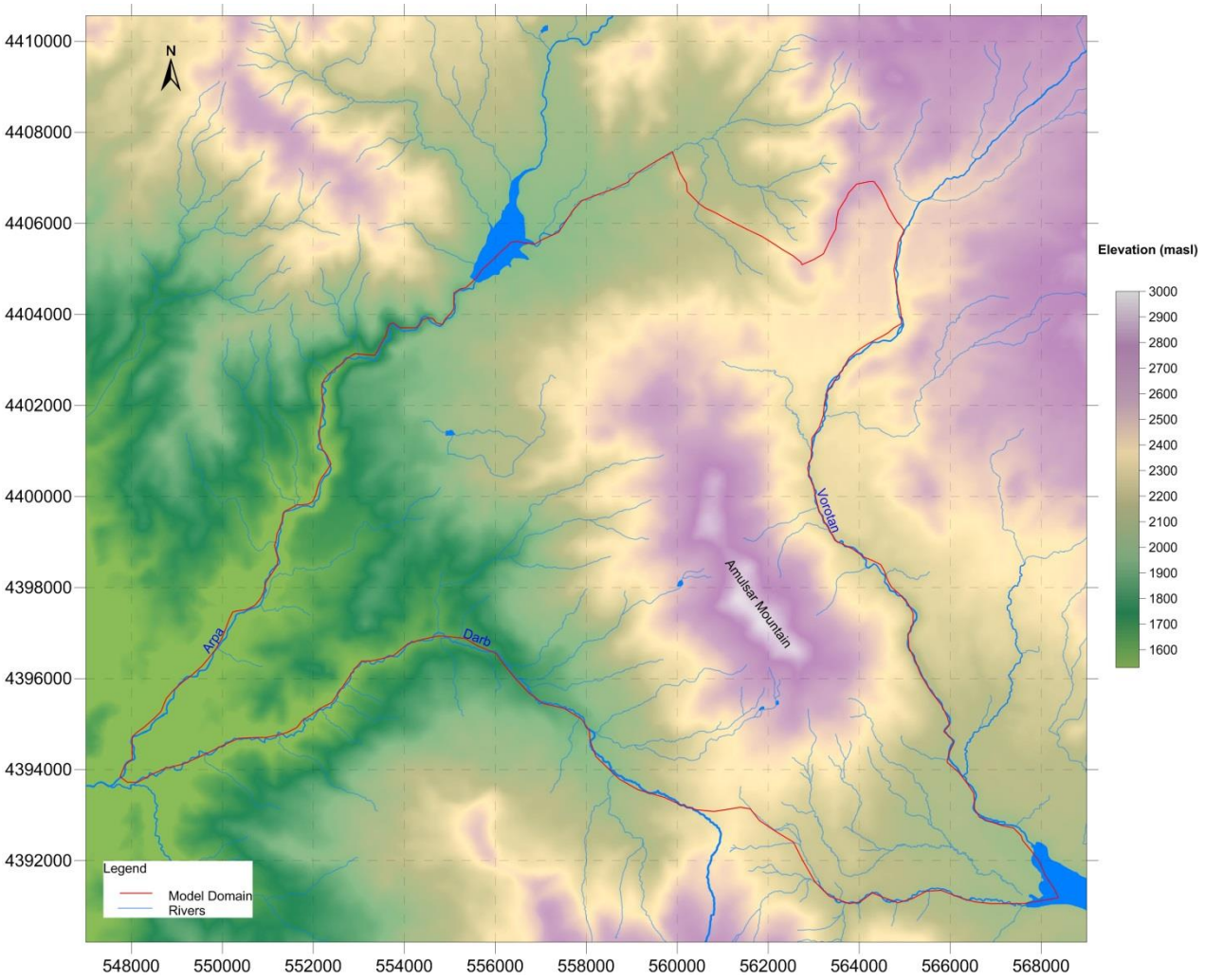

Figure 1: Topography, Amulsar Project and Surrounding Area

4.2 Groundwater Recharge

Based on estimates of groundwater recharge described in Chapter 4.8 of the ESIA, a range of groundwater recharge values between 50 mm/yr and 300 mm/yr was used in model calibration. Calibration commenced with recharge applied uniformly at 300 mm/yr across the model domain. As part of the calibration process, variable, topographically-correlated recharge rates were used.

4.3 Delineation of Hydrogeological Units

Hydrogeological units were delineated in the groundwater flow model based on:

- Outcrop areas in the Lydian geological model and the published regional geology map (USSR, 1981);
- Thicknesses of the colluvium and Cenozoic Basalt Flows based on site investigation in the HLF, BRSF/crusher and ore body areas and in historically investigated sites along the Vorotan valley and northeast of the HLF; and
- Extent, distribution and thickness of the VC and LV presented in cross-sections of the Lydian geological model (Holcombe, 2013; Lydian International *et al*, 2013).

The structural geology of the ore body and surrounding area comprises at least four phases of faulting of an initially interlayered sequence of the VC and the LVA. This structural detail cannot reasonably be represented in the groundwater flow. The extent of the VC unit has therefore been approximated as a vertically continuous unit based on sections of the geological model, with smaller bodies of LVA included within the delineated extent.

The VC body delineated in the groundwater model has an outcrop area similar to that indicated on the Lydian geological map, but includes areas along the mountain ridge where surficial argillic LVA is very thin. It occurs beneath and surrounding the Tigranes and Artavazdes peaks, beneath and surrounding the Erato peak, and extending east toward the Vorotan River. The VC body extends to an elevation of 2,550 masl beneath North Erato and below 2,600 masl beneath Erato. The VC body shallows significantly between the two peaks and is very thin in the saddle between Erato and Tigranes. It extends to at least 2,500 masl beneath Tigranes and to the south and east, deepening further beneath Artavazdes. To the southwest of Artavazdes the VC outcrops at surface (approximately 100 m thick). Beneath Arshak the VC body extends to approximately 2,700 masl. The termination of the VC outcrop to the east of the Amulsar ridge is not shown in Lydian's geological mapping or on sections. In the groundwater model it is assumed that the area of outcrop of the VC terminates slightly upslope of the Vorotan River. The extent of the VC body represented in the groundwater model is indicated in Figure 2.

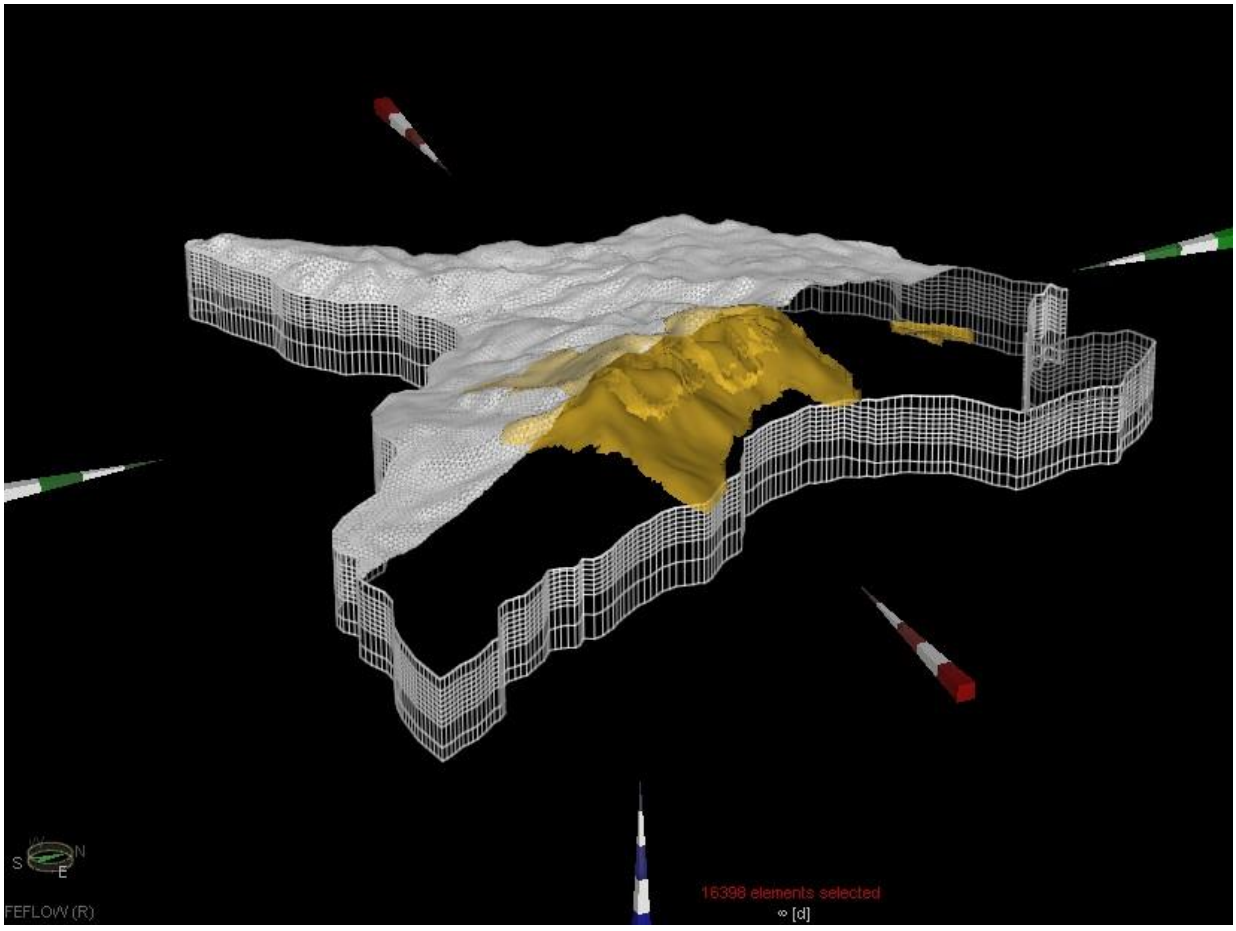

Figure 2: Extent of the VC Unit in the Groundwater Model

Colluvium is thin across much of the Project Area, thickening in stream and river valleys and on the lower river plains. Across the model domain, the colluvium has been delineated at 2 m thickness in areas outside the basalt plateaus and at 5 m on the basalt plateaus (based on drilling observations on the Vorotan plateau) except where mapping or site investigation data indicates greater thickness to be present. Thicker areas of colluvium are represented in the groundwater model as follows:

- Fifteen metres thickness in the centre of the BRSF site decreasing to 10 m on the margins to the northwest and northeast, and increasing again to 15 m in the base of the adjacent river valley;
- Twenty metres thickness in the centre of the valley upslope of the Gndevaz Reservoir;
- Ten metres thickness in stream valleys on the west of Amulsar Mountain mapped as Quaternary sediments on the published regional geological map (USSR, 1981);
- Ten metres increasing to 15 m thickness along the base of the valley forming the BRSF site; and
- Twenty metres thick to the east of Artavazdes peak, based on the delineation of colluvium in this area in the Lydian 3D geological model.

Cenozoic Basalt flows overly the LVA to the north, east, south and west of Amulsar. The thickness of the basalts has been proven on the Vorotan plateau to the east of Amulsar, in the VLF area and on the flanks of the scoria cone adjoining the BRSF site. Boreholes drilled near the peak of the scoria cone encountered greater than 100 m of basalt but did not determine the total thickness. The thickness of the basalt flows represented in the groundwater model is illustrated in Figure 3.

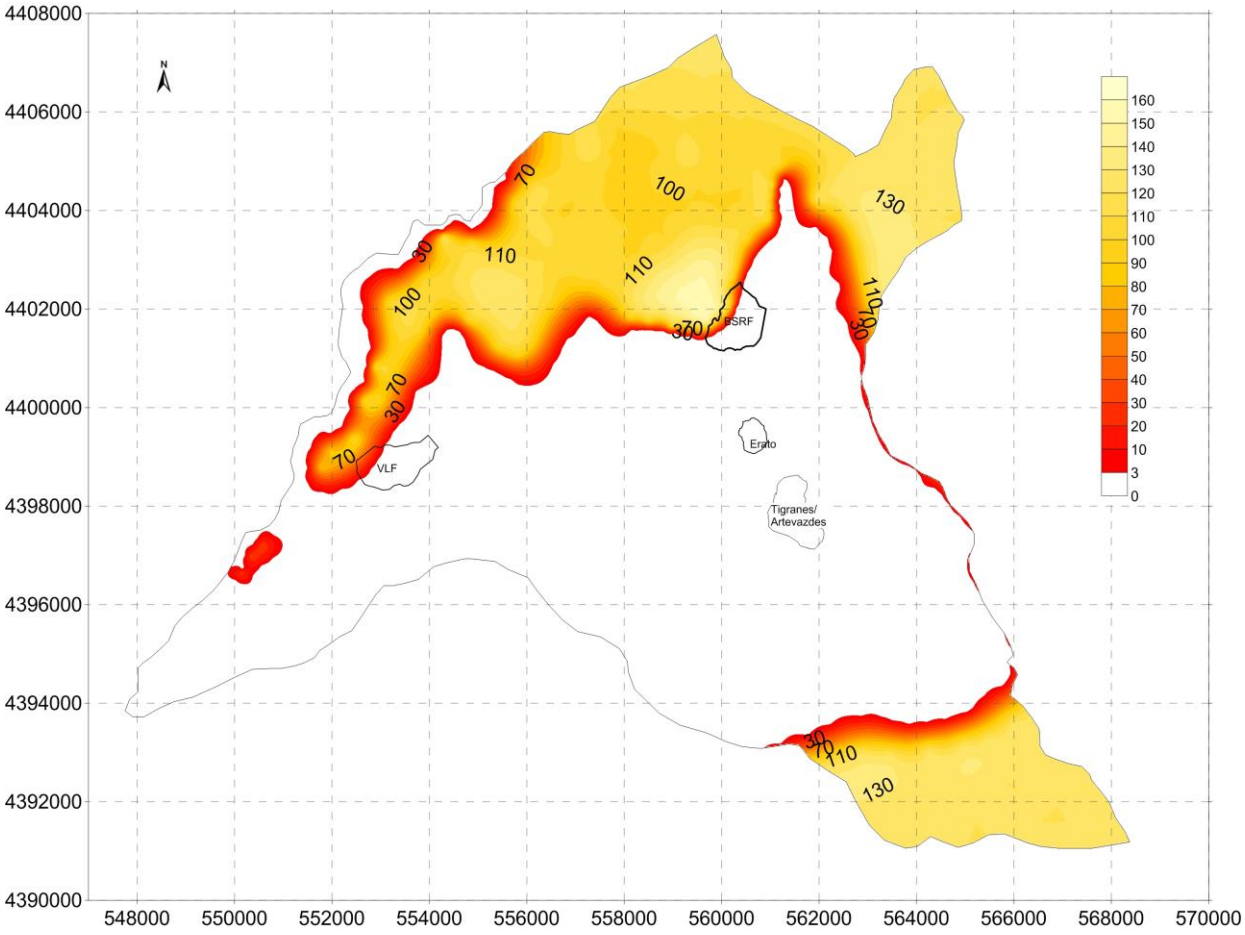

Figure 3: Basalt Thickness (in metres)

The Lower Volcano-sedimentary Sequence (LV) comprises predominantly highly argillically altered andesites at high elevations surrounding Amulsar Mountain. Although the entire LV unit is indicated to be altered in Lydian's geological map, discussions with Lydian's Senior Geologist confirmed that the alteration decreases away from the mountain, and the LV unit is unaltered at lower elevations, as observed at the HLF site (A Turner, Pers. Comm., 2014). The elevation at which the transition from altered to fresh LV occurs is variable surrounding the mountain. In places the transition is clearly visible in aerial imagery of the site; furthermore waste piles generated by construction of the Spandaryan-Kechut tunnel comprise unaltered LV. For the purposes of modelling, it was assumed that the LV is argillically altered above 2,200 masl (above the elevation of the Spandaryan-Kechut tunnel at approximately 2,000 masl).

Hydraulic testing of the LV unit was completed to approximately 100 m depth in the HLF area, the area to the east of Gndevaz and in boreholes higher on Amulsar Mountain. No clear trend with depth was identified where testing was undertaken. It is likely that increased loading and reduced weathering at greater depths will result in a decrease in permeability with depth. An additional hydrogeological unit is therefore delineated in the groundwater model for the deeper LV at greater than 200 m depth.

4.4 Hydraulic Properties

The hydraulic properties data set for the Amulsar Project is presented in Chapter 4.8 of the ESIA. Hydraulic property inputs to the groundwater flow model, and justifications for the values, are presented in Table 1.

Table 1: Hydraulic Properties Inputs, Groundwater Flow Model

Parameter	Argillically Altered LVA	Unaltered LV	Deep LV	Basalt	Silicified Upper Volcano-Sedimentary Sequence (VC)	Colluvium
Horizontal Hydraulic Conductivity (K_h) (m/s)	$8.5x10^{-8}$	$2.5x10^{-6}$	$1.0x10^{-7}$	$1.0x10^{-6}$	$1.0x10^{-7}$	$5.0x10^{-6}$
	Geometric mean of testing surrounding the ore body, at the BRSF site and valley to the east.	Geometric mean of testing at the VLF site, BRSF site and valley to the east.	Golder experience. Applied below 200 m depth based on an assumed decrease in permeability with depth.	Geometric mean of all tests results for the Cenozoic Flow Basalts.	Golder experience. Testing in the VC unit is limited, and both observation and description of the geological model indicate the silicified VC to be highly fractured, and significantly more permeable than the LVA.	Golder experience generally comprises sandy silty clay with gravel/boulders; greater proportion of rock fragments on the mountain slopes.
Anisotropy (K_h:K_v)	1	100	100	10	1	10
	Unit comprises 'amorphous clay' (A Turner, Pers. Comm., 2014).	Given understanding of the geology of the sub-horizontally bedded LV, it has potential to be highly anisotropic.	Given understanding of the geology of the sub-horizontally bedded LV, it has potential to be highly anisotropic.	The layered flow structure of flow basalts will impact some anisotropy.	Fracturing and faulting is reported to be both sub-horizontal and sub-vertical.	Typical value for sediments.
Compressibility (m^2/N)	$2.0x10^{-7}$	$3.0x10^{-10}$	$3.0x10^{-10}$	$3.0x10^{-10}$	$5.0x10^{-10}$	$8.0x10^{-9}$

Parameter	Argillically Altered LVA	Unaltered LV	Deep LV	Basalt	Silicified Upper Volcano-Sedimentary Sequence (VC)	Colluvium
	Domenico and Schwartz (1990)	Domenico and Schwartz (1990)	Domenico and Schwartz (1990)	Domenico and Schwartz (1990)	Domenico and Schwartz (1990)	Domenico and Schwartz (1990) dense sandy gravel
Specific Storage (1/m)	1.96×10^{-3}	3.18×10^{-6}	3.04×10^{-6}	3.04×10^{-6}	5.14×10^{-6}	7.99×10^{-5}
	Calculated from compressibility and porosity.	Calculated from compressibility and porosity.	Calculated from compressibility and porosity.	Calculated from compressibility and porosity.	Calculated from compressibility and porosity.	Calculated from compressibility and porosity.
Specific Yield	0.03	0.04	0.015	0.015	0.04	0.25
	Johnson, 1967	Golder experience	Golder experience	Golder experience	Golder experience	Golder experience
Total Porosity	0.4	0.05	0.02	0.02**	0.05	0.3
	Golder experience (Domenico and Schwartz, 1990).	Golder experience.	Golder experience (Domenico and Schwartz, 1990).	Golder experience (Domenico and Schwartz (1990) and based on observed RQD* average of 0.19 in the 2010 to 2013 dataset.	Golder experience (Domenico and Schwartz (1990) and based on observed RQD average for the silicified volcanics 0.4 in the 2010 to 2013 dataset.	Golder experience.

* *RQD – rock quality designation.*

** *Porosity of basalts will vary as a result of internal flow structure, porosity of flow tops/bottoms will be much greater than this value, which is more representative of flow interiors.*

4.5 Discrete Features Represented in the Model

4.5.1 Spandaryan-Kechut Tunnel

The Spandaryan-Kechut tunnel is 21 km in length and passes through the Amulsar Project area connecting the Kechut and Spandaryan Reservoirs, passing around Amulsar Mountain to the west. Lydian has provided information regarding the tunnel alignment, but has not been able to provide 3-D location information for the tunnel.

The tunnel invert elevation was estimated by interpolation between each point along the tunnel route assuming that the tunnel has a constant gradient between its inlet at the Spandaryan Reservoir, and the outlet above Kechut Reservoir. The inlet and outlet elevations are approximate, estimated from the project Digital Elevation Model. Elevation points are shown in Table 2.

Table 2: Estimated Elevation of the Invert of the Spandaryan-Kechut Tunnel

Point No.	Easting	Northing	Elevation (m)
1	567668	4390995	2033
2	567631	4390959	2030.7
3	567109	4390587	2028.4
4	564087	4391413	2027.9
5	563349	4391969	2026.4
6	561571	4393325	2022.6
7	559684	4394710	2019.1
8	558840	4395317	2017.0
9	558574	4395635	2016.0
10	558092	4396923	2011.8
11	557439	4400050	2009.1
12	556289	4405080	1998

A 2.82 km segment of the tunnel lies outside the groundwater model domain in the southern part of the model adjacent to the Spandaryan Reservoir, representing 13% of the total length of the tunnel.

4.5.2 Faults

A number of fault zones are mapped surrounding and within the Amulsar ore bodies, including the westward dipping shallow Orontes thrust and later steep thrust and reverse fault structures cross-cutting the ridge. Faults have not been represented in the groundwater model because for numerical reasons, the geological model is simplified in the groundwater model. The objective of the groundwater model is to represent the large scale geological and man-made features affecting groundwater flow within the Project Area.

4.6 Calibration Data

The groundwater model was calibrated to the average groundwater elevation recorded in monitoring wells within the Project Area. Wells screened within the colluvium, or in perched groundwater, were not used in the calibration. The calibration data set used the groundwater elevation data available on 11 June 2014, with the exception of the elevation at DDAW007, which has been amended based on conclusions regarding the integrity of this well and validity of groundwater levels described in Chapter 4.8 of the ESIA, and wells at high elevation surrounding Tigranes-Artavazdes, which were updated in late June 2014.

Table 3: Groundwater Elevation Calibration Data

Lydian ID	Easting	Northing	Elevation of well screen mid-point or well base (masl)*	Mean Groundwater Elevation (masl)	Measurement Error Reference Elevation (m)**	Estimated Error on Due to Uncharacterised Seasonal range (m)	Estimated Error (m) +/-
DDAGLP267	561252	4402552	2410	2421	20	5	25
DDAGLP268	561886	4402447	2354	2369	20	5	25
DDAGLP269	562201	4402587	2317	2343	20	5	25
DDAW002	562169	4402759	2306	2335	20	5	25
DDAW003	561490	4402807	2337	2364	20	5	25
DDAW004	560814	4402150	2457	2537	20	5	25
DDAW005	560159	4401267	2549	2561	0.5	10	10.5
DDAW007	561249	4399368	2690	2695	0.5	10	10.5
DDAW009	559342	4399820	2341	2431	20	1	21
DDAW012	560817	4401622	2555	2563	0.5	2	2.5
DDGW005	563068	4403536	2342	2351	20	5	25
DDGW006	563496	4403815	2349	2366	20	5	25
DDGW007	564001	4404566	2364	2394	20	5	25
GGDW002	555309	4401314	1930	1944	0.5	2	2.5
GGDW003A	556155	4401409	2007	2009	0.5	2	2.5
GGDW005	556024	4402134	2016	2022	0.5	1	1.5
GGDW007	552536	4398302	1497	1609	0.5	1	1.5
GGDW008	552932	4398566	1598	1642	0.5	1	1.5
GGDW009	552978	4399660	1583	1660	0.5	1	1.5
GGDW010B	553898	4399557	1729	1775	0.5	0.5	1
GGDW011	554714	4399713	1864	1891	0.5	-10	0 to -10.5
GGDW012	553947	4398843	1753	1789	0.5	1	1.5
GGDW013	553220	4399010	1606	1651	0.5	1	1.5
GGDW014	552385	4398975	1602	1608	0.5	0.5	1
GGDW015	554003	4399203	1738	1775	0.5	1	1.5
GGDW016	552174	4398443	1531	1583	0.5	1	1.5
GGSC002	555495	4402143	2039	2044	0.5	0.5	1
GGSC037	560790	4403154	2412	2412	0.5	1	1.5
GGSC049	560063	4401493	2538	2541	0.5	1	1.5
GGSC050	560542	4401892	2505	2509	0.5	1	1.5
RCAW288	560562	4398393	2548	2583	20	0	20

Lydian ID	Easting	Northing	Elevation of well screen mid-point or well base (masl)*	Mean Groundwater Elevation (masl)	Measurement Error Reference Elevation (m)**	Estimated Error on Due to Uncharacterised Seasonal range (m)	Estimated Error (m) +/-
RCAW289	560537	4398497	2563	2584	20	0.5	20.5
RCAW399	560702	4402856	2448	2472	20	2	22
RCAW400	561263	4402314	2483	2513	20	2	22
RCAW401	561336	4403139	2370	2413	20	0.5	20.5
RCAW403	562432	4402226	2301	2324	20	2	22

* *Where the well screen position is known, the mid-screen elevation has been used as the elevation at which the groundwater elevation is recorded. Where the well screen is unknown, the well base elevation has been used.*

** *Where wells have been surveyed using differential GPS, an error of 0.5 m has been applied. Where well elevation has been estimated based on hand held GPS, an error of 20 m has been applied.*

The model was also calibrated with respect to flow in the Spandaryan-Kechut Tunnel (Figure 4), which has been recorded via spot flow measurements between 2012 and 2014. The mean flow recorded at AWJ6, the outlet of the tunnel at Kechut reservoir, over the monitoring period is 0.19 m^3/s, the minimum flow was 0.07 m^3/s in March 2014 and the maximum flow recorded was 0.29 m^3/s in July 2013. Recent measurements (February to June 2014) have recorded lower flows than during 2012 to 2013.

Figure 4: Spot Flow Measurements at the Spandaryan-Kechut Tunnel Outlet, AWJ6

Calibration used estimates of groundwater base flow to the Darb, Arpa and Vorotan Rivers over the reaches within the model domain. However, the reaches of these rivers which are within the model domain also receive significant flow from catchments on their adjacent banks, outside the model domain. For the Darb River, approximately 30% of the catchment along the modelled boundary is within the model domain; for the Arpa River, approximately 15% of the catchment along the modelled boundary is within the model domain;

and for the Vorotan River, approximately 15% of the catchment along the modelled boundary is within the model domain. This places uncertainty on the possible range in baseflow discharge along the Project Area boundaries which is attributable to discharge from the Project Area.

Baseflow estimates based on continuous flow records at monitoring stations within the Project Area were either unavailable at the time of the model calibration (particularly for tributaries to the major rivers) or not available for concurrent time periods for pairs of points along the major rivers. Baseflow estimates have therefore been based on spot flow measurements during late summer along the major water courses, with the exception of the Arpa River, where the estimate is based on continuous flow records in winter 2012/13. On this basis, the following baseflow discharge rates are estimated:

- A baseflow increase between AW001 to AW003 (10.9 km) on the Vorotan River of 0.7 m^3/s based on measurements in August and September 2010 and August and September 2011. This is equivalent to a baseflow discharge of 0.064 $m^3/s/km$.
- A baseflow increase on the Darb River between AW005 to AW006 (2.9 km) of 0.6 m^3/s to 0.7 m^3/s based on measurements in August and September 2010 and August and September 2011. This is equivalent to a baseflow discharge of between 0.21 $m^3/s/km$ and 0.24 $m^3/s/km$. It is notable that the flow at AW004, on a tributary to the Darb River 1 km upstream of AW005, is almost identical to that at AW005. The contributing catchment between AW004 and AW006 is more than double that between AW005 and AW006.
- Spot flow data suggest that the upper reach of the Arpa River may be a losing reach immediately downstream of the Kechut Reservoir. However, baseflow is observed in the lower reaches within the project area. The median baseflow rate between Arpa 2 to Arpa 3 (3.9 km) over the period November 2012 and February 2013 was 0.1 m^3/s (average 0.11 m^3/s). This is equivalent to a baseflow of 0.026 $m^3/s/km$.

Flows recorded in perennial springs observed within the Project Area were not used to directly calibrate the model as measurements are insufficient to estimate a mean annual discharge. Perennial springs were included in the groundwater model as seepage faces; for this reason the elevation of the perennial springs was not used as a groundwater elevation calibration point. However, the overall distribution of springs was used to guide the expected distribution of zones of seepage or areas where flowing artesian conditions were possible within the model domain.

5.0 GROUNDWATER MODELLING

5.1 Modelling Approach and Model Scenarios

The purpose of the modelling is to represent the conceptual hydrogeological model numerically and to predict the potential groundwater-related impacts associated with mine operations and closure/post closure. A 3-D numerical modelling approach was used to simulate the groundwater flow regime in order to represent spatial variations in material properties and recharge and the location of rivers controlling groundwater discharge. The model approach has been selected to be commensurate with the level of knowledge and available hydrogeological data.

A steady state modelling approach was used to achieve the modelling objectives, consistent with the site conditions where hydrogeological data indicates that the maximum depth of the open pits will be close to or possibly just intersect the water table.

Three steady state scenarios have been developed: baseline conditions, operational conditions and post-closure. The baseline scenario represents a calibrated steady state model of the current groundwater flow regime. The operational scenario considers steady state conditions at the maximum extent of mining. The closure scenario considers the post-closure state when the pits have been backfilled.

The model considers saturated flow only: the purpose of the model is to estimate the configuration of the water table, groundwater flow paths, and groundwater flow volumes (water balance). This approach is consistent with the modelling objectives.

A saturated flow modelling approach is unable to simulate perched groundwater conditions. The model predicts whether groundwater elevations observed surrounding the Amulsar ridge could reasonably be sustained as part of the saturated groundwater system.

Available data indicates that the water table is present at an elevation of about 2,700 to 2,750 m beneath Amulsar. Data also suggests that isolated (disconnected) bodies of perched groundwater are present in and surrounding the ore body, and also that significant infiltration and 'interflow' of seasonal melt water to high altitude springs occurs during the spring and early summer. The groundwater flow model simulates flow below the water table. For the purposes of the groundwater impact assessment, perched groundwater flows have been estimated using recharge-based calculations and interpretation of observed conditions, as described in Chapter 6.8 of the ESIA.

5.2 Numerical Model Selection

FEFLOW, a state-of-the-practice groundwater modelling code, was used for the modelling work. FEFLOW represents three-dimensional steady-state saturated groundwater flow including seepage from the mountain slopes and pit slopes, if required.

5.3 3-D Model Design

5.3.1 Model Grid and Model Domain

The model domain and supermesh polygons are shown in Figures 5 and 6. The model domain has been delineated based on regional hydrogeological boundaries surrounding the areas for the pits, BRSF and HLF.

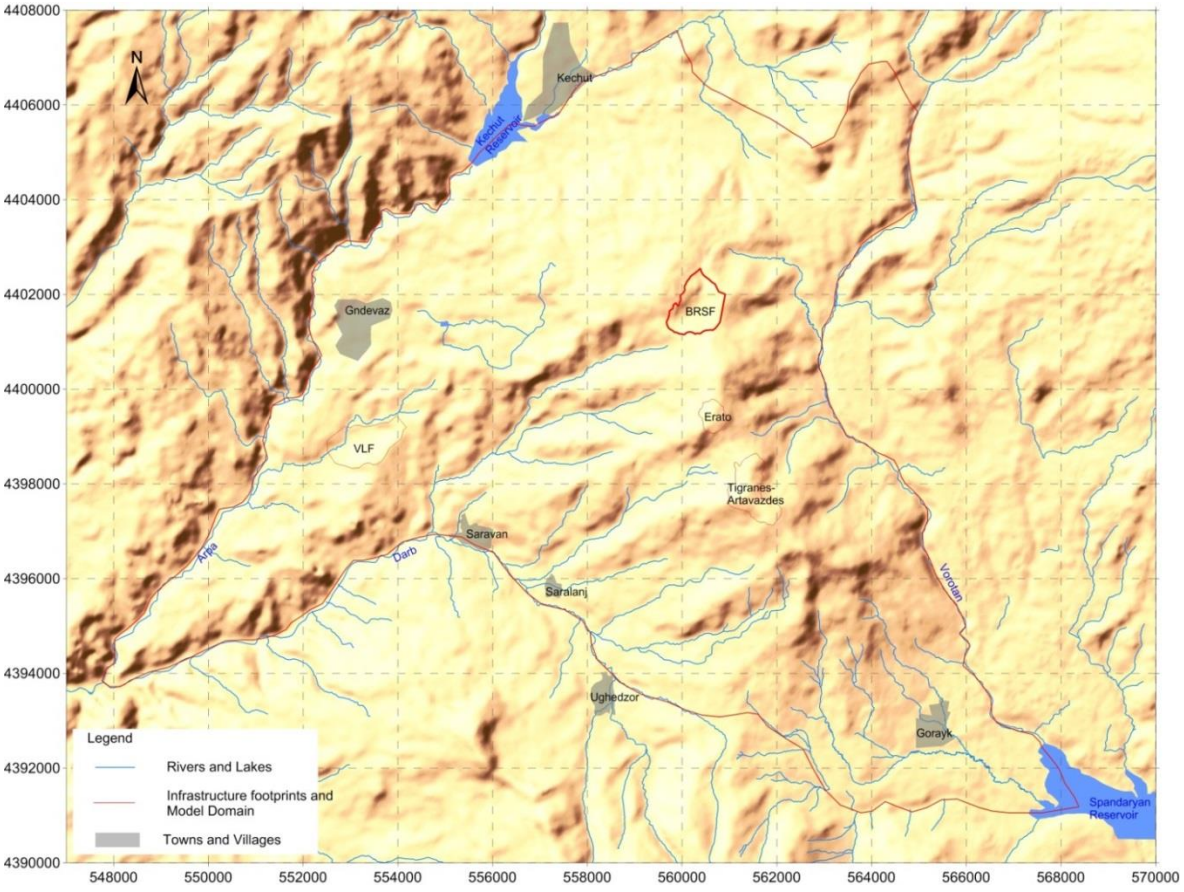

Figure 5: Model Domain and Location of Significant Mine Infrastructure

5.3.1.1 Horizontal Model Discretisation

The horizontal model grid is shown in Figure 6. The grid has been delineated on an approximately 100 m element dimension, with refinement in the areas of interest surrounding the key mine features.

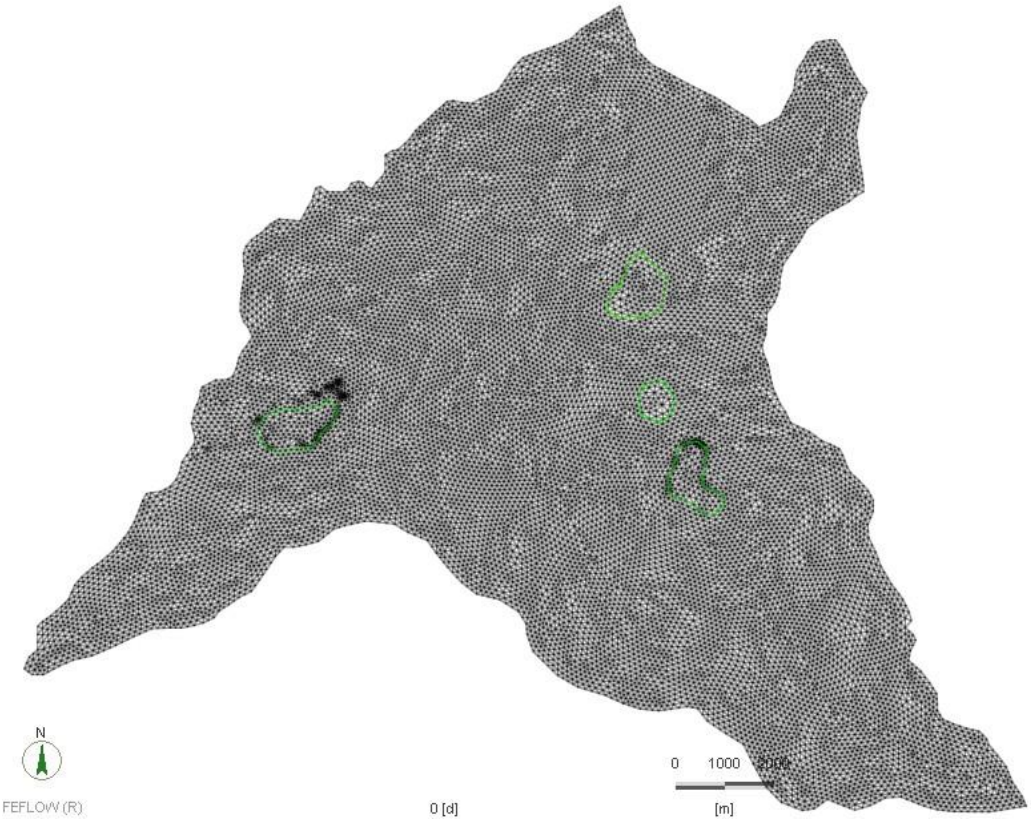

Figure 6: Model Grid

5.3.1.2 Vertical Model Discretisation

The model base has been delineated as a no-flow boundary at a depth of 800 m bGL. This is based on an assumption that hydraulic conductivity of the bedrock decreases with depth and flow will predominantly occur in the upper hundreds of metres of the bedrock, with negligible flow at depth, causing flow lines to mirror bedrock topography.

Vertical discretisation of the model has been based both on lithological variation, and the desired resolution of the model in areas of interest. The following layers are present in the model:

- Layer 1: Represents the colluvium, and is present across the model domain at a minimum thickness of 2 m;
- Layer 2: Represents the Cenozoic Basalt Flows, where the basalt is absent, this layer has a thickness of 1 m and is assigned properties equivalent to the underlying unit;
- Layers 3 to 9 are 50 m thick in order to discretise variation in non-layered lithological units (the VC and LVA). The VC extends to Layer 9 beneath the ore bodies; the LVA extends to the base of the model beneath the ore bodies. Across the remainder of the model domain, Layer 7 and below comprises the deep andesite; and
- Layers 10 and 11: Layer 10 is 200 m in thickness, and as above, comprises deep andesite across most of the model domain. Layer 11 accommodates the remaining thickness to place the model base at 800 m below ground surface.

Figures 7 and 8 shows west-east section lines through the centre of the model domain, illustrating the layers described above.

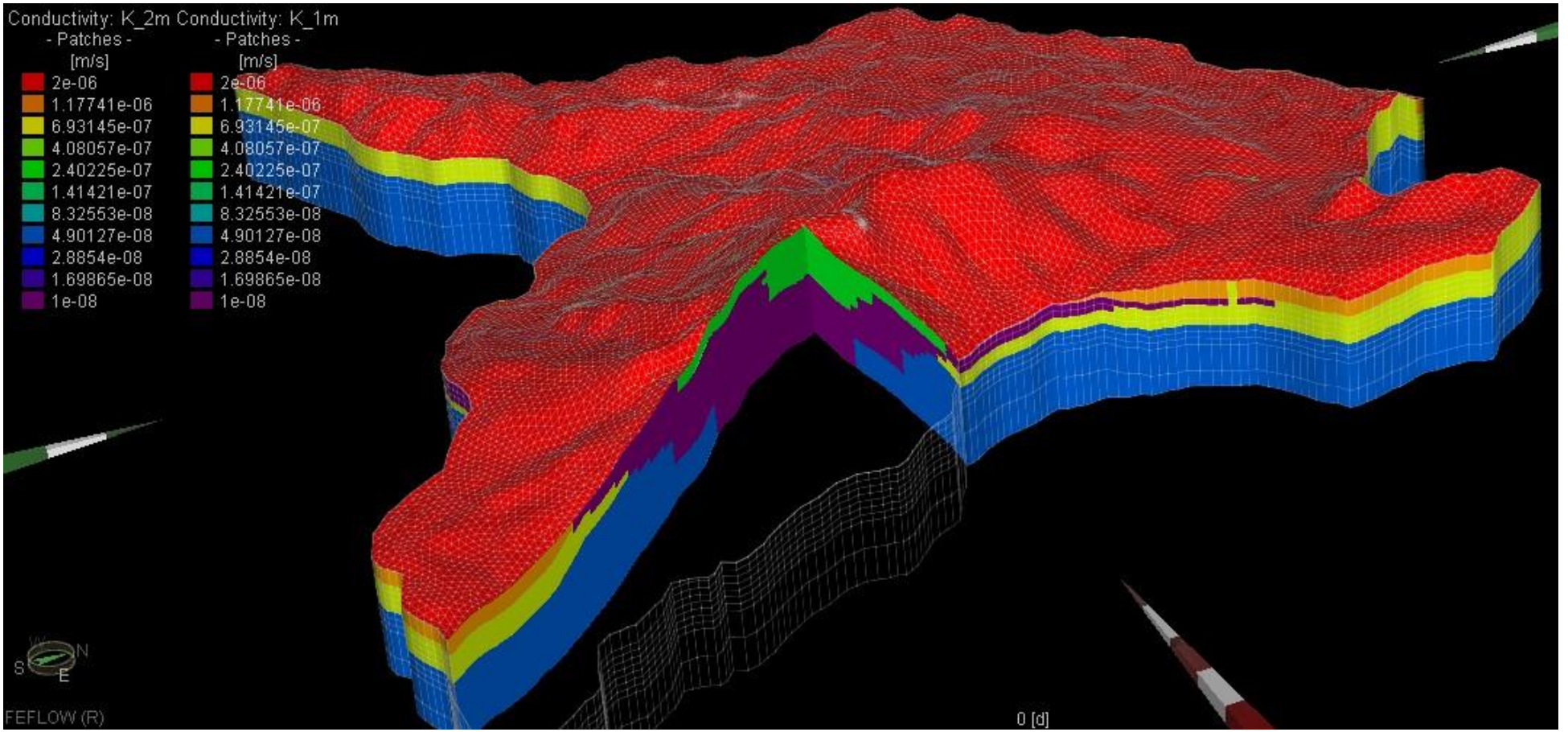

Figure 7: Cutaway view showing sections through Artavazdes (west to east, centre and west of model domain), illustrating layering and hydraulic conductivity domains

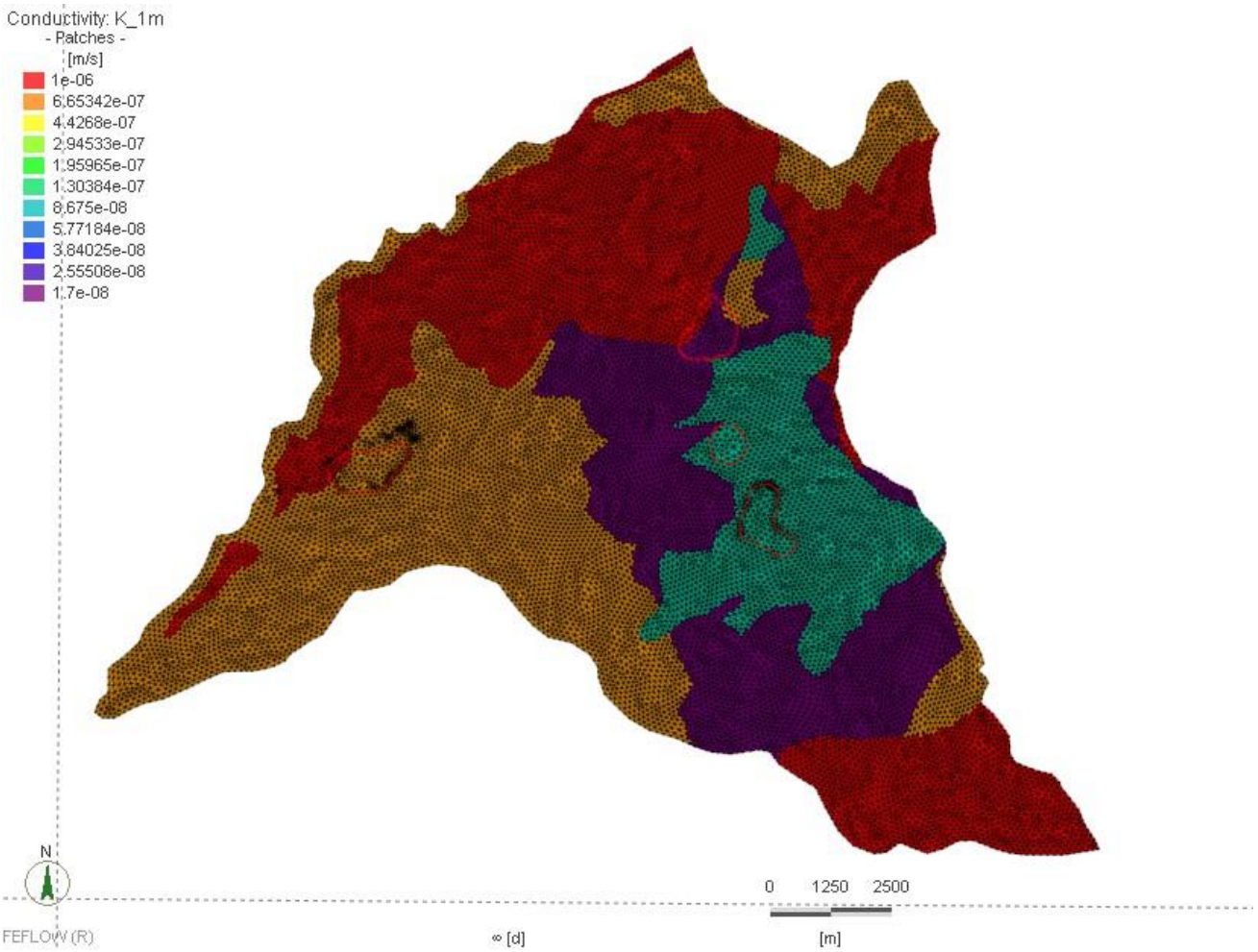

Figure 8: Layer 2 of the Groundwater Model. Red – Cenozoic Basalt Flows, yellow – fresh LV, purple – argillic LV, teal – VC

5.3.2 Boundary Conditions

The following perimeter hydraulic boundaries are defined in the model:

- Constant head boundaries with head at ground surface elevation between ground surface and 100 m depth following the Arpa, Darb and Vorotan Rivers, no flow at greater depth;
- A no-flow boundary along the southern model boundary following assumed groundwater flow lines parallel to the dominant direction of surface water flow (assigned between Saralanj on the upper reaches of the Darb River, and the lower reaches of the Porsughlu River above Gorayk);
- A no-flow boundary following the topographic watershed boundaries along the northern model boundary between Kechut Reservoir and the Vorotan River;
- Seepage faces have been defined along the lower reaches of significant tributaries where it is likely that groundwater discharge is occurring. This includes the tributary which discharges to the Vorotan River from the valley east of the BRSF site, where flowing artesian conditions are observed along the stream valley, and the significant tributary to the Darb River southeast of the VLF site;
- Seepage faces were also assigned at the location of perennial springs identified in the winter 2013/14 spring survey;

- The Spandaryan-Kechut tunnel is represented in the model as a seepage face boundary (drain). A small portion of the tunnel (approximately 2.8 km of its 21 km length) lies outside the model domain on the southern boundary of the model; and
- Recharge has been defined across the upper model surface and a no-flow boundary across the model base.

Boundary conditions assigned along the model perimeter and upper surface are shown in Figure 9. The representation of the Spandaryan-Kechut tunnel is illustrated in Figure 10.

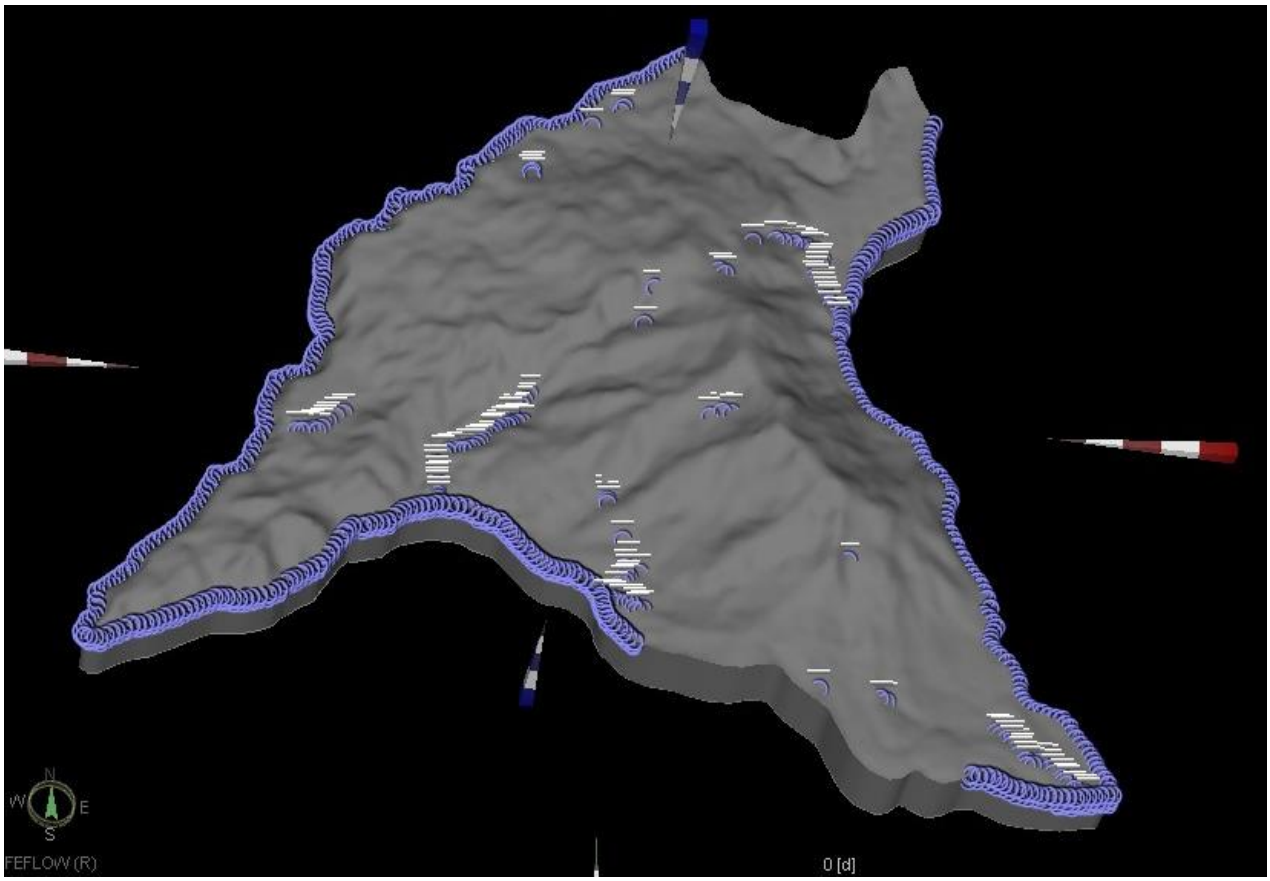

Figure 9: Hydraulic Boundary Conditions

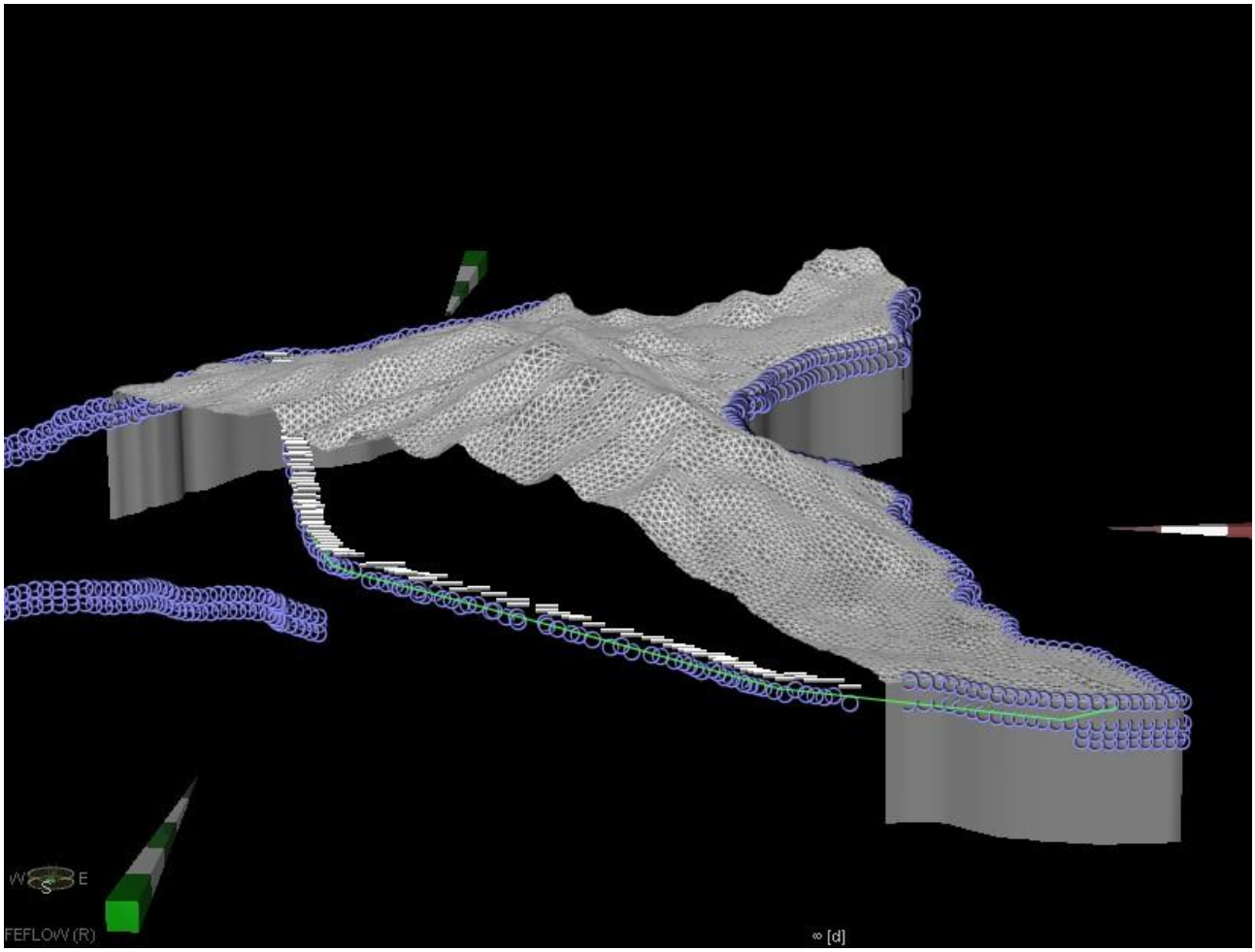

Figure 10: Representation of the Spandaryan-Kechut Tunnel in the Groundwater Model

5.3.3 Initial Conditions

Steady state models were initiated with a hydraulic head of 5,000 m, above the highest ground surface elevation to ensure that all seepage face boundaries defined within the model were retained in the solution.

For the operational phase model, the model was initiated with heads derived from the steady state baseline model, except in the vicinity of the proposed pits, where heads interpolated from the average groundwater elevation surface water were applied in Slices 1 to 5.

5.3.4 Mining Operation Scenario

The mining operation scenario considers steady state flow with the pits at their maximum extent. This is represented by amendment of the model topography to show the pit surfaces, and placement of seepage nodes over the pit faces to calculate seepage into the pits. The model considers inflow to both pits at their maximum extent. This is conservative, but will overestimate the peak inflow, as in reality both pits will not be open simultaneously as the Tigranes-Artavazdes pit will be backfilled as the Erato pit is developed. The limitations of the groundwater model in representing pit inflow and alternative approaches to estimate inflow are discussed further in Section 5.5.2.

Recharge over the pit area is the same as the baseline. The presence of the pit will result in capture of precipitation, but pit dewatering as part of mining operations will remove the majority of this water. There will continue to be infiltration in pit area, but it may not be greater than current recharge rates given the mine water management system and relatively low permeability of the underlying rock.

Leakage from the HLF has been calculated in the modelling for the purposes of the hydrogeological risk assessment of the facility (Golder, 2014)). This assessment indicates that leakage from the HLF (estimated to be equivalent to about 2 mm/yr at steady state in the later years of mine life when Phase 3 is operational) will be significantly lower than the estimated regional recharge rate. The influence of this reduced recharge has been represented in the operational modelling scenario.

The eastern portion of the BRSF is underlain by naturally low permeability clay materials derived from the underlying Lower Volcanics. The western portion of the BRSF will be developed over "engineered" (compacted) native low-permeability soils comprising colluvium and glacial sediments. The BRSF will have an underdrainage layer, directing seepage through the barren rock to a seepage collection system via pipework laid along the central existing drainage channel. Development of the BRSF will intercept recharge within the site footprint, reducing recharge to springs in the southern portion of the site and reducing recharge to groundwater within the basalts to the northwest of the facility.

Modelling of unsaturated flow in the BRSF (GRE, 2014a) indicates that a saturated zone is likely to be present within the central basal seepage collection system drain, allowing leakage to groundwater to occur. GRE (2014c) predicts operational and post-closure groundwater infiltration rates to four discrete areas of the BRSF footprint: the area immediately surrounding the main drainage, the areas overlying the Cenozoic Flow Basalts, the area overlying the Lower Volcanics and the area where spring discharge currently occurs (Figure 11). Two dimensional unsaturated flow section models have been used to calculate infiltration rates in each area. In the area where spring discharge is currently occurring in the central southern portion of the BRSF, GRE (2014c) assumes that negligible leakage to groundwater will occur in operation and closure. The following infiltration rates are calculated based on transient infiltration rates over the 1,000 year post-closure period presented GRE (2014c):

- BRSF stream: 345.3 mm/yr;
- Area overlying Cenozoic Flow Basalts: 0.1 mm/yr in long-term closure;
- Area overlying Lower Volcanics: initially 2 mm/yr, decreasing to 0.3 mm/yr within 350 years and to 0.1 mm/yr after 1,000 years, over the majority of the closure period considered the infiltration rate is approximately 0.2 mm/yr;
- Springs: assumed to be 0 mm/yr.

GRE (2014c) reports a long-term post-closure leakage rate from the BRSF of approximately 14.5 m^3/day, equivalent to a recharge rate of 3.6 mm/yr.

Figure 11: Infiltration Areas, BRSF (GRE, 2014c)

5.3.5 Post-Closure Scenario

The water balance for the partially backfilled Erato pit following closure (Golder, 2014a) indicates that a water body will develop within the permeable backfill with an annual average volume of 21,140 m^3 and an annual average water level of 2,628 masl. The infiltration rate from this water body, based on the assumed average pit base hydraulic conductivity, is calculated to be 21,135 m^3/month. This is equivalent to 27.0 m/yr over the water body area. The volume and infiltration rate from the pit lake is very sensitive to the assumed bedrock permeability, and also to the assumed runoff coefficients. The water balance model assumes a 40% runoff rate from the pit walls. For the purposes of the post-closure modelling scenario, it is assumed that the long-term average infiltration rate on the pit walls will be 20 mm/yr, whilst that in the base the pit over the water body area will be 27.0 m/yr (Figure 15). This equates to an equivalent annual average recharge across the entire pit footprint of 536 mm/yr.

In post closure, backfilling of the Tigranes-Artavazdes pit will result in reduced recharge from the backfilled pit footprint area. The rate of infiltration from the backfill along the pit walls and in the pit base, predicted through unsaturated flow and soil water balance modelling (GRE, 2014b) is shown in Figures 12 and 13.

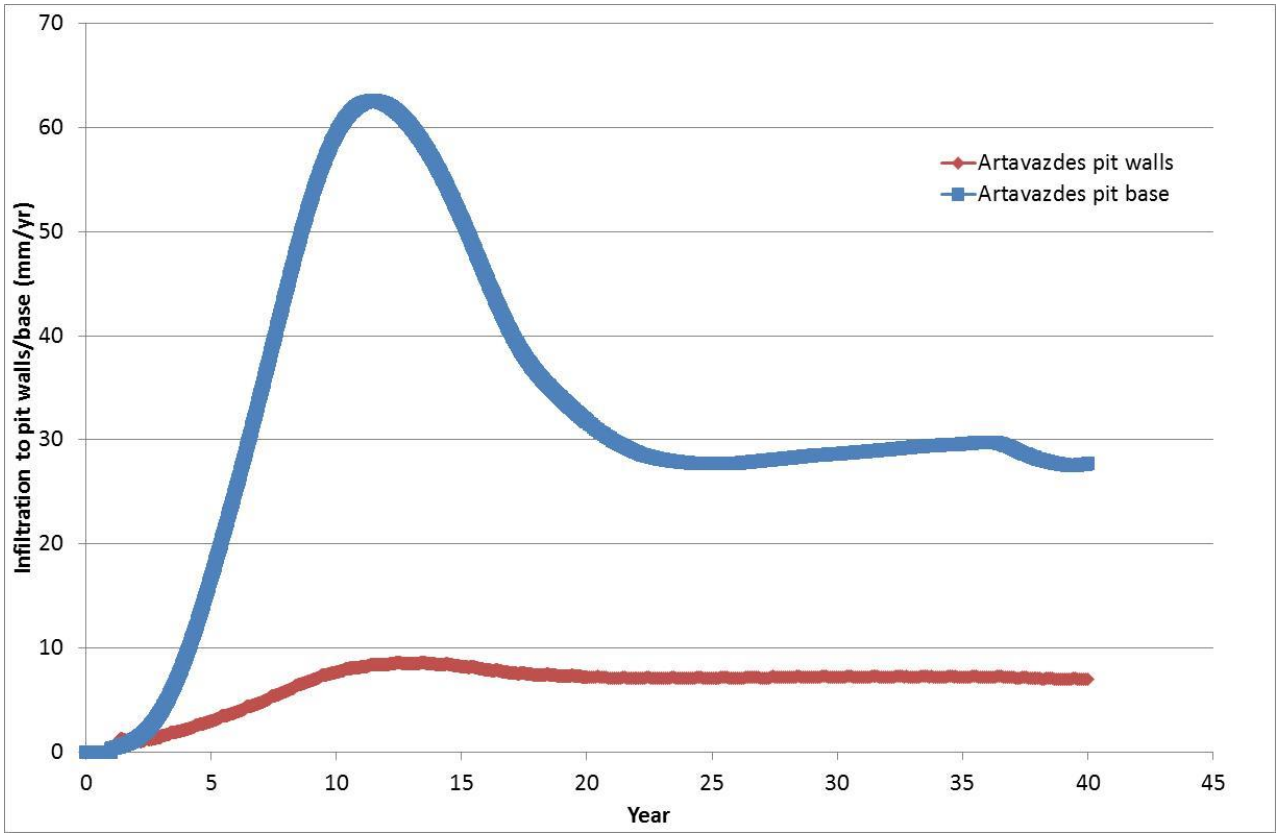

Figure 12: Predicted Infiltration Rates from Artavazdes Pit (GRE, 2014b)

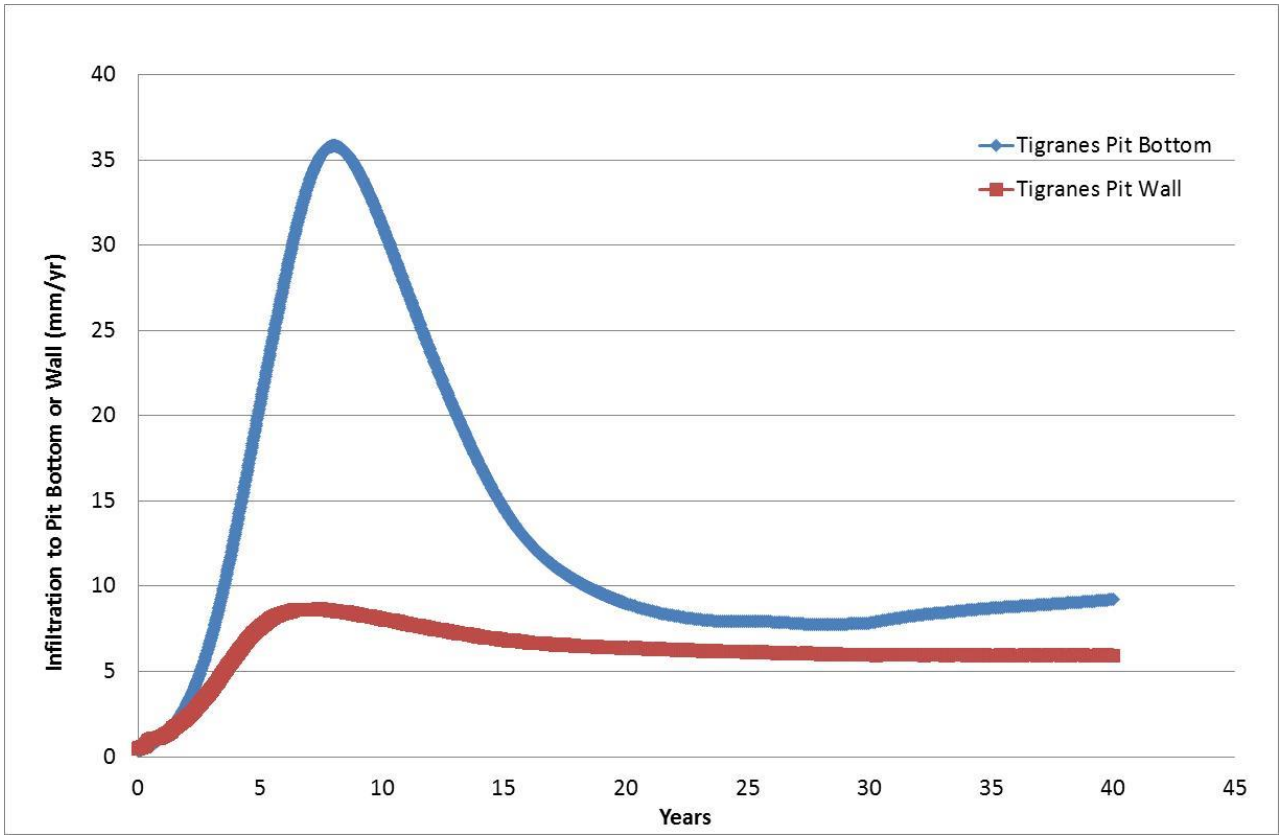

Figure 13: Predicted Infiltration Rates from Tigranes pit (GRE, 2014b)

An initial pulse of recharge occurs as a result of high infiltration rates prior to placement of the engineered cover. Whilst this pulse is significantly above the long-term post closure infiltration rate, it is less than existing conditions. Throughout the closure and post-closure period, the effect of backfilling the pits will be to reduce infiltration to groundwater and subsequently reduce baseflow to surrounding springs and stream. This effect will be most pronounced under the long term closure condition.

The unsaturated flow modelling of the backfill material indicates that this material will not be saturated based on predicted infiltration rates through the engineered cover.

Modelling assumes that the backfill will be above the water table. Based on investigations, it is possible that backfill material in the base of the Tigranes and Artavazdes pits may be below the water table during closure. The rate of infiltration from the base of the backfill will be controlled by the climate driven water balance at the surface of the backfill and is not very sensitive to the backfill thickness. As recharge from the backfilled pit area is controlled by the climate driven water balance and infiltration at surface, saturation in the base of the waste is assumed not to significantly influence the predicted infiltration rate over the pit area.

The southern portion of the Tigranes-Artavazdes pit (known as Arshak), extending towards Artavazdes peak, will not be backfilled at closure. Modelling of infiltration in closure (GRE, 2014b) indicates that a seasonal water body may develop, dependent on the hydraulic conductivity of the bedrock underlying the pit. Modelling suggests that infiltration rates may be high for a short period during operations. Over the modelled period from 15 years to 40 years post-closure, the average annual infiltration rate from the pit base is between 136 mm/yr and 142 mm/yr, with a multi-year average of 139 mm/yr. This is less than the estimated baseline recharge rate of 200 mm/yr. As there is some uncertainty regarding the baseline recharge rate, a model scenario has been completed assuming Arshak pit water body recharge similar to existing conditions.

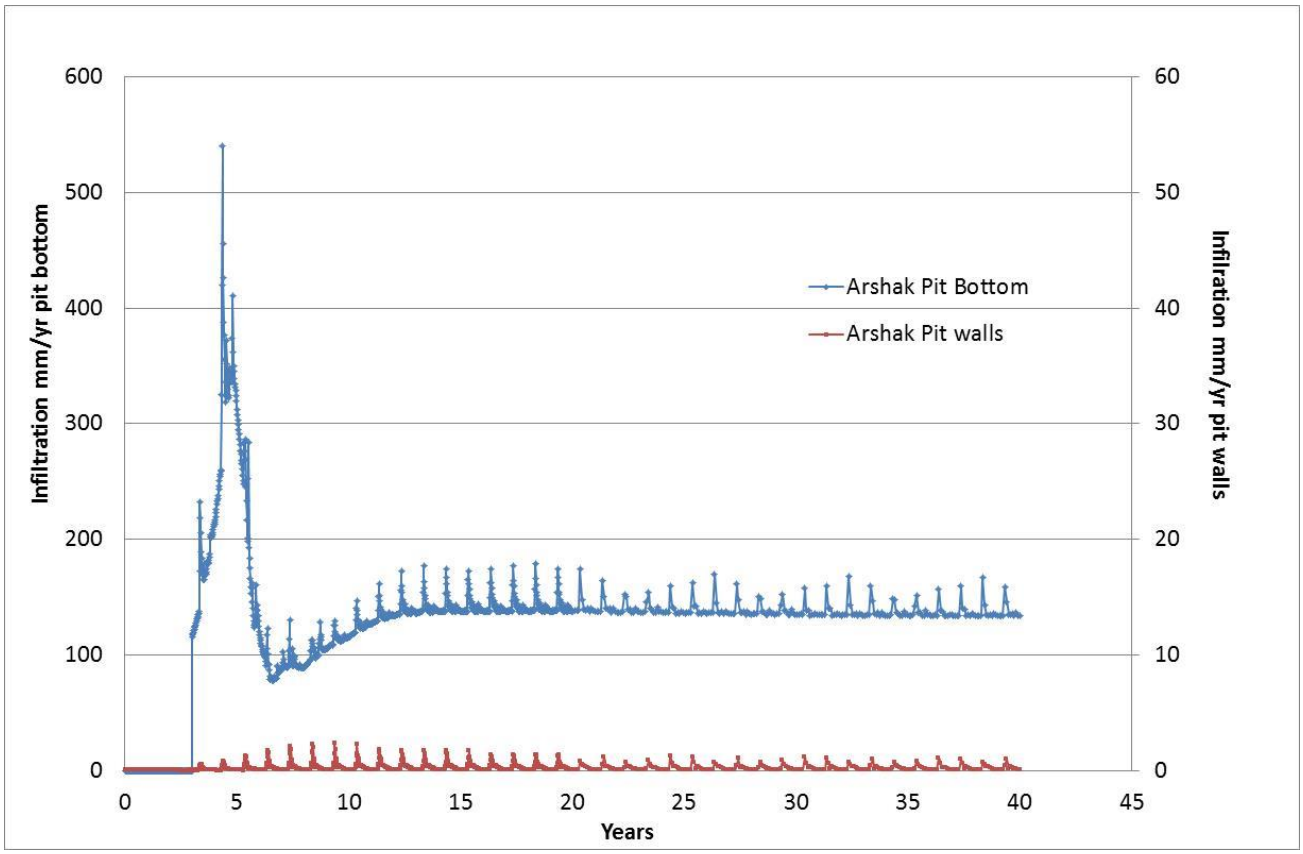

Figure 14: Predicted Post Closure Infiltration, Tigranes-Artavazdes (Arshak) Open Pit (GRE, 2014b)

The predicted change in groundwater recharge patterns in the backfilled Tigranes-Artavazdes pit represents a reduction in infiltration rates through the closure period. The period of peak impact in terms of water quantity is in the long-term post-closure phase when the backfill areas have been covered. The impact on

water quantity has therefore been assessed as a steady state model representing long-term post-closure conditions, with the following rates of infiltration applied in the pit area:

- Tigranes pit base: 10 mm/yr;
- Tigranes pit walls: 6 mm/yr;
- Artavazdes (mid area) pit base: 30 mm/yr;
- Artavazdes (mid area) pit walls: 8 mm/yr;
- Arshak open pit, pit base: 139 mm/yr; and
- Arshak open pit, pit walls: 2 mm/yr.

The pit floor and pit wall areas for Tigranes-Artavazdes have been defined by GRE (2014b). The pit backfill material is not represented in the post-closure model. This is because the infiltration rate at the base of the backfill has been calculated using a local scale unsaturated flow model. Representing the backfill in the groundwater flow model would cause the model to recalculate flow through this volume, and yield a different infiltration rate compared to the unsaturated flow model. The infiltration areas defined in the groundwater model to reflect post-closure pit infiltration are illustrated in Figure 15.

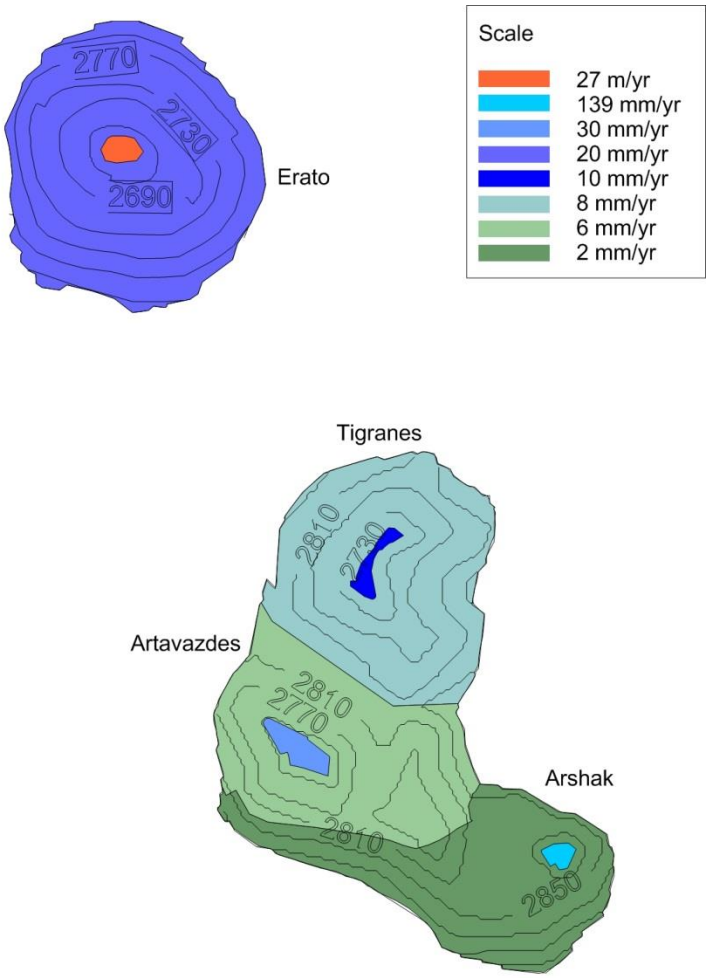

Figure 15: Infiltration Rates to Pit Areas, Post Closure Scenario

In the post-closure phase, the engineered liner of the HLF will continue to inhibit recharge within the HLF footprint and the evapotranspirative (store-and-release) cover will minimise infiltration into the facility, reducing the head on the liner. The HLF has been simulated in the post-closure scenario with a recharge rate of 0.4 mm/yr based on the post-closure leakage rate calculated by the HLF impact assessment GoldSim model (Golder, 2014b). In the long-term (over hundreds of years) the geomembrane liner component of the basal liner of the HLF will degrade, and the HLF will have a lesser influence on the groundwater flow regime. Uncertainty in leakage from the HLF facility has been evaluated further in the HLF impact assessment (Golder, 2014b).

The BRSF will have an underdrainage layer, directing seepage through the barren rock to a seepage collection system. Development of the BRSF will intercept recharge within the site footprint, reducing discharge to springs in the southern portion of the site and reducing groundwater flow to the northwest from the facility. The drainage system will continue to operate in closure and post-closure.

As in the operational case, infiltration to the base of the BRSF in the closure scenario is based on modelled infiltration rates in four areas of the facility footprint, defined in GRE (2014c).

Uncertainty in the extent of the saturated area at the base of the BRSF, the head of water acting on the base area, and water available for infiltration in closure in the BRSF has been modelled to determine the potential range of post-closure impacts. This scenario considers an infiltration rate from the base of the facility of 5 mm/yr in areas away from the basal drain (the average infiltration rate across the entire footprint area will be much greater than 5 mm/yr as infiltration through the facility base is non-uniform and the majority of infiltration will occur surrounding the basal drain). A fixed head of 0.1 m above ground surface has been applied in a localised area in the 25 m surrounding the basal drain. The basal drain is assumed to be underlain by natural soils, or a compacted soil liner permeability of $1x10^{-9}$ m/s. The proportion of the BRSF footprint which is assumed to include a constant saturated head of 0.1 m is illustrated in Figure 16.

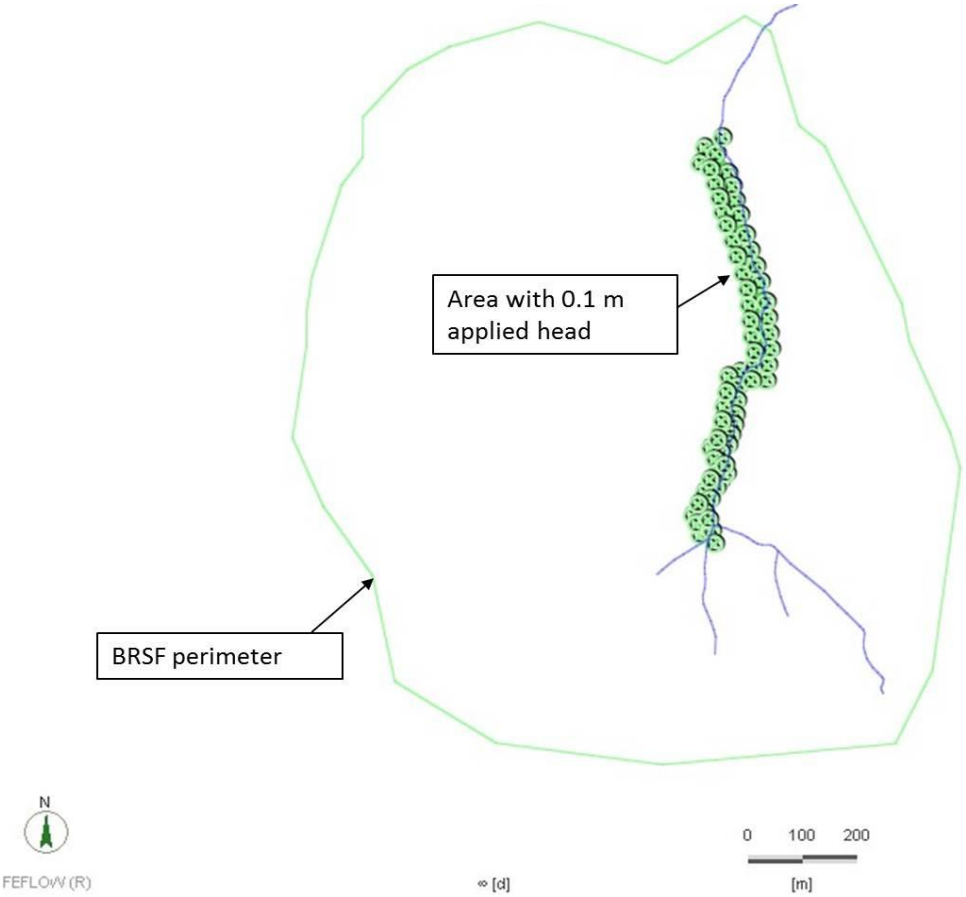

Figure 16: Area within BRSF Assigned a Constant Head of 0.1 m, Closure Scenario

5.4 3-D Model Calibration

The model was calibrated to average groundwater elevation shown in Table 3, to groundwater flow in the Spandaryan-Kechut tunnel and to other hydrologic parameters described in Section 4.6.

The position of the water table within the model domain was simulated using the 'phreatic' surface definition for the upper surface in FEFLOW.

Calibration with respect to hydraulic head (groundwater elevation) was undertaken with respect only to those wells and springs which tap/or are fed by the saturated groundwater flow system. Less weight was placed on calibration of the groundwater elevations in wells high on the mountain peaks (above 2,600 masl) than those at lower elevation because of the perched conditions.

The following parameters were evaluated during model calibration:

- Recharge rates, and distribution;
- Hydraulic conductivity (including anisotropy); and
- The extent of groundwater seepage along streams within the Project Area.

The final numerical solution is accurate to an error criterion of less than $1x10^{-7}$, approximately equivalent to +/- 0.03 cm of head. The final model water balance error is less than 0.001%.

Final values post-calibration are described in Table 4.

Table 4: Calibrated Model Input Parameters

Parameter	Initial Value	Final Value
Recharge		
BRSF valley and adjacent valley basins	300 mm/yr	250 mm/yr
Remaining area	300 mm/yr	200 mm/yr
Hydraulic Conductivity and Anisotropy		
Colluvium	$5x10^{-6}$ m/s K_h:K_v: 10	$2x10^{-6}$ m/s K_h:K_v: 10
Upper Volcanics (VC)	$1x10^{-7}$ m/s K_h:K_v:10	$2x10^{-7}$ m/s K_h:K_v: 1
Argillically altered LVA	$8.5x10^{-8}$ m/s K_h:K_v:1	$1x10^{-8}$ m/s K_h:K_v: 1
Unaltered LV	$2.5x10^{-6}$ m/s K_h:K_v:100	$6x10^{-7}$ m/s K_h:K_v: 100
Deep LV (below 200 m)	$1x10^{-7}$ m/s K_h:K_v:100	$5x10^{-8}$ m/s K_h:K_v: 50

The error in the modelled water table elevation with respect to observed hydraulic heads in the calibrated model is shown in Appendix B.

The model predicts flow exiting the Spandaryan-Kechut tunnel from the model domain is 0.14 m^3/s. Scaled proportional to the length of the tunnel including the portion outside the model domain, this would be equivalent to a total groundwater inflow of 0.16 m^3/s. This is similar to the observed average flow of 0.19 m^3/s, particularly as recent data suggests historical measurements may have slightly overestimated actual flows.

The model predicts the following baseflows along river segments described above:

- Vorotan River AW001 to AW003: model calculated flow of 0.13 m^3/s (observed flow from the whole contributing catchment of 0.7 m^3/s, approximately 20% of the catchment is estimated to lie within the model domain, suggesting a contribution of approximately 0.14 m^3/s);
- Arpa River Arpa 1 to Arpa 2: model calculated flow of 0.093 m^3/s (observed flow from the whole contributing catchment of 0.1 m^3/s, approximately 60% of the catchment is estimated to lie within the model domain, suggesting a contribution of approximately 0.06 m^3/s); and
- Darb River AW005 to AW006: model calculated flow of 0.062 m^3/s (observed flow from the whole contributing catchment 0.6 to 0.7 m^3/s, approximately 45% of the catchment is estimated to lie within the model domain, suggesting a contribution of approximately 0.3 m^3/s).

Both due to the contribution of out-of-domain flows to the observed river flows, and because estimates of annual average baseflow are based on summer spot flow measurements, the flows for calibration purposes are uncertain. Modelled flow in the Vorotan River along the AW001 and AW003 segment are a reasonable match to observed flows, and this is the location where the baseflow estimate is most reliable as summer spot measurements show a clear recession curve. Modelled flow in the Arpa River between Arpa 1 and Arpa 2 is approximately 60% of observed, given the uncertainties, this is considered within the range of error on the baseflow estimate. Modelled flows in the Darb River section are not similar to observed flows, but baseflow discharge in the AW005 to AW006 section is high given the incremental increase in topographic catchment between these two locations, such that this result is reasonable.

The calibrated model results provide a good match to overall trends in groundwater elevation across the Project Area, and the model predicts reasonable flows in large scale hydrologic features such as the Spandaryan-Kechut tunnel. However, within all areas where a higher spatial resolution of groundwater elevation information is available, a single hydraulic conductivity domain for each hydrogeological unit is not able to accurately represent the observed head distribution. This is because the model is not able to simulate short length-scale variation in hydraulic head as the result of local scale variation in hydraulic properties or discrete features (faults).

- The calibrated model hydraulic conductivities are generally lower than values measured in hydraulic testing. Monitoring wells were installed screened across flowing zones, or where groundwater was encountered within the lithological sequence. It is usual for wells to test the more permeable zones within an overall low-permeability geological sequence. In addition:
  - The hydraulic conductivities recorded in testing covered a large range and given the size of the testing data set, the error of the mean value is large; and
  - Initial estimates of hydraulic conductivity were generally based on the geometric mean of the testing data set; it is possible that the large scale hydraulic conductivity is not represented by the mean of local-scale testing.

Given these factors, the final calibrated hydraulic conductivity values are considered to be representative of the observed ranges.

The calibration process has considered only the optimum fit with the application of a single hydraulic conductivity value for each hydrogeological unit. It is likely that some variation from the observed conditions is attributable to spatial variation in the (kilometre-scale average) hydraulic conductivity within units across the Project Area. This is evident with respect to calibration of wells installed in the argillic LVA at the BRSF site and surrounding the ore bodies. A good calibration cannot be obtained for these two areas using a single hydraulic conductivity value. Given the uncertainties involved in characterising field-scale permeability of fractured rock, it is not possible to further refine the bounds on hydraulic conductivity for sub-domains within lithological units from the existing data set. It is also likely to be the case with regard to the colluvium, which on steep slopes of the mountain comprises predominantly cobbles and boulder, but on the lower plains is likely to comprise silty clay alluvium along the stream valleys and more gravelly/cobbly silty clay on the interfluves. Detailed information to represent these variations is limited. The resulting model calibration is considered to represent the conceptual groundwater model and be suitable for predictive purposes.

There is greater uncertainty in the hydraulic conductivity of some units (such as the colluvium and VC units) and there is also some uncertainty regarding the recharge rate. This leads to a non-unique calibration solution with respect to hydraulic heads. However, as the model has been calibrated to both head (groundwater elevations within the Project Area) and flow in the Spandaryan-Kechut tunnel, this provides confidence on the large-scale behaviour of the groundwater system. The model is very sensitive to the hydraulic conductivity of the colluvium (sensitivity analysis presented below). Assuming a lower hydraulic conductivity for the colluvium requires an unreasonably low recharge rate that produces an underestimate of groundwater discharge to the Spandaryan-Kechut tunnel.

The following features of the groundwater flow system were identified during the model calibration process:

- Groundwater levels on the west of the Amulsar Mountain ridge and in the BRSF site cannot be matched using a single hydraulic conductivity value for the argillically-altered andesite, even using variable distributed recharge rates. Groundwater levels in the BRSF site are under-predicted by the current model, whilst those on the west of the mountain ridge are over-predicted;
- Groundwater elevations surrounding the ore bodies are highly variable and cannot be well matched based on the current representation of the geological model. This is a result of model scale, geological variability and localised perched recharge/discharge conditions; and
- The groundwater model calibration is very sensitive to the assumed hydraulic conductivity of the colluvium, which is variable across the Project Area.

5.5 3-D Model Results

5.5.1 Baseline Scenario

Groundwater elevation contours for the baseline scenario are shown in Appendix C. Particle pathlines representing groundwater pathways from the BRSF site, the HLF site and the ore bodies are also shown. The groundwater model simulates key aspects of the conceptual model developed based on physical observations, including:

- Water table elevation of between 2,700 masl and 2,740 masl beneath the Amulsar ridge, extending northeast to southwest largely mirroring topography;
- Radial groundwater flow away from the Amulsar Mountain ridge, with flow to the east (to the River Vorotan) and west (predominantly to the River Darb) from the Tigranes-Artavazdes pit, and flow predominantly to the west to the River Arpa from the Erato pit. The model suggests that where flow does occur east from Erato, the groundwater enters the Arpa catchment;
- Groundwater flow is initially to the northwest from the BRSF site before turning west to discharge predominantly to the Arpa River downstream of the Kechut Reservoir;
- Groundwater flow westward from the HLF site toward the Arpa River;
- A shallow near-surface water table to the west, south and northwest of the Amulsar ridge with discharge to perennial springs on the flanks of the ridge, and in the valley east of the BRSF site. The model predicts groundwater elevation at ground surface in the base of the BRSF site;
- Groundwater discharge to the stream along the base of the HLF valley, consistent with observed heads, which are very close to ground surface in proximity to the stream, local discharge to the stream with groundwater flow at depth and beneath the northern portions of the HLF toward the Arpa River;
- A deep water table (in excess of 100 m) in the basalts to the northwest and west of the Amulsar ridge; and
- Discharge from springs at the base of the Basalt sequence adjacent to Kechut Reservoir.

The model indicates that the Spandaryan-Kechut tunnel intersects the water table along its length (seepage nodes applied along the path of the tunnel are active in the final solution). In the south and centre of the model the tunnel has little influence on the water table. In the north of the model area there is a small influence. Overall, the groundwater contribution area (capture zone) of the tunnel is localised (Figure B11). Simulated groundwater flow pathlines indicate that groundwater flow originating from the Erato, Tigranes and Artavazdes peaks and from the BRSF site does not reach the tunnel.

The predicted water table elevation in the baseline scenario is approximately 2,720 masl beneath the Tigranes-Artavazdes pit and approximately 2,700 masl beneath the Erato pit. This is slightly higher than the monitoring data (Figure 17). As noted above, a good calibration was not achieved in the mountain area, likely as a result of the simplification of the geological conceptual model in the groundwater model. The groundwater model over-predicts heads to the west of the ridge, and under-predicts heads beneath Artavazdes. The groundwater model therefore suggests that the base of both the Erato pit (base 2,620 masl) and Tigranes pit (base 2,680 masl) will be below the water table. Observed level data suggests that the Erato pit base will be above the water table, whilst the base of the Tigranes pit may intersect the water table.

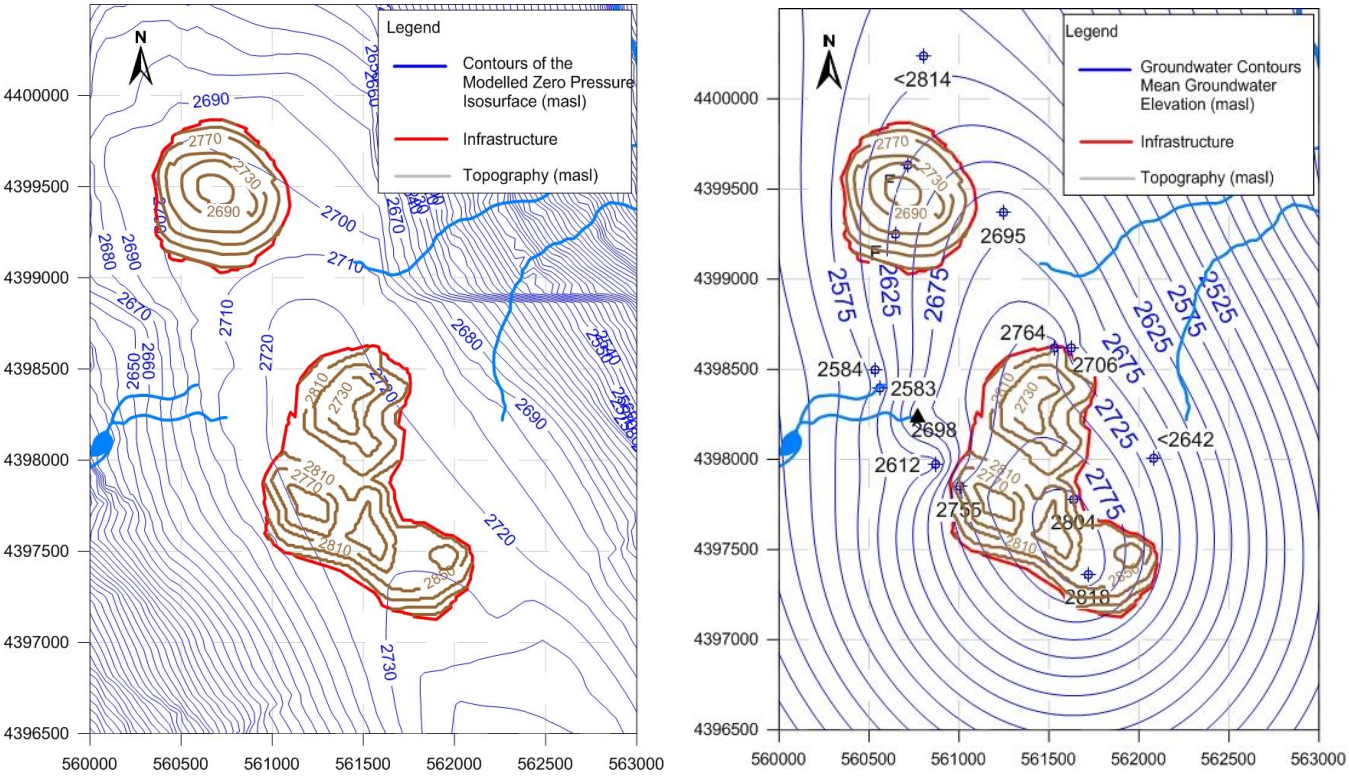

Figure 17: Contours of the Zero Pressure Isosurface beneath Proposed Pits, and Observed Mean Water Table Elevation

Given the steep hydraulic gradients and short length scale variation in hydraulic heads observed along the Amulsar ridge, there is some uncertainty regarding which wells reflect the elevation of the water table, and which reflect perched water tables within the LVA/VC. The results of the groundwater model suggest that in general, the groundwater levels in wells which have remained open could reasonably represent the water table surface, given the understanding of the permeability of the surrounding material and likely recharge rates.

Calculated groundwater discharges to significant features in the baseline model are shown in Table 5.

Table 5: Groundwater Discharges Predicted by the Groundwater Model

Area	Net Discharge m^3/s	Net Discharge L/s
Arpa River and Kechut	0.37	366
Darb River	0.18	180
Vorotan River	0.20	198
Upper Lake Spandaryan	0.002	1.91
HLF site stream	0.003	2.71
Stream south of HLF site	0.031	30.9
Stream in basin east of BRSF site (to mouth of valley)	0.009	8.71
Amulsar springs	0.008	8.15
BRSF springs	Negligible	
Springs west of BRSF	0.0002	0.22
Springs from Basalts adjacent to Kechut Reservoir	0.003	3.44
Spandaryan-Kechut tunnel	0.14	137

Groundwater flows to the major rivers and the Spandaryan-Kechut tunnel are discussed with regard to the model calibration, above. The model underestimates discharge from the springs in the centre of the BRSF footprint, because the model underestimates heads in the BRSF area. Springs to the west of the BRSF were observed to be wet but with no measurable flow in November 2013 and with a discharge of 9 L/s from the spring cluster in May 2014.

Discharge at location FM-5 at the mouth of the basin east of the BRSF is shown in Figure 17 for spring 2012. The spring melt water discharge peak passes relatively rapidly, and flow in the stream in late June is between 7 L/s and 9 L/s. This is a good fit to the predicted groundwater discharge.

Spring discharges recorded surrounding the Artavazdes, Tigranes and Erato peaks in November 2013 totalled less than 0.5 L/s, although not all potentially flowing springs were visited in the survey. May 2014 discharge from the spring clusters represented in the groundwater model was approximately 15 L/s. Many more ephemeral springs were identified to be flowing in the May 2014 spring survey; however these springs are considered to represent discharge of snow melt water 'interflow' passing through the soils and shallow rocks to discharge downslope.

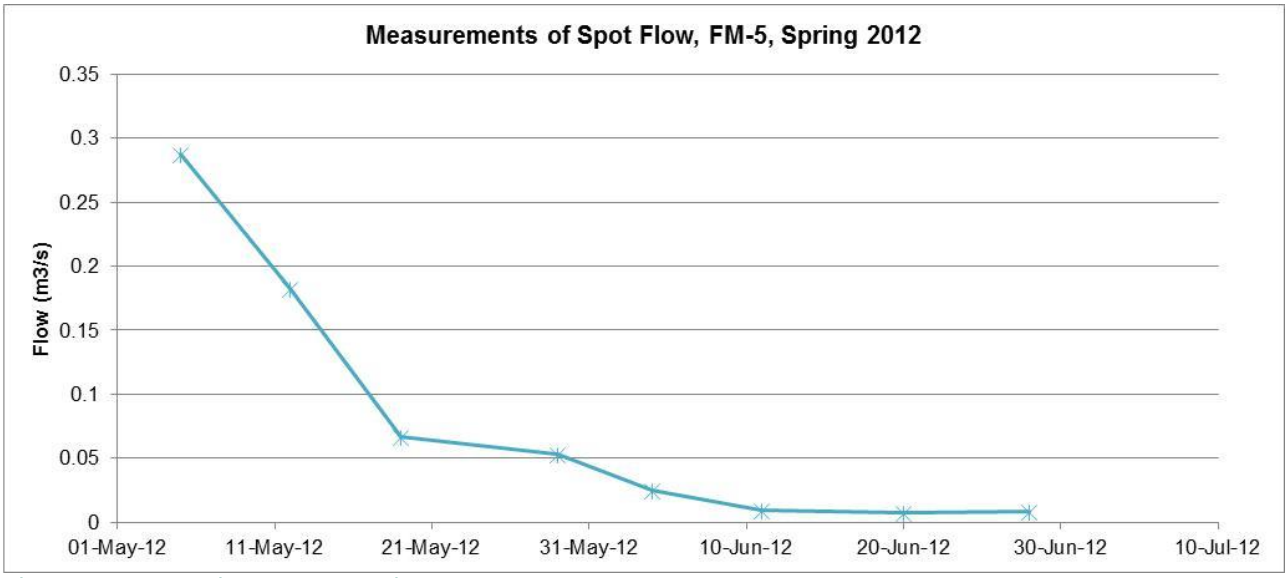

Figure 18: Stream Flow at FM-5, Spring 2012

Figure B2 shows the saturated domain (where groundwater pressure is above zero). Not all of the springs or areas of groundwater seepage in the project area are mapped, or explicitly represented in the groundwater model. Areas where the upper layer of the model is saturated (shown in blue) reflect expected zones of potential seepage and groundwater discharge. The extent to which discharge occurs will depend on the permeability of the colluvium at surface, which is likely to be locally variable. The model shows discharge zones in river and stream valleys, and on the flanks of the Amulsar ridge. This distribution is relatively well matched to observed areas of spring discharge in the November 2013 and May 2014 spring surveys.

5.5.2 Operational Scenario Effects

5.5.2.1 Pit Inflow during Mining Operations

There are three sources of groundwater inflow to the pits during mining:

1) Seasonal perched water inflow from snow melt which infiltrates to ground within the area immediately surrounding the pits and that may flow through the sub-surface towards the pit and reach the pit sump.

2) Transient inflows during excavation from perched water bodies supported within the complex faulted geology of the pit.

3) Year-round inflow from groundwater where the bases of the pits extend below the water table. This may occur in the base of both the Artavazdes and Tigranes pits which are interpreted to be mined to a depth of about 45 m and 70 m, respectively, below the existing water table. The base of the Erato pit is interpreted to at or slightly above the existing water table.

Perched Water Inflow

The perched inflows are not modelled by the steady state saturated flow model. Perched water inflow to the pits from localised permanent or semi-permanent bodies supported within the complex geology surrounding the ore bodies will be a function of snow accumulation and melt and the underlying geology. Perched water inflows will occur throughout the mine life being greatest at the end of mine life when the pit is deepest. This perched inflow has been estimated based on simplifying assumptions and should be managed with an adaptive water management approach for the pit water depending on operational observations.

An estimate of transient seasonal perched water inflow the pits has been made based on the estimated recharge rate in the pit vicinity and the possible topographic/geological controls on perched flow to the pits, combined with observation of ephemeral spring flows under current conditions.

Based on observations and the groundwater model calibration, the recharge rate at the peak of Amulsar Mountain is likely to be between 200 mm/yr and 250 mm/yr; most of this (90%) occurring during the spring snow melt, with the remainder probably occurring in autumn before the winter freeze, and negligible inflow in winter when the ground is snow covered. Spring flows in the May 2014 survey also give a good indication of the extent of infiltration and discharge of seasonal melt water. The observation of spring flow response to the snow melt indicates the shallow flow system on the high mountain is relatively permeable with a quick response to recharge (probably via fractures and faults in the VC) therefore we have assumed that similar behaviour could occur at the pits given the pervasive fracturing/faulting.

The area that may provide seasonal perched inflow to the final pit extents has been estimated based on topography, the final pit depth and observed discharge locations. Based on this area and observed flows we have estimated the seasonal perched water inflow to the each pit at maximum extent. As noted above, in the intermediate term, recharge rates will also govern any permanent groundwater inflow to Tigranes; there will be a short period of higher flows associated with storage changes, but after a period of no more than a year it is probable that groundwater inflows will stabilise to a recharge-driven rate.

Table 6: Estimate of Seasonal Perched Water Inflows to the Erato and Tigranes-Artavazdes Pits

	Estimated Perched Seepage Contribution Area (m^2)	Inflow in May/June/July (m^3/hr for 90 days) (0.9R)	Inflow in Sept/Oct (m^3/hr for 30 days) (0.1R)	As Annual Average Equivalent Flow Rate (m^3/hr)
Erato	294,850	25-31	8-10	7-8
Tigranes-Artavazdes	542,130	45-56	15-19	12-15

Inflows in Table 6 represent maximum inflows at the ultimate pit extent. The Tigranes-Artavazdes pit will be partially backfilled when the Erato pit reaches its maximum extent. The flows indicated will not therefore occur simultaneously, and perched water inflows to Tigranes-Artavazdes are likely to reduce as the pit is backfilled.

Groundwater Inflow

The groundwater model is large scale and its objective is to replicate the broad features of the groundwater flow system to support the groundwater impact assessment. It represents the geology surrounding the pits in a simplified condition. The model is not capable of accurately simulating groundwater inflows into the pit in such a hydrogeological system. Furthermore, the geometry of the pit area is such that any intermediate/long-term groundwater inflow to the pits will be controlled by the rate of recharge as the entire system is free draining toward the bounding river valleys. This places a limit on the possible maximum inflow rates.

The measured and model-predicted steady state groundwater elevations below the Erato and Tigranes/Artavazdes pits are at least 60 m to 140 m below current ground surface – measured groundwater elevation approximately 2,625 to 2,775 m, respectively. This indicates that sustained and year-round groundwater inflow to the pits will occur only when the pit floors are mined below these approximate elevations in the later years of mining.

The operational scenario modelled the effect of dewatering the final pit extent under steady state conditions. This scenario is conservative, as in reality both pits will not be open at their full extent simultaneously. Backfilling of Tigranes-Artavazdes will occur during excavation of Erato. The model predicts the annual average steady state groundwater inflows into the two pits as follows:

- Erato: 185 m^3/d; and
- Tigranes-Artavazdes: 37 m^3/d.

However, because the calibrated baseline model significantly over predicts the groundwater elevations at Erato, the modelled groundwater inflow to the Erato pit at the end of mining is not valid. Observed

groundwater elevations suggest that the planned base of the Erato pit would be at or slightly above the water table, such that permanent groundwater inflow to this pit at the end of mining is likely to be minimal.

The calibrated baseline model under-predicts the groundwater elevation beneath Artavazdes and Tigranes pits. The predicted groundwater inflow to these pits at the full pit extent is likely to be underestimated. Based on the difference between the predicted and measured groundwater elevations at Tigranes/Artavazdes, we estimate that the steady-state groundwater inflow to the pits at the full pit extent (Year 3 of the mine life) could be in the range of 100 m^3/d to 250 m^3/d.

Backfilling will occur predominantly in the deeper parts of the Tigranes-Artavazdes pit, in the vicinity of the current peaks for Tigranes and Artavazdes. The shallowest portion of the pit (beneath Arshak peak) will not be backfilled. The Arshak portion of the Tigranes-Artavazdes pit is between 10 m and 30 m above the permanent water table. As a result, permanent groundwater inflow to the pit is likely to cease as backfilling proceeds.

5.5.2.2 Mountain Peak Springs

The baseline model simulated groundwater flow to perennial springs to the west of main pits, and to the south of Tigranes-Artavazdes. The groundwater model provides an indication of the extent of influence of pit dewatering on the water table surrounding the mountain peak, and the resultant impact to spring flows.

Figures B12 and B13 (Appendix B) illustrate the extent of the zones surrounding the mountain where the water table is at surface in the baseline and operational scenario models. These are areas where seepage may occur within the pits and where spring discharge is likely to occur on the mountain flanks. There is a limited decrease in the extent of saturation on the mountain flanks surrounding the pits at the end of mining, the maximum elevation of the saturated/spring zone decreased by typically approximately 30 m in the operational case in the area east and west of the pits. The effect on the potential seepage zone is limited because pit dewatering will create only local drawdown and will not materially influence the extent of any existing seepage zones at lower elevations surrounding the pits. None of the perennial springs observed in the November 2013 spring survey are located above the elevation of the pit base. All lie within the potential seepage zone in both the baseline and operational models.

At the end of mining, model results indicate that the overall flow in the mountain springs could decrease by about 0.85 L/s (10%). This is the result of capture of groundwater recharge in the pit area which would otherwise feed these springs. The model therefore suggests that pit dewatering should not affect the overall distribution of perennial springs, but may result in a small decrease in the spring discharge. The model simulates annual average conditions. The results therefore potentially suggest that some springs which currently flow at a very low rate during winter may become ephemeral (dry during the winter months) at the end of mining. As described above, the model underestimates heads in the Tigranes-Artavazdes area, and as such may underestimate the extent of the capture zone surrounding this pit and influence of local spring flows.

In the BRSF, the reduction in recharge results in a decrease in the water table elevation particularly in the southern portion of the site, such that groundwater discharge may no longer occur in this catchment at the end of operations.

The model predicts that groundwater discharge to the stream in the valley east of the BRSF will decrease from an annual average of 8.7 L/s to 6.6 L/s during operations, a decrease of 24%. This change will be sensitive to the infiltration rate to the BRSF, spring discharges into the BRSF basal drain and the maximum permeability specification of the basal liner. A decrease in flow of 0.1 L/s (36%) is predicted in the spring cluster west of the BRSF. The impact on discharge to the valley east of the BRSF under conditions with a higher leakage rate from the BRSF is discussed in Section 5.5.3.

5.5.2.3 Change in Hydraulic Heads, Pit Area, BRSF and HLF

The change in hydraulic head at wells used as observations points in the groundwater model between the baseline and operational scenarios is illustrated in Figure B15 (Appendix B). The largest change is observed in the vicinity of the BRSF, where reduced recharge results locally in an approximately 60 m decline in water table elevation on the southern side of the facility. Significant drawdown (greater than 20 m) is also

observed in wells immediately adjacent to the Tigranes-Artavazdes pit and in DDAW007 adjacent to Erato. This decline would take place gradually over time as the groundwater system re-equilibrates to a new steady state condition in response to the changes in recharge.

Reduced recharge across the HLF footprint has a significant impact on groundwater heads beneath the HLF in the groundwater model. A decrease of 10 m is observed on the southeastern boundary and in the centre of the site, reducing in wells in proximity to the main drainage to a minimum of 3 m in GGDW016. Currently perennial flow in the stream within the HLF site is not observed. However, reduction in groundwater levels surrounding the site is likely to result in a reduction in seasonal baseflow, and to any permanent baseflow to the stream southwest of the site. These groundwater elevation and discharge changes would occur gradually as the groundwater system responds to the new recharge conditions.

5.5.2.4 Groundwater Flow Pathlines

Groundwater flow directions from each of the facilities in the operational scenario is similar to the baseline case (Figure B16, Appendix B). Any leakage from the BRSF would flow northwest toward the Arpa River. Any leakage from the HLF would flow to the west toward the Arpa River.

The groundwater model underestimates heads beneath the Tigranes-Artavazdes pit, therefore is likely that the model underestimates the capture zone associated with pit dewatering. The model indicates that infiltration through the pit walls in operation will flow in groundwater both east to the Vorotan River and west to the Darb River. At Erato, the model suggests that a greater portion of recharge through the pit walls will be captured in the pit sump. This is because this pit is modelled to be mined further below the water table. It is possible that site conditions will result in less groundwater capture during operations and infiltration through the pit walls will follow pathways more similar to the post-closure scenario.

5.5.2.5 Change in Regional Groundwater Discharge

Overall, the modelling indicates that at the end of mining there could be a small decrease in the amount of baseflow discharging to the Arpa, Darb and Vorotan rivers and their tributaries draining from Amulsar. The decrease is estimated to be 3% of the current baseflow deriving from the catchment within the Project Area in the Vorotan River, 2% in the Arpa River and 1% in the Darb River.

Groundwater discharge to the Spandaryan-Kechut tunnel is predicted to decrease by 1% by the end of the operational period.

Groundwater discharge to the tributary of the Darb River southeast of the HLF is predicted to decrease by approximately 2% by the end of the operational period.

Groundwater discharge to the Madicenk springs is predicted to decrease by approximately 10% as a result of operation of the mine, due primarily to the reduction in recharge beneath the BRSF.

5.5.3 Post Closure Scenario

The post-closure scenario considers the effect of reduced recharge in the vicinity of the backfilled Tigranes-Artavazdes pit and increased recharge from the open portion of the Tigranes-Artavazdes (Arshak) pit and permeable backfill in Erato pit on groundwater levels and spring flows (where replicated by the regional groundwater flow model). The post-closure model has considered the steady state condition representative of long-term closure conditions. As described above, two closure scenarios were considered to evaluate uncertainty associated with the potential leakage rate from the BRSF in closure and infiltration from the southern portion of the Artavazdes pit.

5.5.3.1 Mountain Peak Springs

The baseline model simulated groundwater flow to perennial springs to the west of the pits, and to the south of Tigranes-Artavazdes. The groundwater model provides an indication of the extent of influence of backfilling of the Tigranes-Artavazdes pit and capture of surface water in the post-closure Erato pit on the water table surrounding the mountain peak, and the resultant impact to spring flows.

Figures B19 and B20 (Appendix B) illustrate the extent of the zones surrounding the mountain where the water table is at surface in the baseline and post-closure scenario models. These are areas where seepage may occur within the pits and where spring discharge is likely to occur on the mountain flanks. There is a slight increase in the maximum elevation of the seepage zone surrounding Erato as a result of increased recharge in this area following closure, increasing the maximum elevation by approximately 20 m to 30 m. There a slight decrease in the maximum elevation of the seepage zone surrounding Tigranes-Artavazdes, with a decrease of less than 20 m to 30 m as a result of reduction in recharge due to backfilling of the pits. The perennial springs observed in the November 2013 spring survey are at elevations below the area where seepage is predicted to cease in post-closure.

In post-closure, modelling indicates that the flow in the high mountain springs simulated in the groundwater model could decrease by between 0.12 and 0.47 L/s (1% to 6%) from baseline conditions. The effect of reduced recharge due to backfilling and placement of a store and release soil cover in the Tigranes-Artavzdes pit area is offset by the influence of increased recharge in the vicinity of the Erato pit, resulting in a small net change in spring flow. It is likely that the influence of these factors will affect different areas of the mountain differently, and springs to the east and west of Tigranes-Artavazdes are likely to show a reduction in flow, whilst those in the vicinity of Erato may show an increase in flow. The influence of springs surrounding the Tigranes-Artavazdes pit is reduced in the scenario considering infiltration from the Arshak pit at the baseline recharge rate. Model pathlines suggest that infiltration from the base of the Erato pit in closure will result in limited localised discharge to the high mountain springs with most flow within the groundwater system beneath the lower elevations on Amulsar.

The model simulates annual average steady-state conditions. The results therefore potentially suggest that some springs which currently flow at a very low rate during winter, particularly in the vicinity of Tigranes-Artavazdes, may become ephemeral (dry during the winter months) at the end of mining.

In the BRSF, the reduction in recharge results in a decrease in the water table elevation in the long-term during operation and closure, particularly in the southern portion of the site, such that groundwater discharge may no longer occur in the headwaters of this catchment in post-closure. Discharge from springs in the valley west of the BRSF are also reduced in the post-closure scenario by between 14% and 20% in comparison to baseline conditions, dependent on the post-closure leakage rate. Discharge from these springs is sensitive to the amount of recharge in the BRSF footprint.

The model predicts that groundwater discharge to the stream in the valley east of the BRSF will decrease from an annual average of 8.7 L/s to between 6.9 L/s and 7.8 L/s in post-closure, a decrease of between 11% and 21%. Variation in the predicted post-closure discharge is the result of response of groundwater heads in this area to leakage from the BRSF: lower leakage from the BRSF in closure will result in a decrease in groundwater levels in the valley east of the facility, reducing groundwater discharge to the springs and stream in this valley. Modelling indicates that spring flow and groundwater discharge in the valley east of the BRSF is also sensitive to recharge in the BRSF area.

5.5.3.2 Change in Hydraulic Heads, Pit Area, BRSF and HLF

The change in hydraulic head at wells used as observations points in the groundwater model between the baseline and post-closure scenarios is illustrated in Figure B21 and B22 (Appendix B).

The greatest change is observed on the southern side of the BRSF, where a long-term progressive decrease in groundwater level of between 50 m and 60 m is predicted in the post-closure scenario, and between 40 m and 50 m in the sensitivity analysis scenario. A significant change is also predicted on the southern side of the Tigranes-Artavazdes pit, where long-term steady state post-closure groundwater levels are approximately 40 m lower than baseline, and 20 m to 25 m lower than baseline in the sensitivity analysis. Change in groundwater elevations is likely to occur progressively through operation and in the decade following closure. Model results suggest that the impact of backfilling of the Tigranes-Artavazdes pit on groundwater heads beneath the peak, and therefore springs flows, will be greater in post-closure than during operation. This may be an artefact of the model, as the underestimation of heads beneath Tigranes-Artavazdes is likely to result in an underestimation of impacts on local groundwater heads and spring flows.

An increase in groundwater elevation is observed in the vicinity of the Erato pit as a result of increased recharge; between 9 m and 16 m increase in head is predicted at DDAW007.

The groundwater flow model indicates that reduced recharge across the HLF footprint has a significant impact on groundwater heads beneath the HLF. A decrease in groundwater elevation of 13 m is observed on the southeastern boundary and in the centre of the site, reducing in wells in proximity to the main drainage to a minimum of 4 m in GGDW016. Currently perennial flow in the stream within the HLF site is not observed. However, a reduction in groundwater levels surrounding the site may result in a reduction in seasonal baseflow, and to any permanent baseflow to the stream southwest of the site. Impacts on flow in this stream are discussed further in Golder (2014b).

Conditions in post-closure surrounding the BRSF are similar to those at the end of operations, with a significant decrease in groundwater levels (and therefore spring flows) in the southern portion of the BRSF footprint. Any leakage from the basal drain would reduce the groundwater level decline in the northern portion of the site.

Groundwater elevations beneath the BRSF and pit areas are sensitive to change in recharge/leakage rates during operation and closure due to their geographic location. These facilities are located along the Amulsar ridge and have little or no upgradient catchment to support groundwater flow, therefore local changes to recharge in these areas result in significant localised changes in groundwater head.

5.5.3.3 Leakage from the BRSF Basal Drain

The post-closure scenario predicts a leakage rate of between 15 m^3/day and 158 m^3/day (0.2 L/s to 1.8 L/s) from the basal drain of the BRSF in closure (the former replicating the leakage rate predicted by GRE (2014c)). The upper bound value, equates to an average infiltration rate across the facility footprint of 47 mm/yr.

The modelling completed indicates that springs to the west and east of the BRSF are sensitive to recharge in the BRSF area, as is stream flow to the east of the facility. In the event that infiltration to the facility in closure is higher than predicted by GRE (2014a, 2014c), where reductions in spring flow and groundwater discharge are predicted, the flow reduction will be less under conditions of higher leakage from the BRSF.

5.5.3.4 Change in Regional Groundwater Discharge

The modelling indicates that at the end of mining there could be a small decrease in the amount of baseflow discharging to the Arpa, Darb and Vorotan rivers and their tributaries draining from Amulsar. The decrease is estimated to be 2% of the current baseflow deriving from the catchment within the Project Area in the Vorotan River, 2% in the Arpa River and 1% in the Darb River. The predicted change in baseflow shows only minor sensitivity to uncertainty in the leakage rates from the mine facilities in closure.

Groundwater discharge to the Spandaryan-Kechut tunnel is predicted to decrease by between 1% and 3% in the post-closure scenario.

Groundwater discharge to the tributary of the Darb River southeast of the HLF is predicted to decrease by 2% in post-closure.

Groundwater discharge to the Madicenk springs is predicted to decrease by between 7% and 8% in post closure. This range indicates some sensitivity to the rate of leakage from the BRSF (and therefore change in groundwater elevation beneath the BRSF and the hydraulic gradient in the Basalts feeding these springs).

5.5.3.5 Groundwater Flow Pathlines

Groundwater flow from each of the facilities in the post-closure scenario is similar to the baseline case (Figure B23, Appendix B). Leakage from the BRSF flows northwest toward the Arpa River. The drain simulated within the BRSF in the closure sensitivity analysis has the potential to both capture or discharge water in the model. As the base of the site lies above the water table in the central and northern areas, there is a net discharge from this drain. Leakage from the HLF flows to the west toward the Arpa River.

Leakage from the base of the Artavazdes-Tigranes pit in closure infiltrates to the water table and the migrates to the east toward the Vorotan River and to the west to the Darb River. Infiltration to the base of the Erato pit flows in an approximately radial pattern over a large area, with discharge to the Arpa, Darb and Vorotan Rivers.

Simulated particles released from the mine facilities do not discharge to the Spandaryan-Kechut tunnel. Particles pass under the tunnel (i.e., a deep groundwater flow path) and discharge to streams and rivers at lower elevations. This suggests that water quality in the tunnel may not be affected by discharge from the facilities.

5.5.4 Sensitivity Analysis

A sensitivity analysis was undertaken to assess the sensitivity of the baseline model with regard to those parameters identified to be most sensitive to the model calibration. The sensitivity of the model to the following parameters was determined:

- Colluvium hydraulic conductivity - evaluation of a 10-fold increase and decrease in hydraulic conductivity from the final calibration value;
- Argillic andesite hydraulic conductivity - evaluation of a 10-fold increase and decrease in hydraulic conductivity from the final calibration value; and
- Recharge, evaluation of the influence of an increase and decrease of 100 mm/yr from the final calibration value.

The changed in predicted hydraulic head in each sensitivity analysis in comparison to the baseline case is presented in Appendix C. Change in predicted flow in the Spandaryan-Kechut tunnel, and change in predicted head beneath Tigranes-Artavazdes and Erato peaks is shown in Table 7.

Table 7: Sensitivity Analysis Results

Sensitivity Analysis*	Flow in the Spandaryan-Kechut Tunnel (m^3/s)	Head beneath Tigranes-Artavazdes (masl)	Head beneath Erato (masl)
Base case	0.137	2,720	2,700
SA1 – colluvium, lower permeability	0.144	2,880	2,880
SA2 – colluvium, higher permeability	0.097	2,370	2,350
SA3 – argillic LVA, lower permeability	0.113	2,880-2,930	2,730
SA4 – argillic LVA, higher permeability	0.150	2,490	2,480
SA5 – lower recharge	0.033	2,370-2,380	2,340 – 2,360
SA6 – higher recharge	0.257	Above ground surface	Above ground surface

* *Hydraulic conductivities were increased and decreased by a factor of 10; recharge was increased and decreased by 100 mm/yr*

The model is most sensitive to the recharge rate. Changing recharge affects the head across the model domain, but has a greater influence at higher elevations (greater distance from the constraining boundaries) than at lower elevations. Decreasing the recharge value by 100 mm/yr has a greater influence on heads than increasing recharge by 100 mm/yr, with an average (root mean square) decrease of 188 m in scenario SA5 and an average increase of 137 m in scenario SA6. Groundwater flow in the model is proportional to the square of the infiltration rate per unit area. Therefore, increasing the recharge rate by 100 mm/yr (1.5 times the baseline rate across much of the model domain) approximately doubles discharge to the Spandaryan-Kechut tunnel, whilst decreasing by 100 mm/yr (halving across much of the model domain) results in a 4-fold decrease in flow.

The model is sensitivity to hydraulic conductivity of the colluvium and argillic LVA units. Changing the hydraulic conductivity of the colluvium by an order of magnitude results in an increase in head of up to 190 m (for a decrease in permeability), or a decrease in head of over 300 m at observation point at high elevations (for an increase in permeability). Decreasing and increasing the hydraulic conductivity of the argillic LVA unit by an order of magnitude results in an increase in heads of up to 240 m, or decrease in head of over 220 m, respectively in observation points at high elevations. The distribution of the sensitivity effects differs. Changing the hydraulic conductivity of the argillic LVA unit strongly influences heads in the mountain area, but does not significantly influence heads on the lower plains (e.g. in the vicinity of the HLF), where the fresh LVA outcrops. Changing the hydraulic conductivity of the colluvium has a moderate influence at low elevations (resulting in changes in the tens of metres), but a much greater influence at high elevations. It is likely that heads on the lower plains (such as the HLF area) are similarly highly sensitive to the hydraulic conductivity of the fresh LVA unit, though at lower elevations the degree of sensitivity is less due to the effect on the fixed boundary heads.

The predicted discharge from the Spandaryan-Kechut tunnel does not respond significantly to a decrease in hydraulic conductivity of the colluvium (showing only a 5% increase in response to a 10-fold change), but has a greater response to an increase in hydraulic conductivity (showing a 30% decrease in response to a 10-fold change). Discharge from the tunnel decreases with increased hydraulic conductivity; this is because a less proportion of the tunnel length is below the water table in the higher permeability scenario. Similarly, a decrease in colluvium hydraulic conductivity generally raises the water table, increasing the length over which discharge to the tunnel occurs. Discharge from the Spandaryan-Kechut tunnel is not highly sensitive to the assumed hydraulic conductivity of the argillic LVA. A 10-fold change in hydraulic conductivity of the LVA results in a 10% increase or 18% decrease in tunnel discharge.

The high sensitivity of heads in the vicinity of the ore bodies to changes in both hydraulic conductivity and recharge means that estimates of pit inflow is very sensitive to these parameters. In scenarios where the water table is below the pit base (SA2, SA4, SA5) the models do not predict any groundwater inflow to the pits. In scenarios where the heads surrounding the pits are much higher than in the baseline model (SA1, SA3 and SA6) estimates of groundwater inflow would be greater. However, as monitoring data for the groundwater elevation surrounding the peak indicates that the water table is approximately 2,625 (+/- 20) masl below Erato, and 2,750 (+/- 20) masl below the southern portion of Tigranes-Artavazdes and 2,755 (+/- 20) masl beneath the western portion of Tigranes-Artavazdes, a sensitivity analysis to generate quantitative ranges of inflow in these scenarios has not been undertaken.

Leakage from the HLF and BRSF facilities will be a function of the performance of the engineered liner and the infiltration rates to these facilities. The possible range of leakage from the HLF has been evaluated in the HLF groundwater risk assessment (Golder, 2014b). The sensitivity of leakage from the BRSF to the assumed basal liner hydraulic conductivity of between $1x10^{-9}$ m/s and $1x10^{-8}$ m/s has been evaluated in the post-closure scenarios described in Section 5.5.

6.0 CONCLUSIONS

A 3-D steady state saturated flow groundwater model has been developed using the code FEFLOW to simulate groundwater flow in the vicinity of the proposed Amulsar mine development under baseline conditions. This model has then been used as a basis for the development of a steady state model to represent post-closure conditions following completion of the proposed development, and a transient model to consider groundwater inflows into the open pits at their maximum extent.

The groundwater model represents five hydrogeological units distributed across the project area. The model includes a highly simplified representation of the faulted LVA/VC sequence which hosts the ore bodies, represented as the VC unit.

6.1 Baseline Conditions

The model is able to reasonably reproduce key aspects of the groundwater flow system, including:

- Radial flow away from the Amulsar Mountain ridge, with flow to the east (to the River Vorotan) and west (predominantly to the River Darb) from the Tigranes-Artavazdes pit, and flow predominantly to the west to the River Arpa from the Erato pit. The model suggests that where flow does occur east from Erato, this groundwater enters the Arpa catchment;
- Flow initially northwest from the BSRF site before turning west to discharge predominantly to the Arpa River downstream of the Kechut Reservoir;
- Flow westward from the HLF toward the Arpa River;
- A water table with groundwater elevations 2,700 masl and 2,740 masl beneath the Amulsar ridge, extending northeast to southwest largely mirroring topography;
- A shallow near-surface water table to the west, south and northwest of the Amulsar ridge with discharge to perennial springs on the flanks of the ridge, and in the valley east of the BSRF site. The model represents the groundwater elevation at surface in the base of the BRSF site;
- Groundwater discharge to the stream passing along the base of the HLF valley consistent with the observed heads, which are very close to surface in proximity to the stream, local discharge to the stream with flow at depth and beneath the northern portions of the HLF toward the Arpa River;
- A deeper water table in the basalts to the northwest and west of the Amulsar ridge; and
- Discharge from springs at the base of the Basalt sequence adjacent to Kechut reservoir.

The calibrated groundwater model indicates that observed groundwater levels could be sustained by a groundwater recharge rate of approximately 200 mm/yr (250 mm/yr in the BRSF site and adjacent valley) across the project area, combined with slightly lower average field scale permeabilities than indicated by hydraulic testing data. This suggests that observed groundwater levels in intact wells along the Amulsar ridge record groundwater levels representative of the water table.

The groundwater model suggests that the Spandaryan-Kechut tunnel is close to the natural water table elevation, intersecting, but not lying significantly below the water table. The tunnel therefore receives groundwater discharge but from a limited and localised area. Groundwater flow from or below the proposed facilities does not discharge to the tunnel.

The groundwater model calibration to observed heads is highly sensitive to the hydraulic conductivities of the colluvium and argillic LVA units and heads in the HLF area and at lower elevations is sensitive to the hydraulic conductivity of the fresh LVA. The model is also highly sensitive to recharge. The predicted discharge from the Spandaryan-Kechut tunnel is moderately sensitive to the hydraulic conductivity of the colluvium (due to its influence on groundwater elevation and therefore the length of the tunnel which is saturated) and highly sensitive to recharge. Although the observed heads surrounding the Amulsar ridge could be matched with alternative combinations of hydraulic conductivity(within the constraints on estimates in each unit), introducing a lower hydraulic conductivity value for the colluvium unit would require a reduction in recharge to match observed heads. This would not provide a result consistent with observed baseflows. Overall, the model calibration is relatively well constrained and the model replicates key features of the hydrogeological regime within the Project Area.

6.2 Operational Conditions

There are three sources of groundwater inflow to the pits during operation:

1) Seasonal perched water inflow from snow melt which infiltrates to ground within the area immediately surrounding the pits and that may flow through the subsurface towards the pit and reach the pit sump.

2) Transient inflows during excavation from perched water bodies supported within the complex faulted geology of the pit.

3) Year-round inflow from groundwater where the bases of the pits extend below the water table. This may occur in the base of both the Artavazdes and Tigranes pits which are interpreted to be mined to a depth of about 45 m to 70 m, respectively, below the existing water table. The base of the Erato pit is interpreted to be at or slightly above the existing water table.

The regional groundwater flow model is not able to represent the hydrogeological regime surrounding the ore bodies with sufficient accuracy to predict rates of permanent groundwater inflow during mining. Similarly, the occurrence of isolated permanent and semi-permanent perched water bodies within the faulted geological sequence cannot be readily predicted and must be dealt with as an operational issue. An estimate has been made of likely rates of seasonal perched water to the pits at their final extent following the spring snow melt, and in late autumn, indicating a peak inflow rate during the spring months of between 25 m^3/hr and 31 m^3/hr to the Erato pit 45 m^3/hr to 56 m^3/hr to the Tigranes-Artavazdes pit.

Operational scenario results suggest that pit dewatering will not permanently dry out any of the observed perennial springs found at a lower elevation than the pit base. However, dewatering may result in a minor reduction in flow in these springs, which may potentially lead to some springs becoming ephemeral with dry periods in the winter.

Pit dewatering is predicted to reduce groundwater elevations by up to 30 m in wells adjacent to Erato, and of up to 20 m in wells adjacent to Tigranes-Artavazdes. Reduced recharge across the HLF footprint has a significant impact on groundwater heads beneath the HLF. A reduction of 10 m is observed on the southeastern boundary, decreasing in wells in proximity to the main drainage to a minimum of 3 m in GGDW016. Reduced recharge in the BRSF site may result in a long-term progressive decrease in heads of up to 60 m in the southern portion of the BRSF. This is likely to influence perennial spring discharges in the south of the BRSF footprint, may result in the complete cessation of discharge from these springs as the water table is predicted to drop below ground surface in this area by the end of operations.

Modelling indicates that in the long-term, low recharge to the BRSF footprint will have a localised significant effect on spring and stream flows. Discharge to springs west of the site are predicted to experience a long term reduction in flow of 36% and the stream east of the site is predicted to experience a reduction in baseflow of 24%. However, such effects are likely to occur over a period of years and may occur in closure rather than during operation. Aggregated post-closure effects and sensitivity to higher leakage rates than predicted by GRE (2014c) are evaluated as part of the post-closure scenario.

Change in groundwater recharge during operations is predicted to have a minor impact on groundwater base flow to the Vorotan, Darb and Arpa Rivers. Model results indicate an approximately 1% to 3% decrease in groundwater baseflow from the catchment area which lies within the Project Area as a result of activity during operations.

6.3 Post-Closure Conditions

In post-closure, the scenario results suggest that, over the Amulsar area, a reduction in spring flows in the southern portion of the ridge due to backfilling of the Tigranes-Artavazdes pit and placement of a store and release evaporative cover will be balanced by increased recharge in the Erato pit, enhancing spring discharge in the northern portion of the ridge. Model results suggest that changes in infiltration in the pit areas will not permanently dry out any of the observed perennial springs found at a lower elevation than the pit floor. However, a reduction in groundwater flow may result in a minor reduction in flow in these springs, which may potentially lead to some springs becoming ephemeral with dry periods in the winter.

Backfilling of the Tigranes-Artavazdes pits is predicted to reduce groundwater elevations by up to 40 m in wells surrounding the pits. Increased recharge in the vicinity of the Erato due to the capture of surface water runoff within the pit is predicted to increase the water table in this area by more than 10 m.

Reduced recharge across the HLF footprint has a significant impact on groundwater heads beneath the HLF. A long-term progressive groundwater level decrease of up to 13 m is predicted on the southeastern

boundary, reducing in wells in proximity to the main drainage to a minimum of 4 m in GGDW016. Reduced recharge in the BRSF site may result in a decrease in heads of up to 60 m in the southern portion of the BRSF. This is likely to influence perennial spring discharges in the south of the BRSF footprint, and may result in the cessation of discharge from these springs as the water table will drop below ground surface in this area in closure.

Unsaturated flow modelling (GRE, 2014c) has predicted that the rate of leakage from BRSF in closure will be approximately 14.6 m^3/day, and this flow is replicated in the post-closure scenario. The post-closure sensitivity analysis scenario has considered the effect of accumulation of water in the basal drainage layer of the BRSF to a depth of 0.1 m over an area of 25 m either side of the main basal drain if constructed with a maximum basal liner permeability between $1x10^{-9}$ m/s. Under these conditions, an annual average leakage of 158 m^3/day is predicted from the BRSF in closure. This rate is considered to be an upper bound on leakage from the facility based on the water balance (GRE, 2014a), which indicates infiltration rates to the facility are likely to be low. The impact of lower leakage rates from the BRSF over the long-term is evaluated as part of the closure scenario.

Change in groundwater recharge following closure and reclamation of the mine facilities is predicted to have a minimal impact on groundwater baseflow to the Vorotan, Darb and Arpa Rivers. Model results indicate a decrease in groundwater baseflow deriving from catchments within the Project Area of between 1% and 2% in the Vorotan River, 2% in the Arpa River and 1% in the Darb River.

The regional groundwater flow model indicates that leakage from the BRSF and mine pits will not discharge to the Spandaryan-Kechut tunnel. Simulated groundwater flow pathlines pass under the tunnel and continue downgradient to discharge to streams and rivers at lower elevations. This suggests that water quality in the tunnel may not be affected by discharge from the facilities.

7.0 REFERENCES

1) Domenico, P A and Schwartz, F W 1990. *Physical and Chemical Hydrogeology*, 1st Edition. J Wiley & Sons, New York.

2) Golder, 2014a. Technical Memorandum. Amulsar Gold Project, Post Closure Water Balance, Erato Pit. 14514150095.503 Version B.4. 4 August 2014.

3) Golder, 2014b. Amulsar Gold Project, Hydrogeological Risk Assessment, Proposed Heap Leach Facility. Ref 14514150095.509 Version B.1. August 2014.

4) GRE, 2014a. Technical Memorandum, Amulsar BRSF Seepage Model. Ref 13-1064, 14 July 2014.

5) GRE, 2014b. Technical Memorandum, Amulsar Pit Seepage Model, Ref 13-1064. 7 July 2014.

6) GRE, 2014c. BRSF Seepage Source Term for the Regional GW Model. Ref 13-1064. 5 August 2014.

7) Johnson, A I 1967. *Specific yield — compilation of specific yields for various materials*. US Geological Survey Water Supply Paper 1662-D.

8) Holcombe, R., 2013. Amulsar 3D Geological Model Revision: Summary and Resource Implications November 2013.

9) Lydian International (2013a). Presentation summary entitled “Amulsar, Armenia: An IOCG Chameleon?” by Rod Holcombe, Tim Coughlin, Nick Oliver, Mentor Demi, Hayk Aloyan, Fabian Baker, and Alan Turner, dated September 2013.

10) Turner, A (2014). Discussion between Golder Associates (UK) Ltd and Alan Turner of Lydian International Ltd regarding the Lydian Geological Model, 23 May 2014.

11) USSR (1981), 1:50 000 scale geological map J-38-8-B, Масштао. In Russian, translation provided by Lydian.

Report Signature Page

GOLDER ASSOCIATES (UK) LTD

Hollie Garrick
Hydrogeologist

Carl Nicholas
Project Manager

Date: 21 August 2014

Author: Hollie Garrick/CN/sp

Company Registered in England No. 1125149
At Attenborough House, Browns Lane Business Park, Stanton-on-the-Wolds, Nottinghamshire NG12 5BL
VAT No. 209 0084 92

APPENDIX A

Model Calibration

Table A1: Amulsar Groundwater Model, Calibration Error

Lydian ID	Easting	Northing	Observed Mean Groundwater Elevation (masl)	Calculated Elevation (masl)	Error (m)	Estimated Measurement Error on Observed (m)
DDAGLP267	561252	4402552	2421	2446	25	25
DDAGLP268	561886	4402447	2369	2395	26	25
DDAGLP269	562201	4402587	2343	2349	7	25
DDAW002	562169	4402759	2335	2350	14	25
DDAW003	561490	4402807	2364	2395	31	25
DDAW004	560814	4402150	2537	2457	-80	25
DDAW005	560159	4401267	2561	2538	-24	10.5
DDAW007	561249	4399368	2695	2697	2	0 to +20.5
DDAW009	559342	4399820	2431	2509	77	21
DDAW012	560817	4401622	2563	2543	-20	2.5
DDGW005	563068	4403536	2351	2330	-21	25
DDGW006	563496	4403815	2366	2326	-40	25
DDGW007	564001	4404566	2394	2337	-58	25
GGDW002	555309	4401314	1944	1995	51	2.5
GGDW003A	556155	4401409	2009	2041	32	2.5
GGDW005	556024	4402134	2022	2038	16	1.5
GGDW007	552536	4398302	1609	1577	-33	1.5
GGDW008	552932	4398566	1642	1640	-3	1.5
GGDW009	552978	4399660	1660	1660	-1	1.5
GGDW010B	553898	4399557	1775	1776	1	1
GGDW011	554714	4399713	1891	1879	-12	0 to -10.5
GGDW012	553947	4398843	1789	1752	-37	1.5
GGDW013	553220	4399010	1651	1684	33	1.5
GGDW014	552385	4398975	1608	1613	5	1
GGDW015	554003	4399203	1775	1777	1	1.5
GGDW016	552174	4398443	1583	1567	-16	1.5
GGSC037	560790	4403154	2412	2410	-2	1.5
GGSC049	560063	4401493	2541	2492	-48	1.5
GGSC050	560542	4401892	2509	2497	-12	1.5
RCAW288	560562	4398393	2583	2621	38	20
RCAW289	560537	4398497	2584	2630	46	20.5
RCAW399	560702	4402856	2472	2432	-40	22
RCAW400	561263	4402314	2513	2472	-40	22
RCAW401	561336	4403139	2413	2420	7	20.5

Lydian ID	Easting	Northing	Observed Mean Groundwater Elevation (masl)	Calculated Elevation (masl)	Error (m)	Estimated Measurement Error on Observed (m)
RCAW403	562432	4402226	2324	2321	-4	22
RCAW286	561533	4398618	2764	2714	-50	22
RCAW287	561003	4397849	2755	2712	-44	22
RCAW404	561717	4397364	2818	2722	-96	30
RCAW405a	561640	4397780	2804	2720	-84	22
RCAW407	561625	4398616	2706	2711	5	25
RCAW408	560871	4397975	2612	2697	85	25

RMS	40.2
Abs Mean	30.9
True Mean	-6.4

Model Solution Error	$2.3x10^{-8}$		
Water Balance Error	<0.0001%		

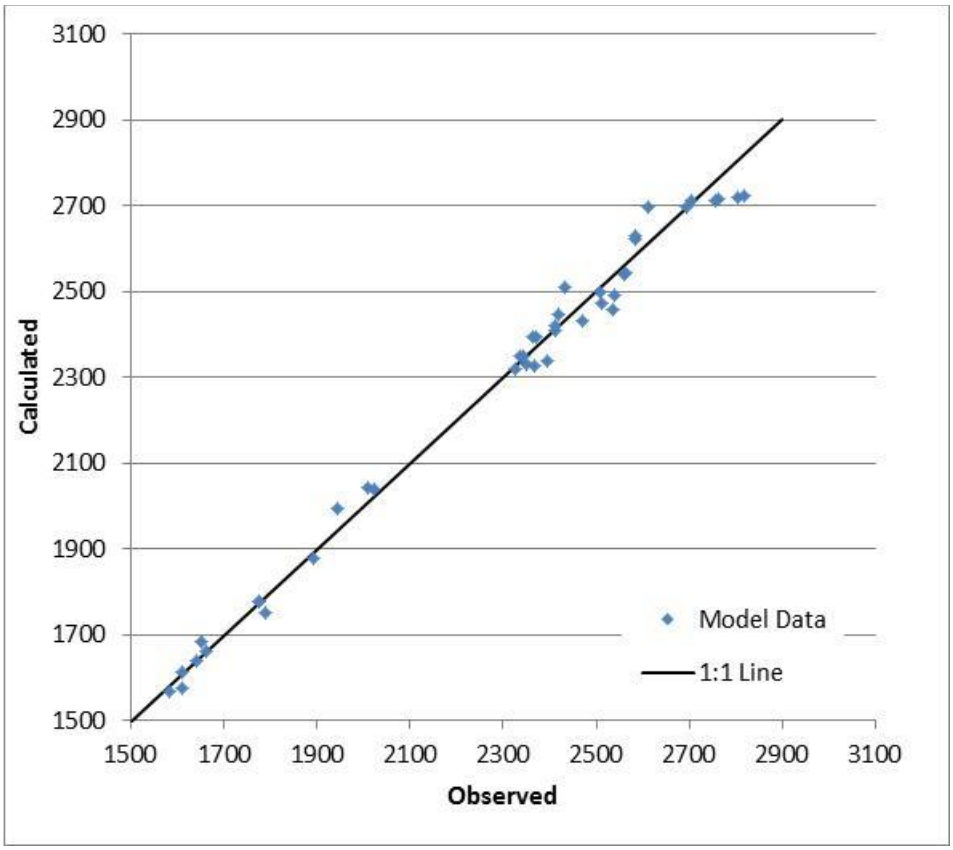

Figure A1: Groundwater Model Calibration Error Distribution

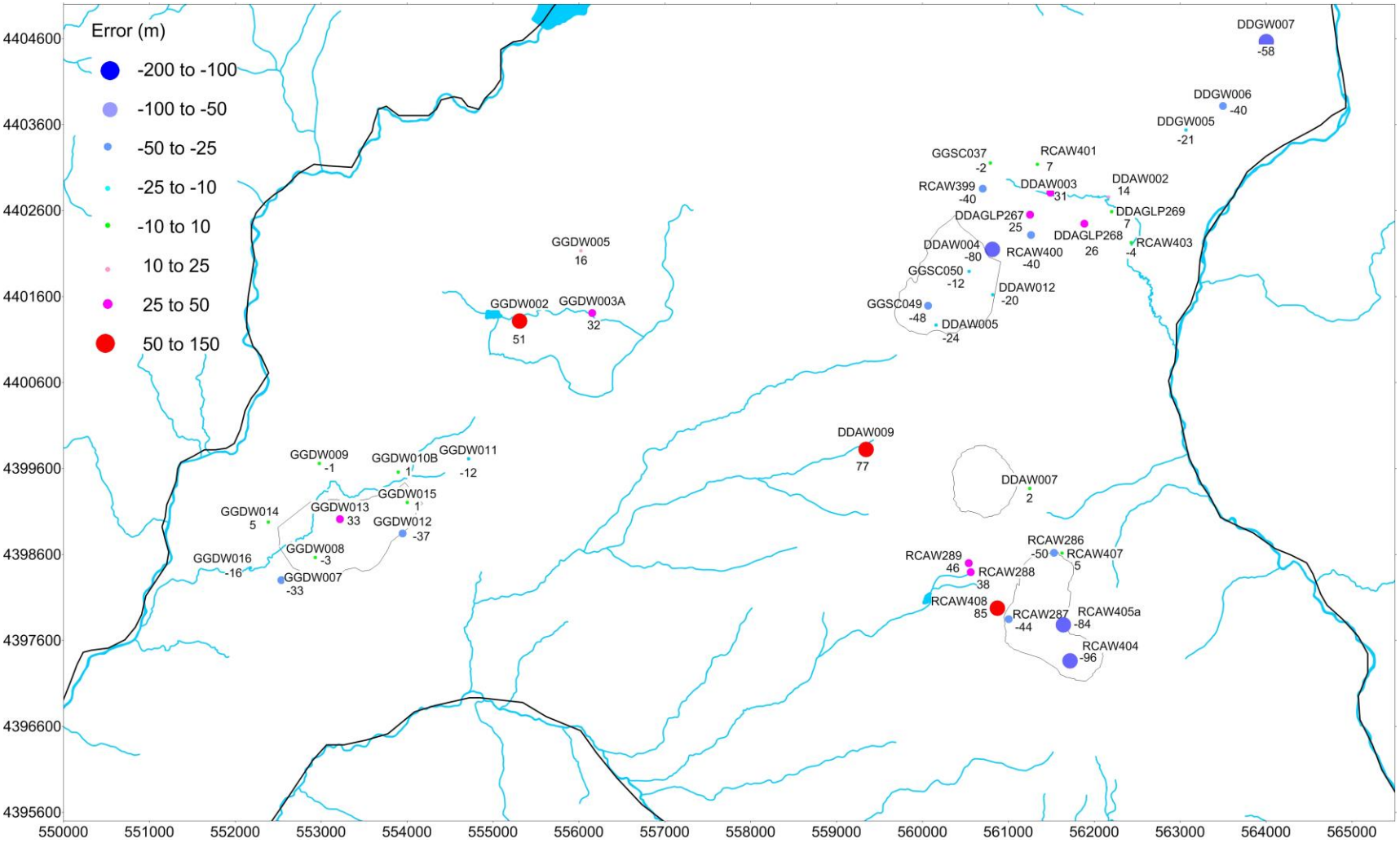

Figure A2: Groundwater Model Calibration Error

APPENDIX B

Groundwater Model Results

Baseline Scenario Model Results

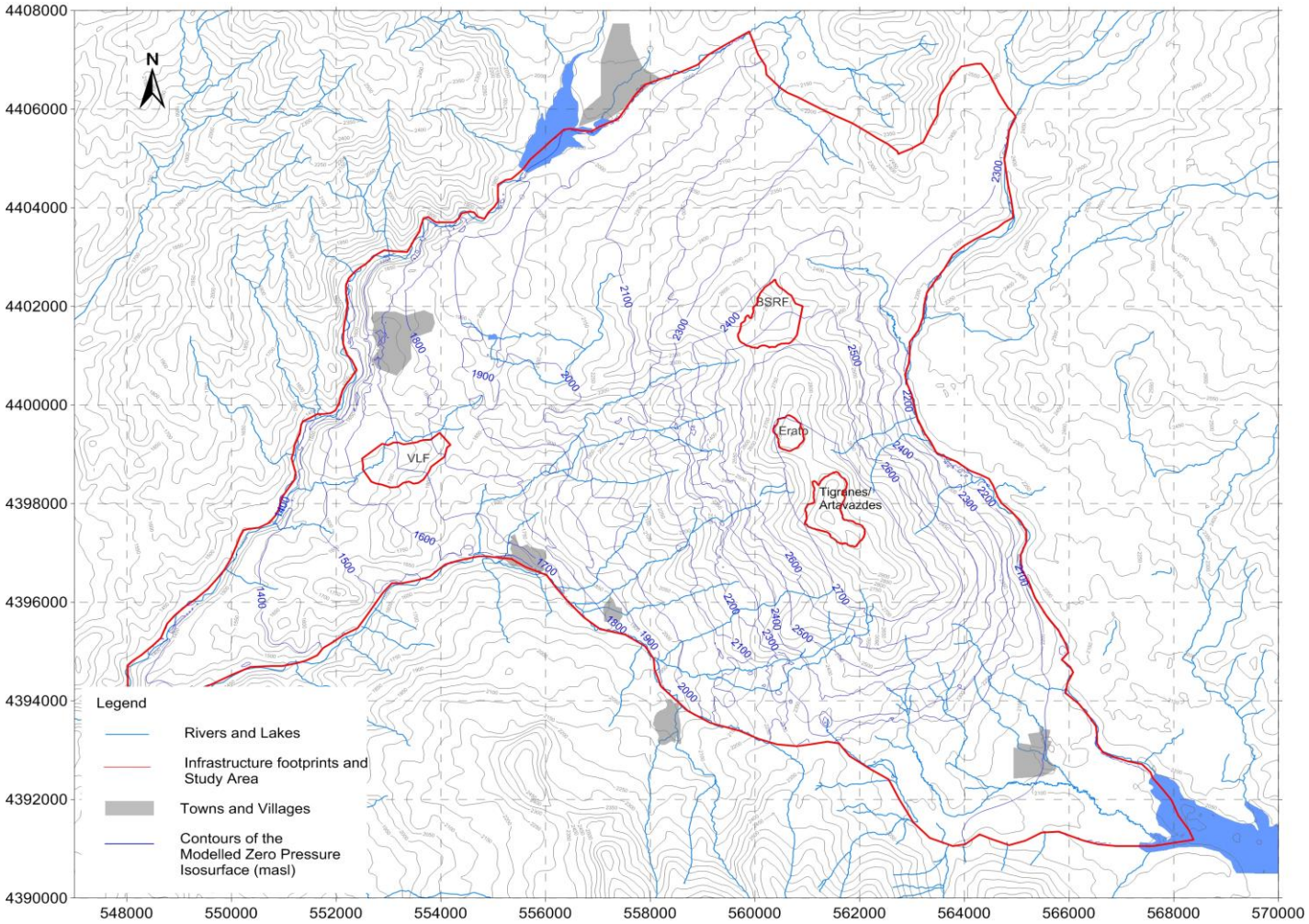

Figure B1: Contours of the Zero Pressure Isosurface, Baseline

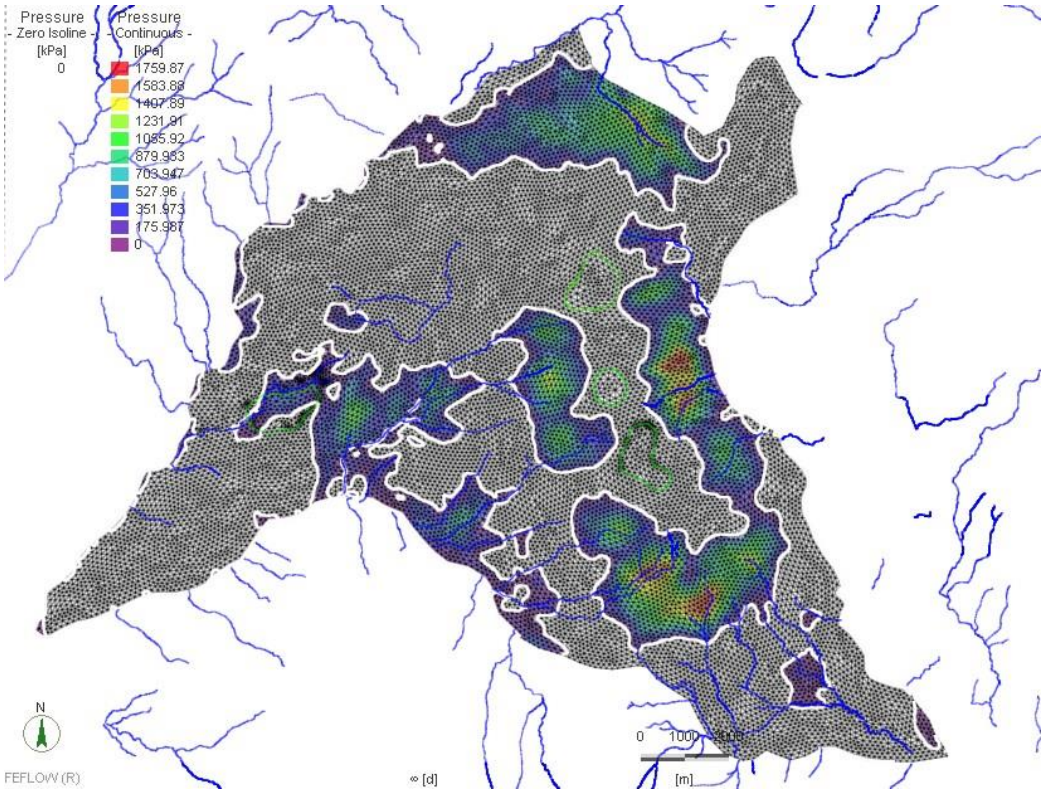

Figure B2: Zero Pressure Isosurface Intersection with Ground Surface, Baseline

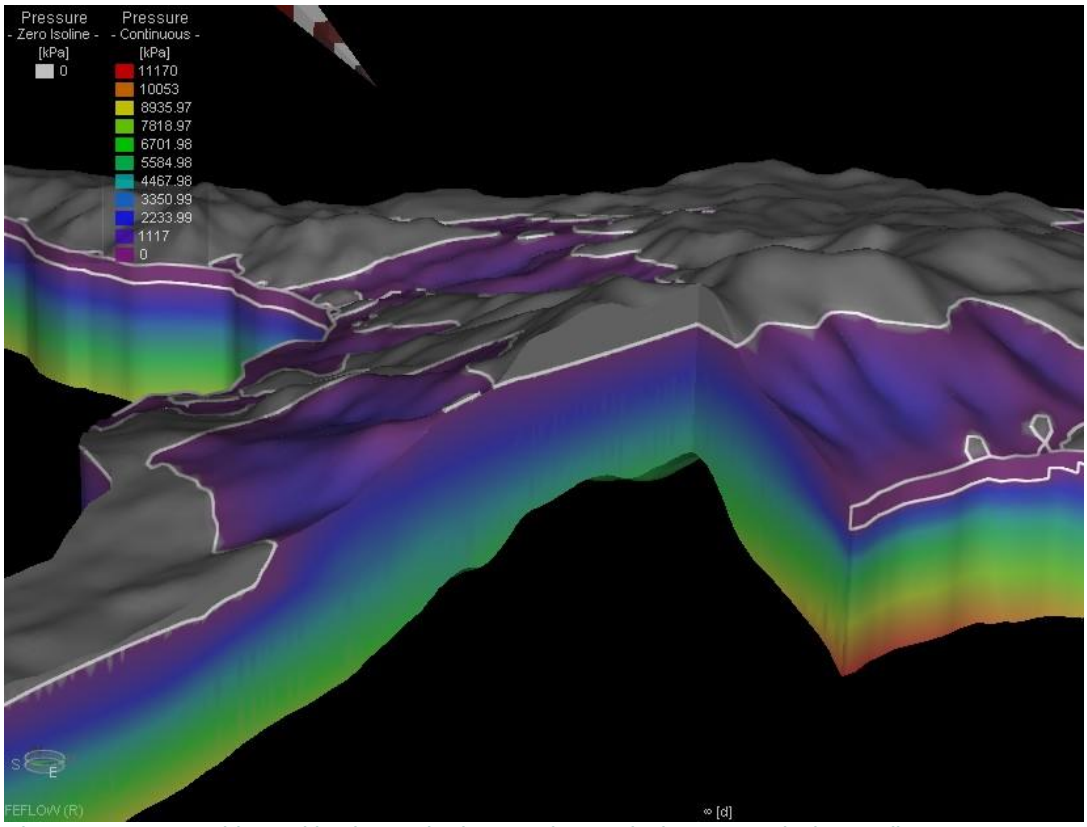

Figure B3: Water Table Position beneath Tigranes (2x Vertical Exaggeration), Baseline

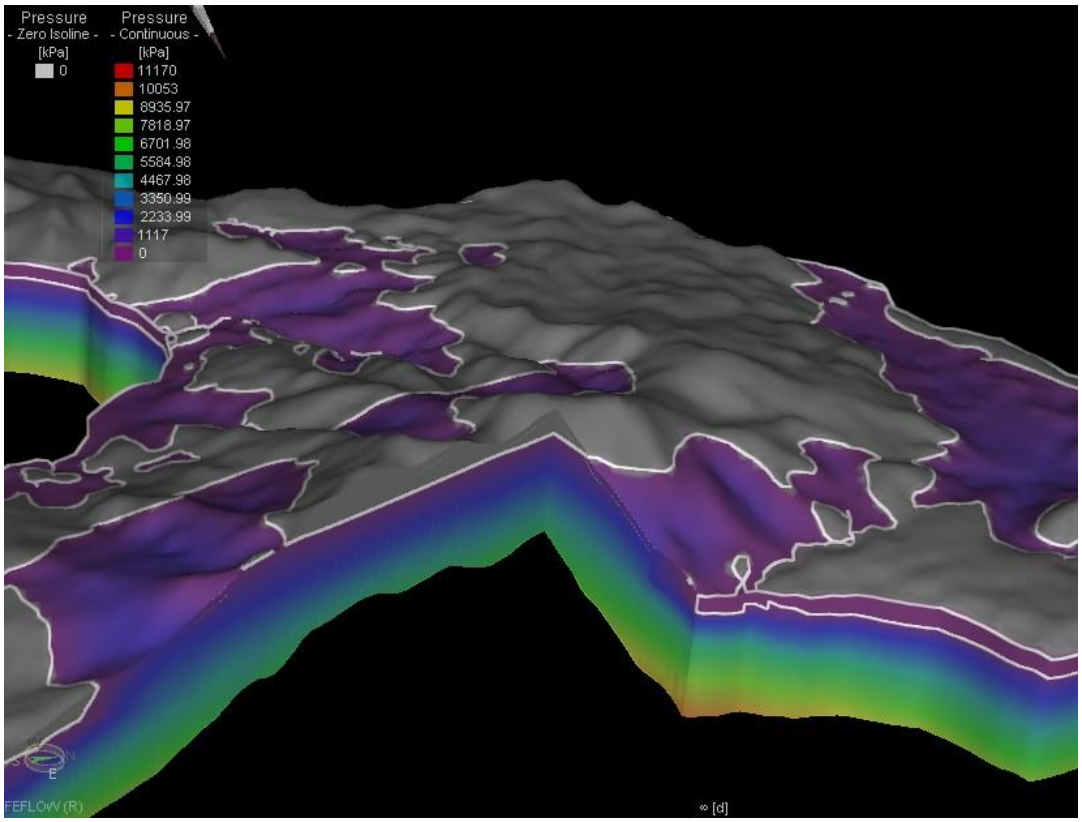

Figure B4: Water Table Positions beneath Erato (2x Vertical Exaggeration), Baseline

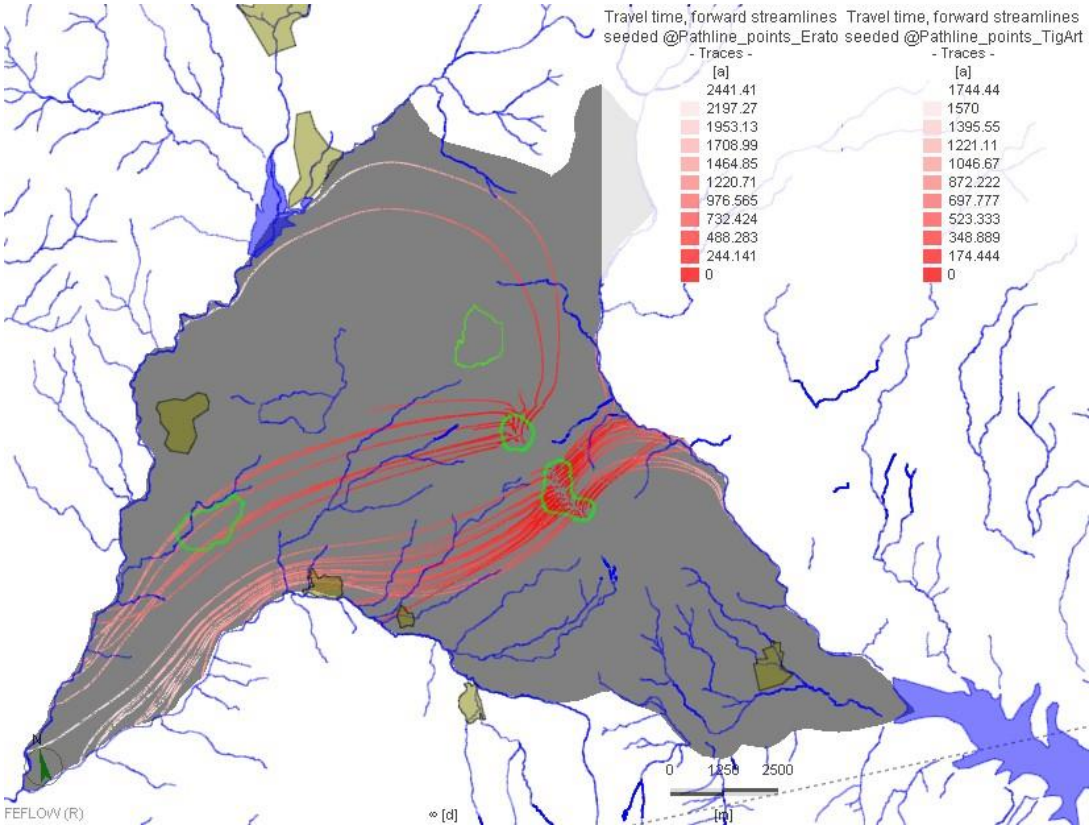

Figure B5: Pathlines, Erato and Tigranes/Artavazdes, Base Case, Plan View, Baseline

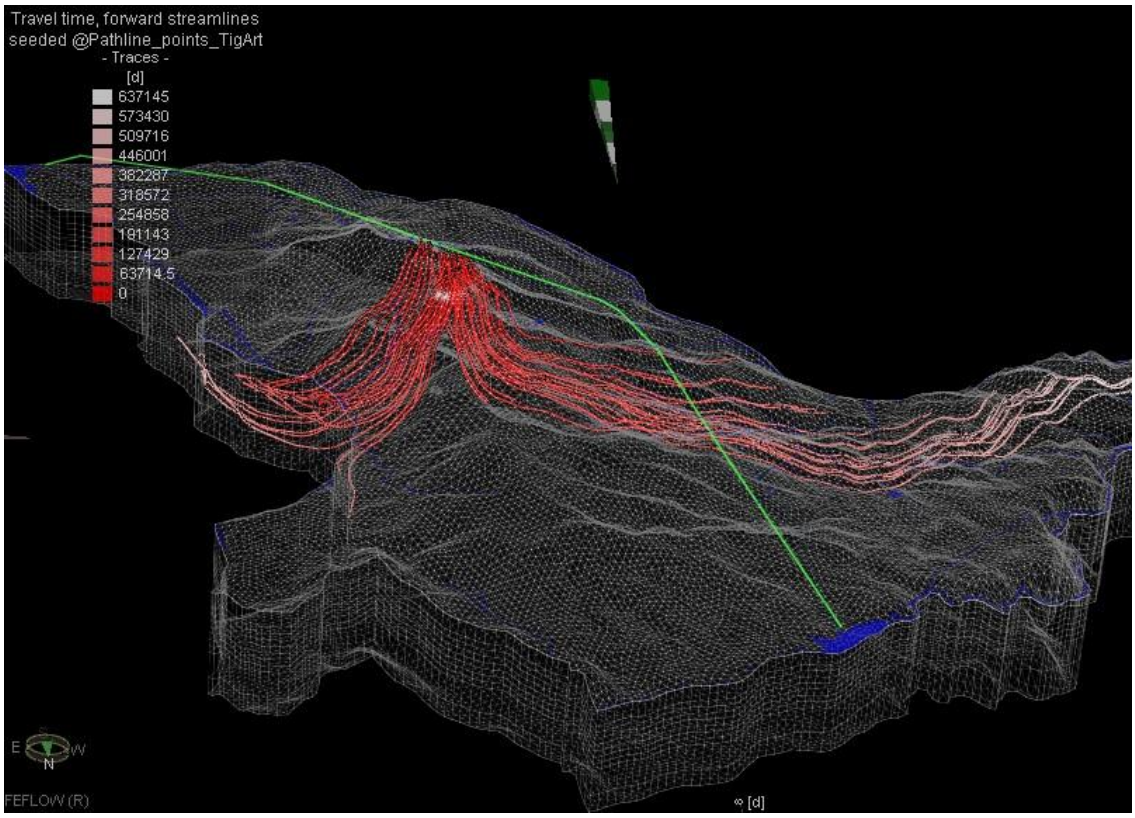

Figure B6: Pathlines from Tigranes/Artavazdes, 3D view, Baseline

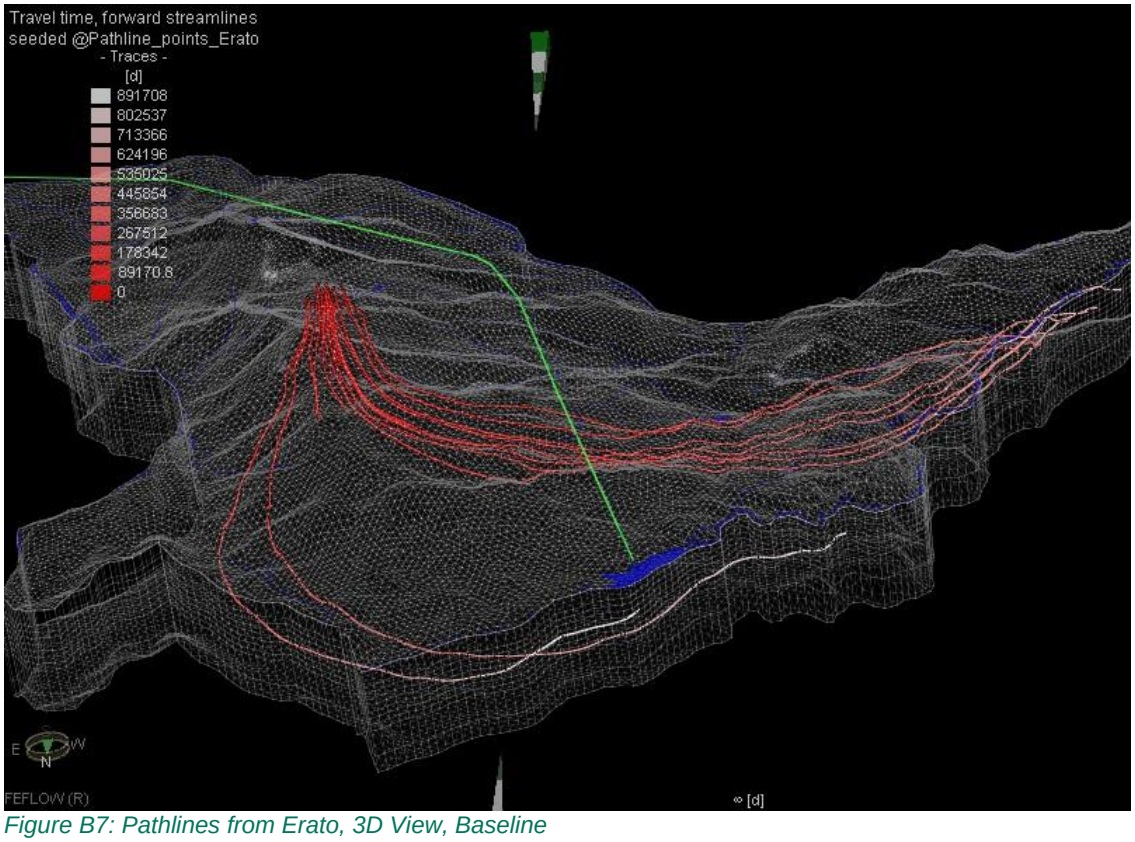

Figure B7: Pathlines from Erato, 3D View, Baseline

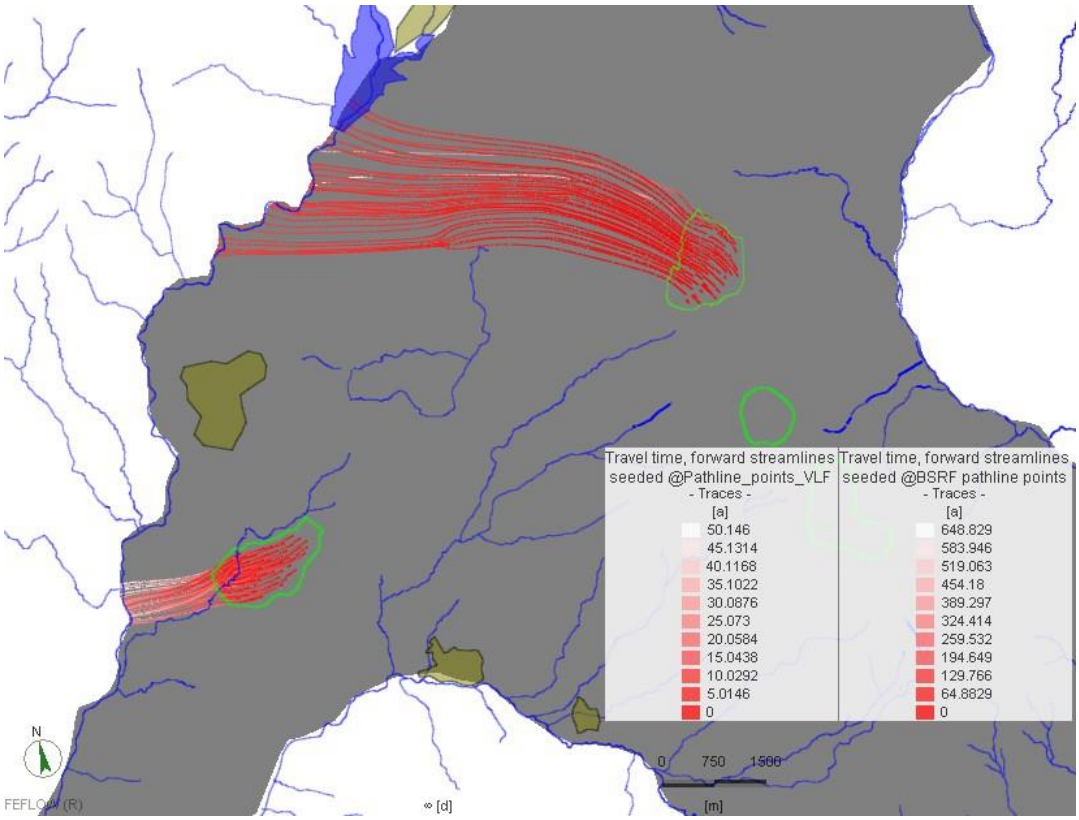

Figure B8: Pathlines from the VLF and BSRF Sites, Baseline, Plan View

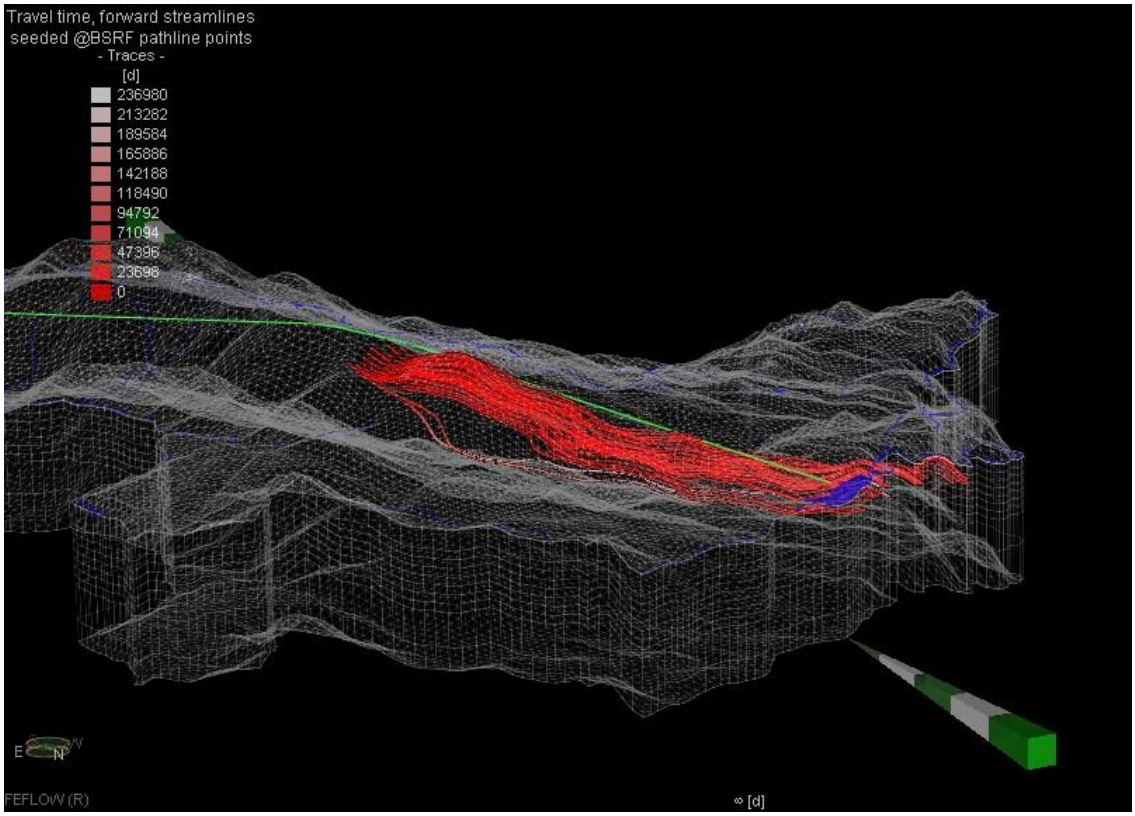

Figure B9: Pathlines from the BSRF, 3D View, Baseline

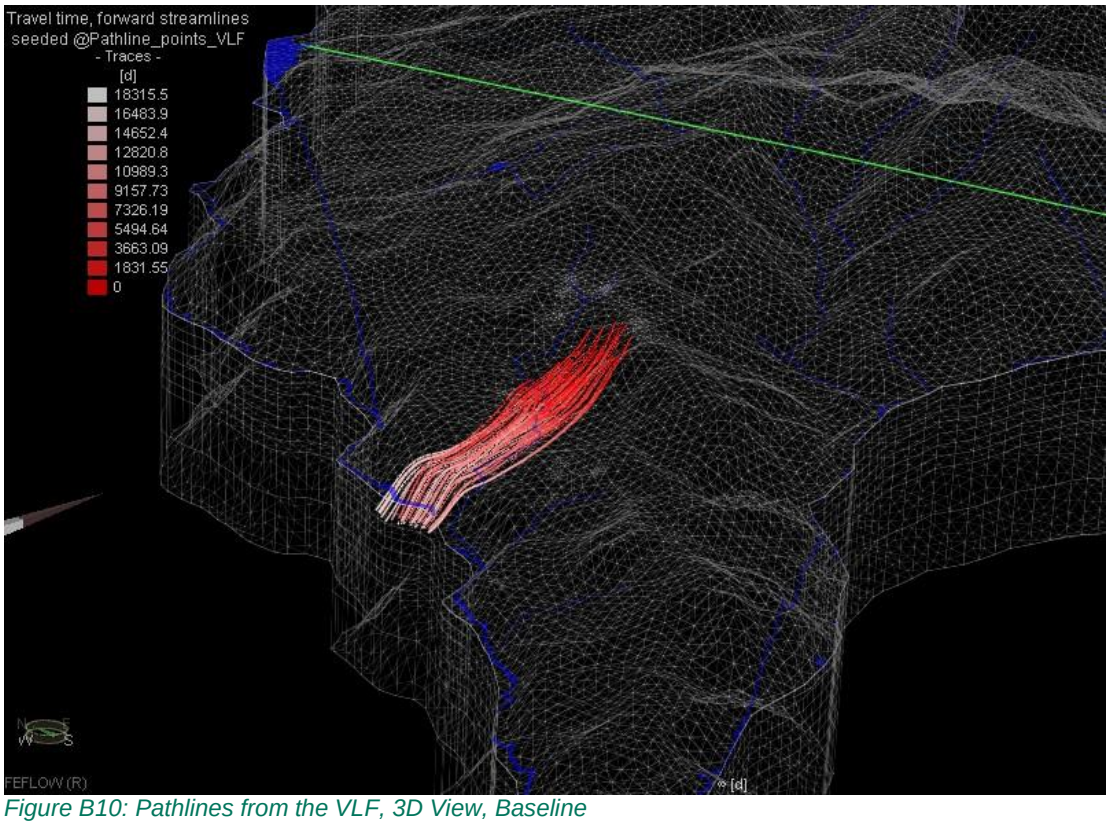

Figure B10: Pathlines from the VLF, 3D View, Baseline

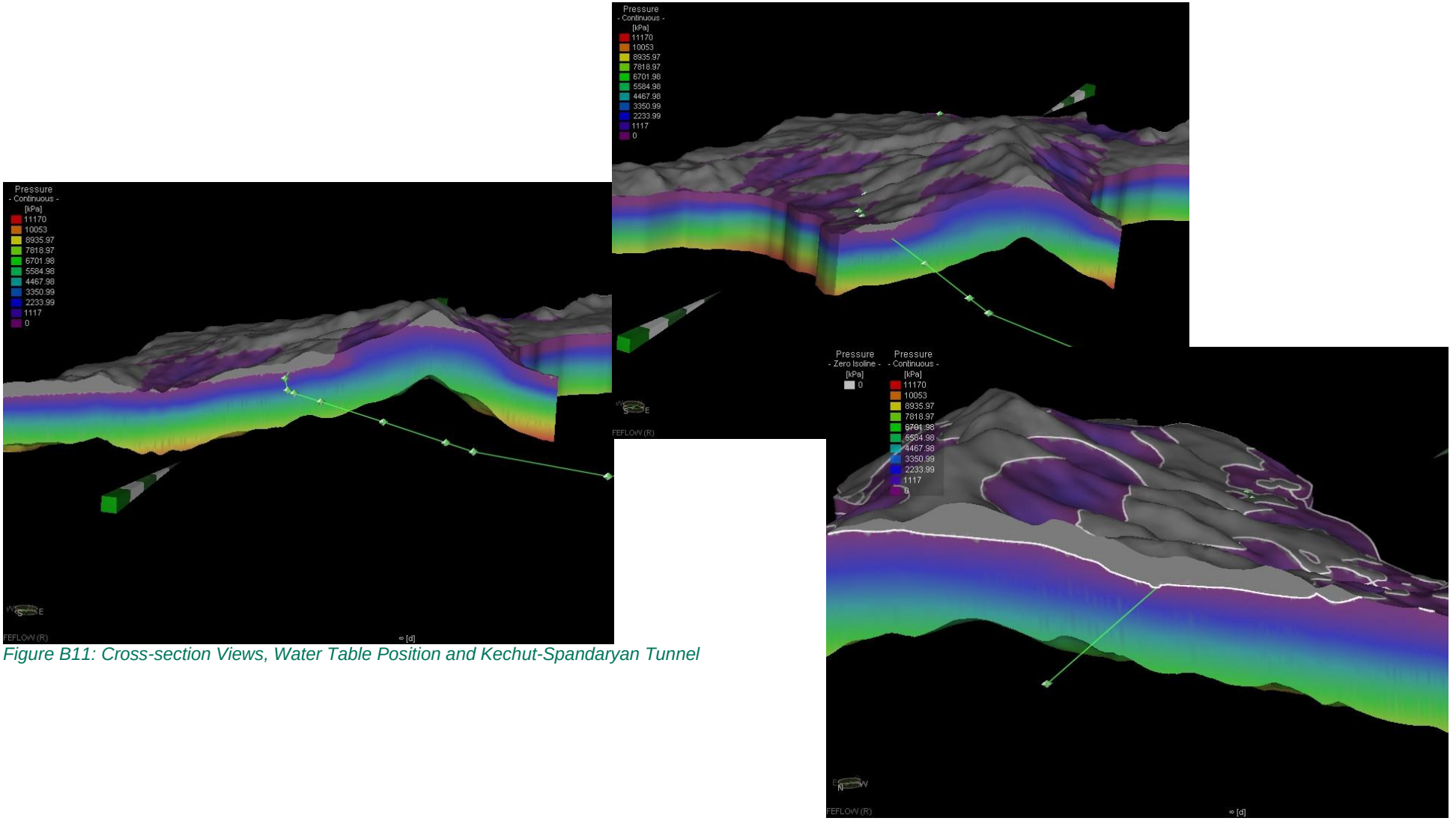

Figure B11: Cross-section Views, Water Table Position and Kechut-Spandaryan Tunnel

Operational Scenario Model Results

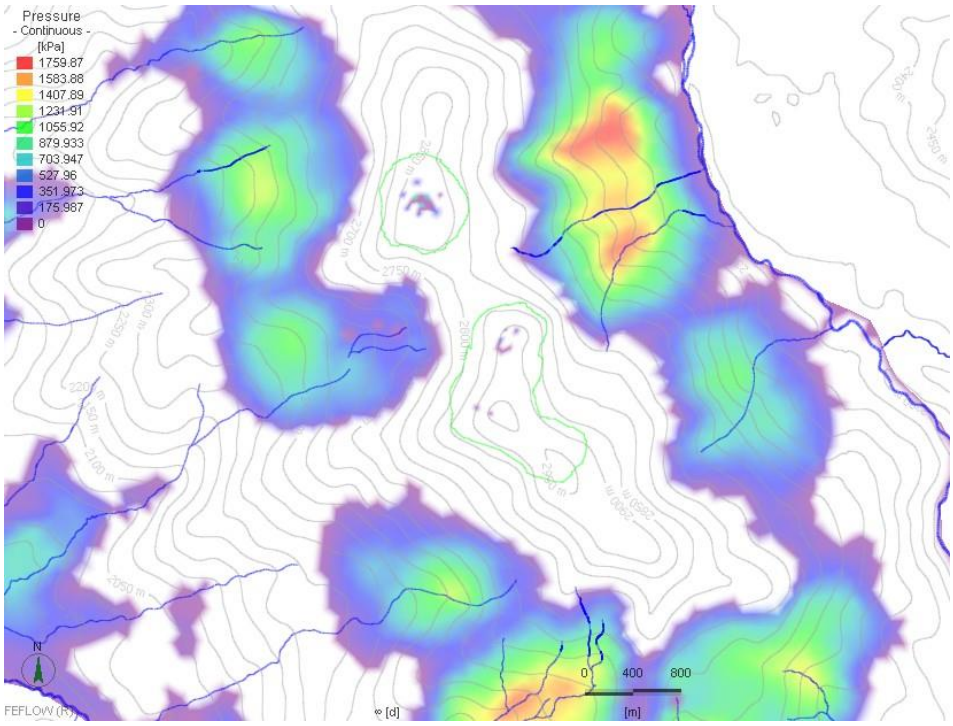

Figure B12: Extent of Saturation in and Surrounding the Pits, Baseline Steady State Water Level (No Dewatering)

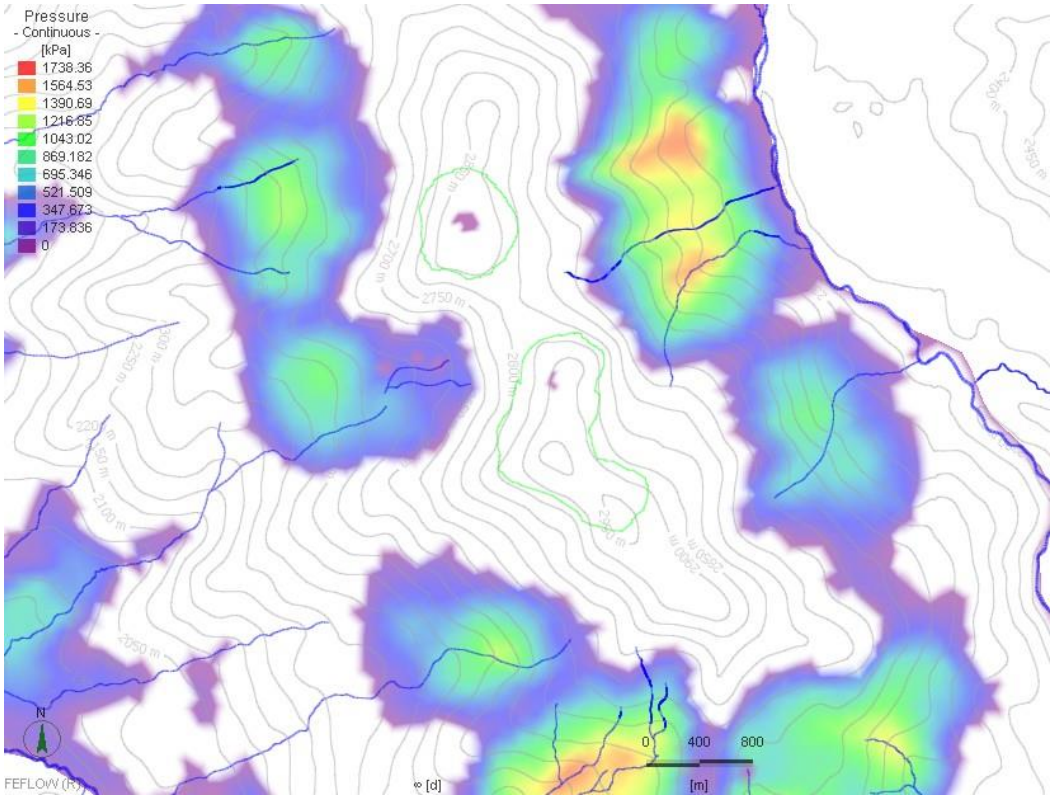

Figure B13: Extent of Saturation in and Surrounding the Pits, Operational Steady State Water Level (Active Dewatering)

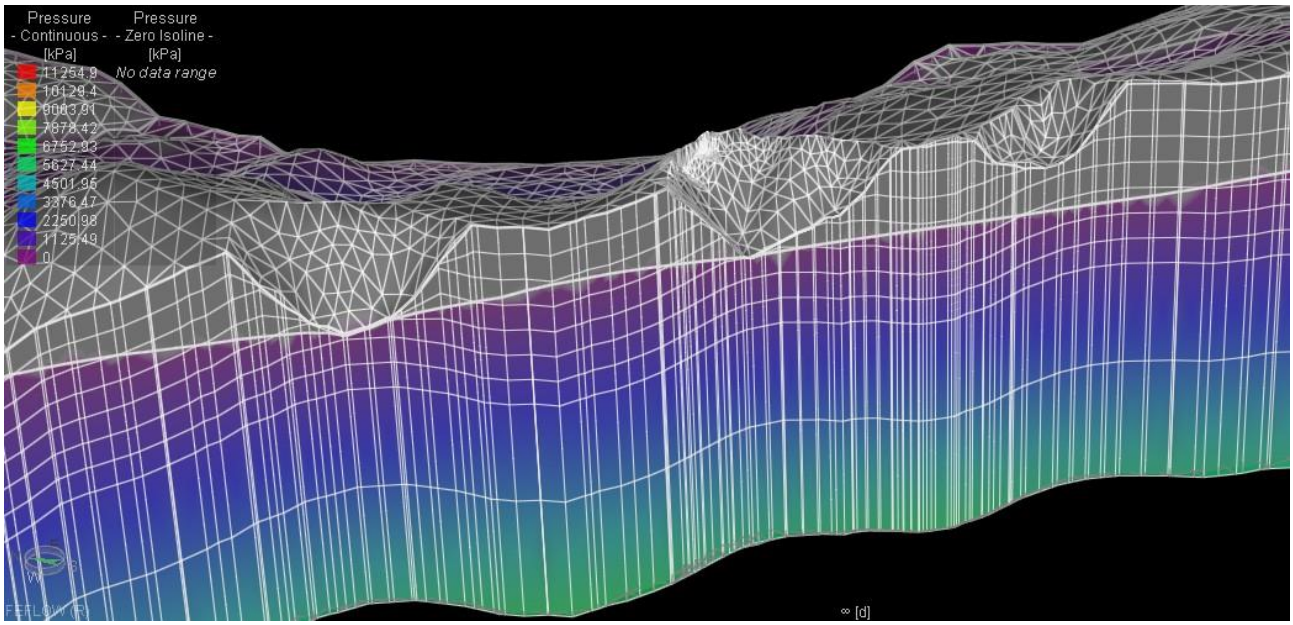

Figure B14: Water Table Elevation beneath the Operational Pits, Steady State Dewatering

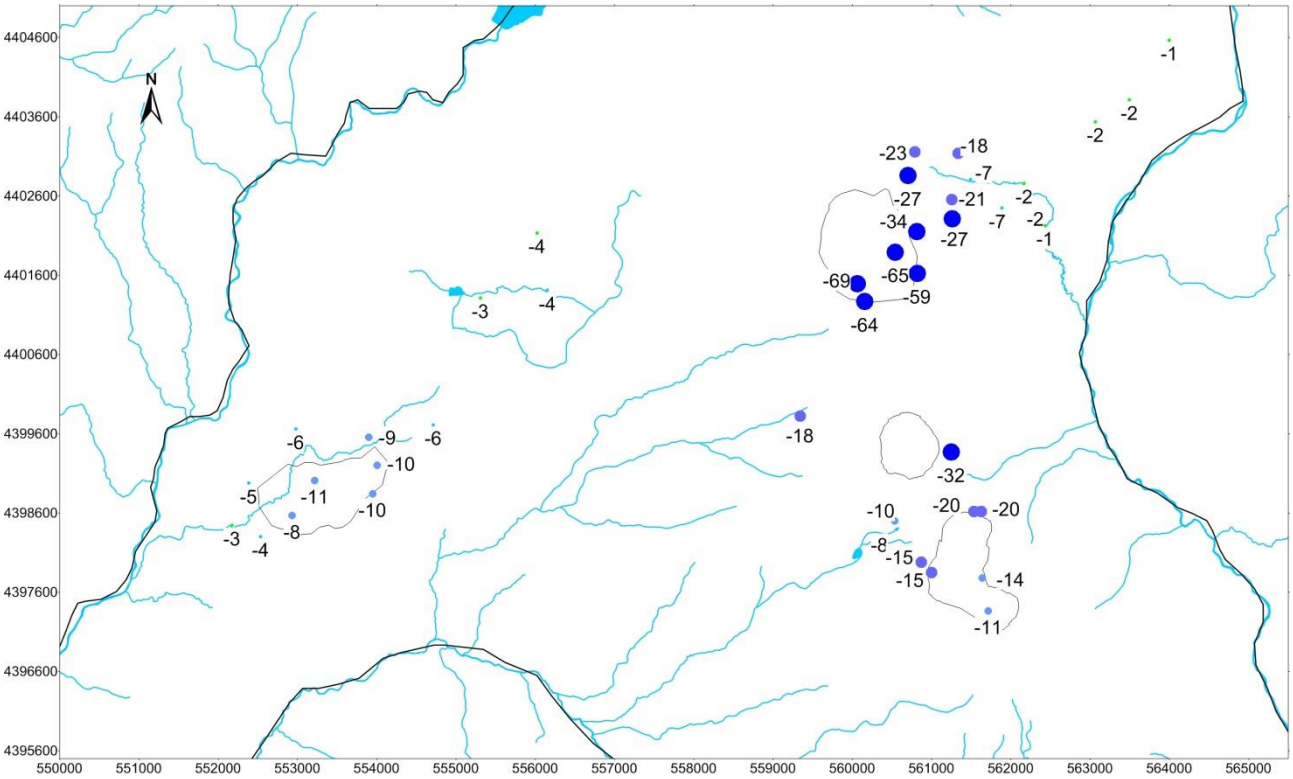

Figure B15: Change in Head at Observations Points, Base Case vs Operational Scenarios

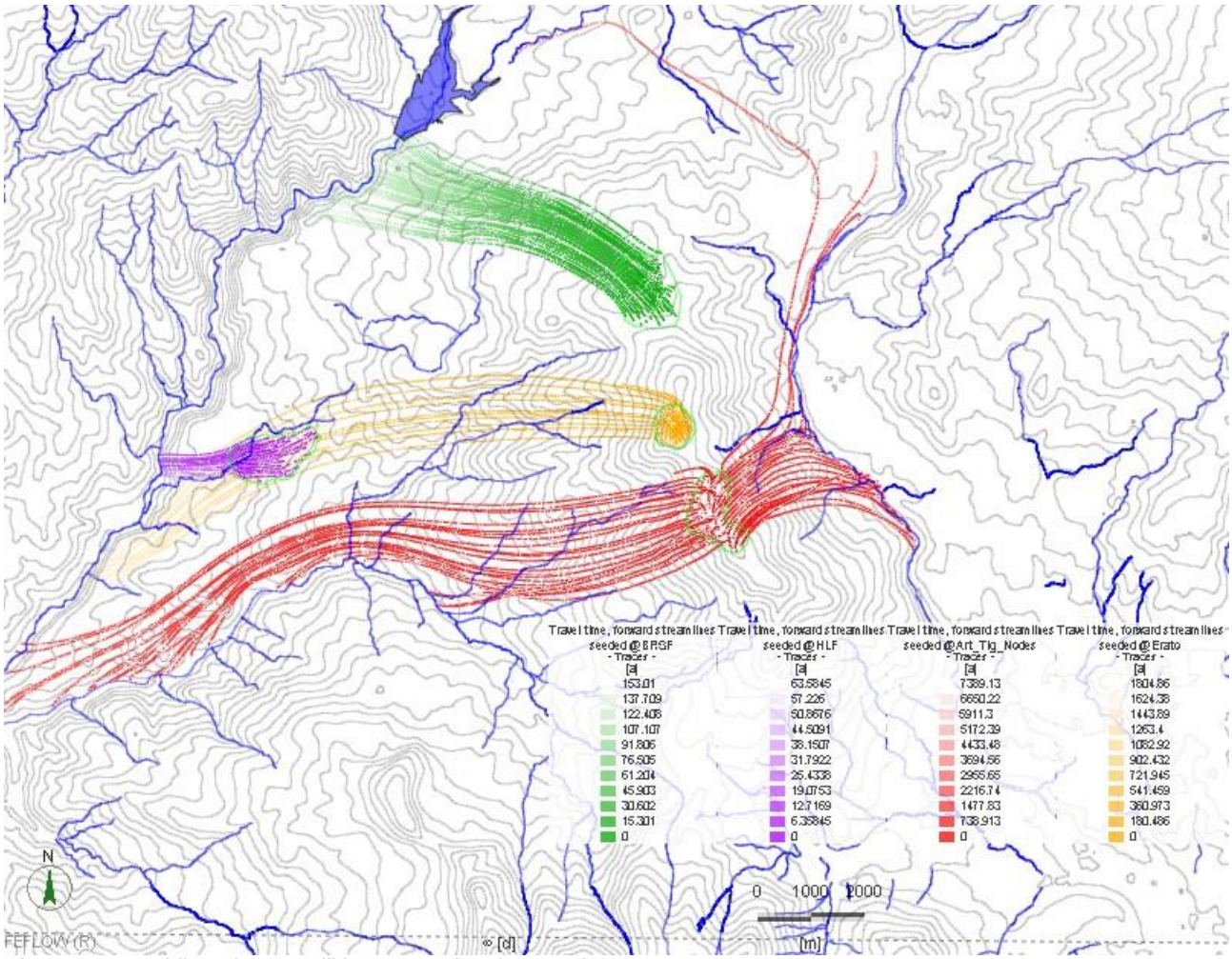

Figure B16: Pathlines from Facilities, Operational Scenario

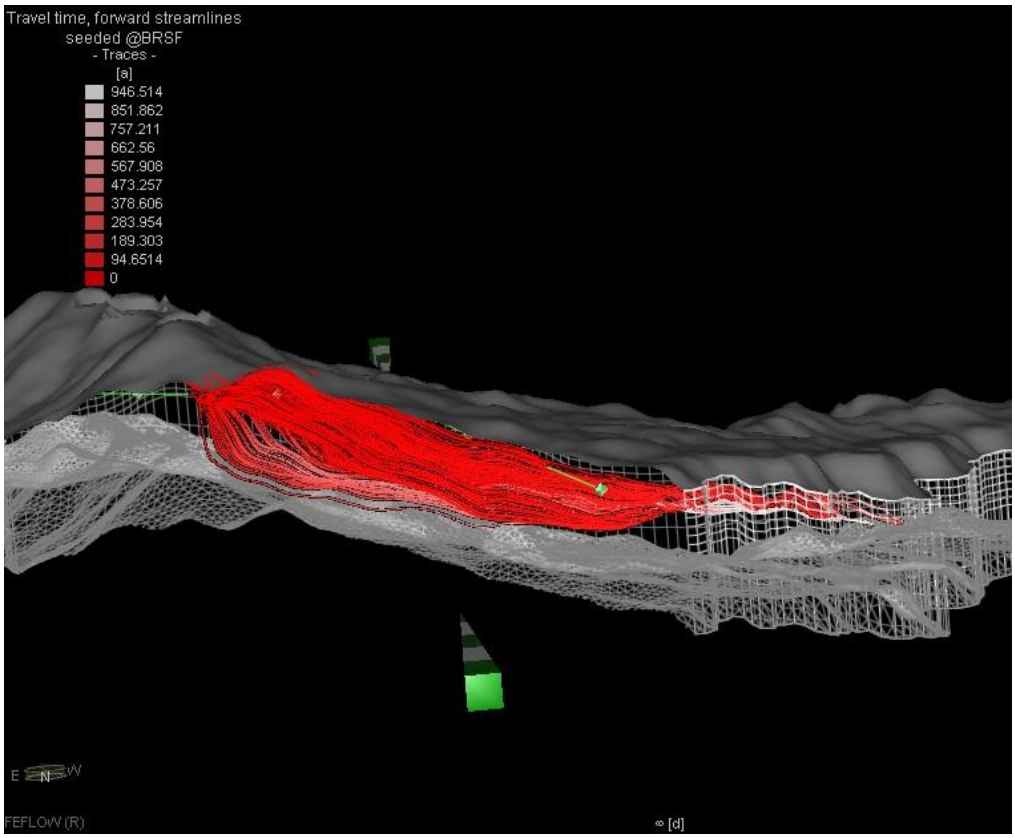

Figure B17: Pathlines, BRSF Operational Scenario

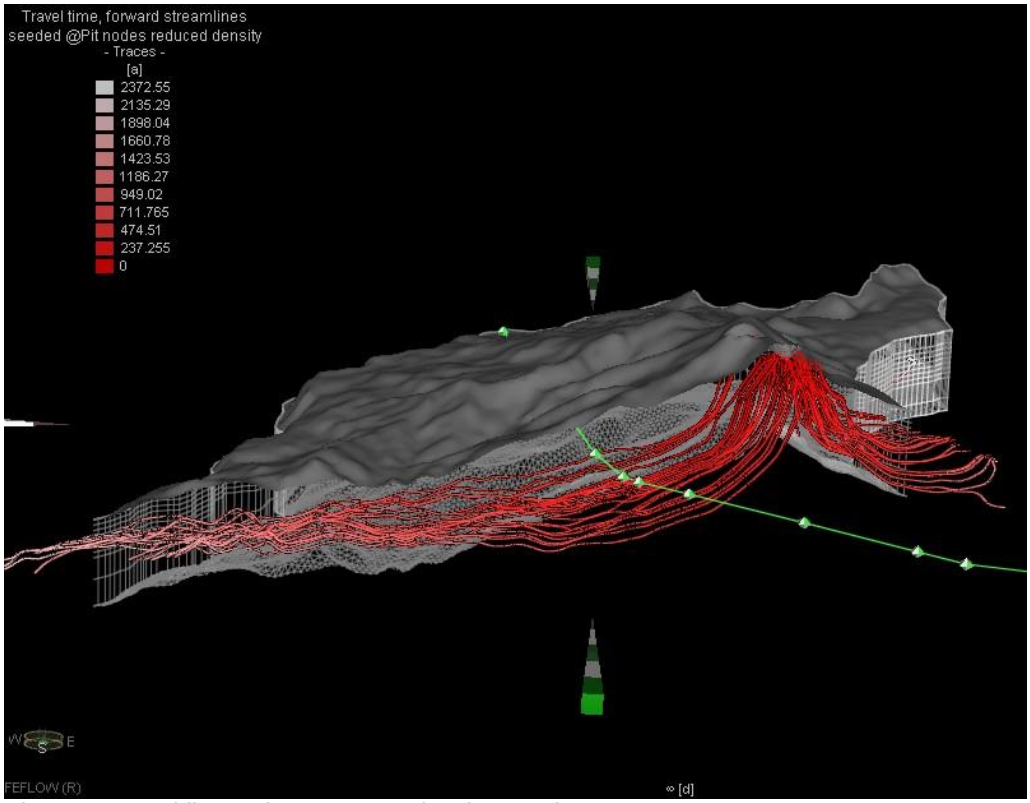

Figure B18: Pathlines, Pit Area, Operational Scenario

Post Closure Scenario Model Results

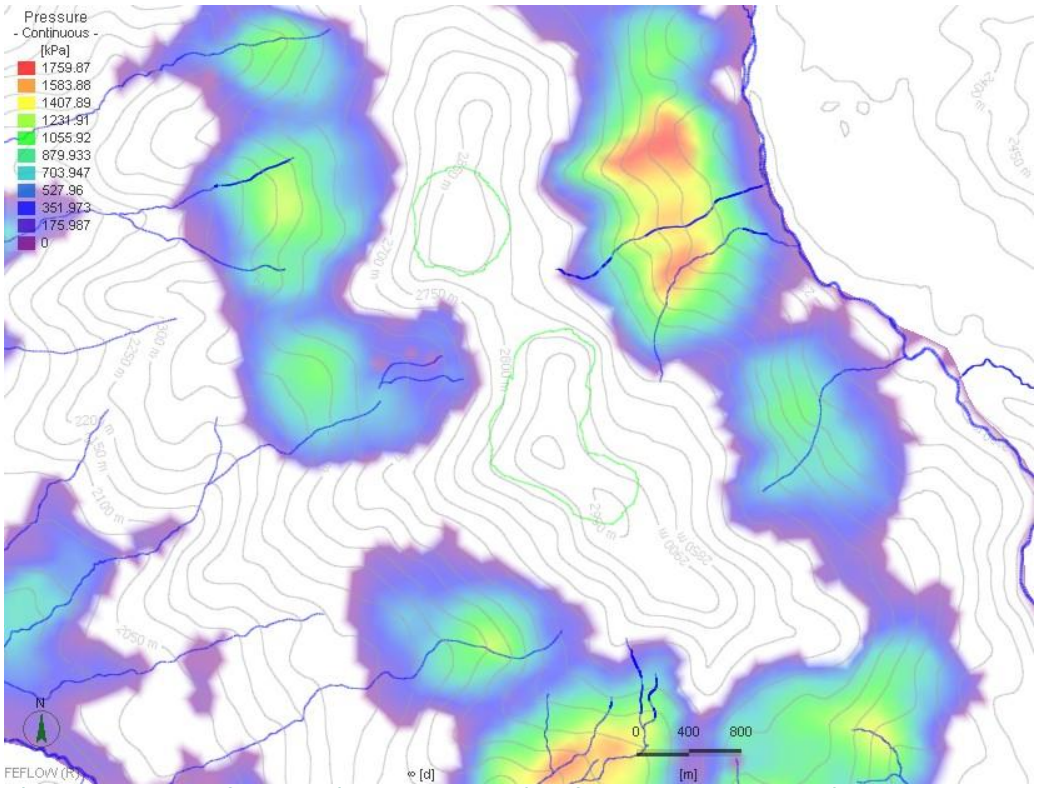

Figure B19: Extent of Saturated Zones at Ground Surface, Base Case Scenario

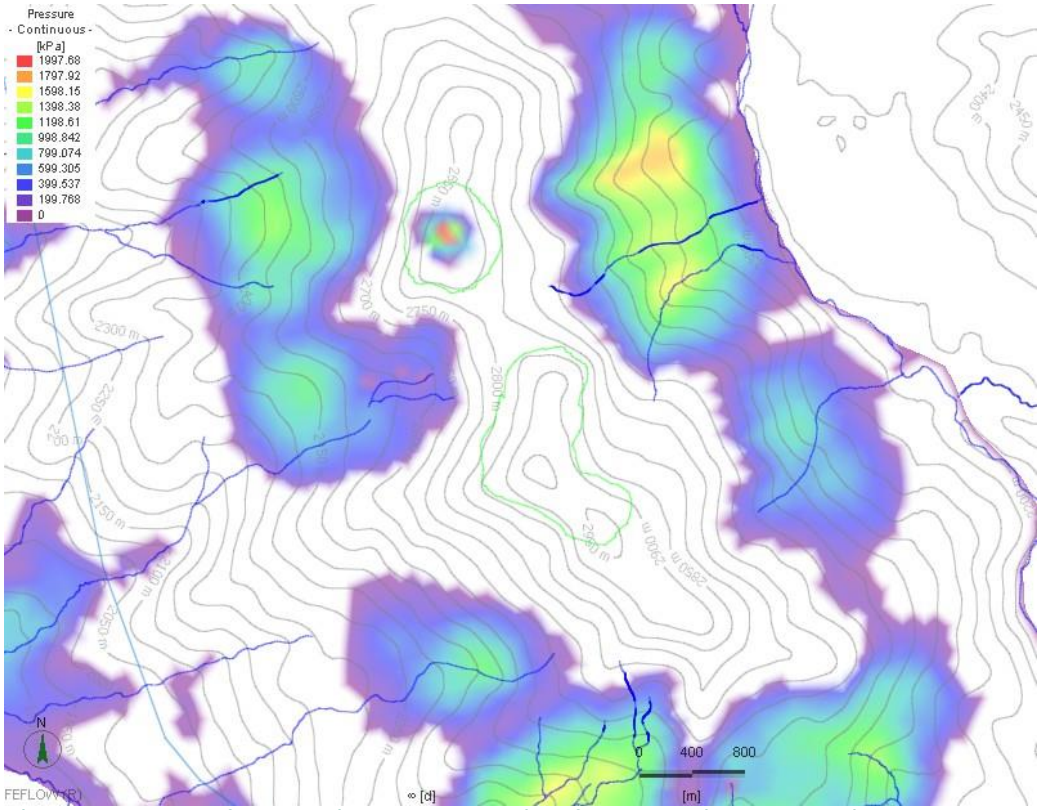

Figure B20: Extent of Saturated Zones at Ground Surface, Post Closure Scenario

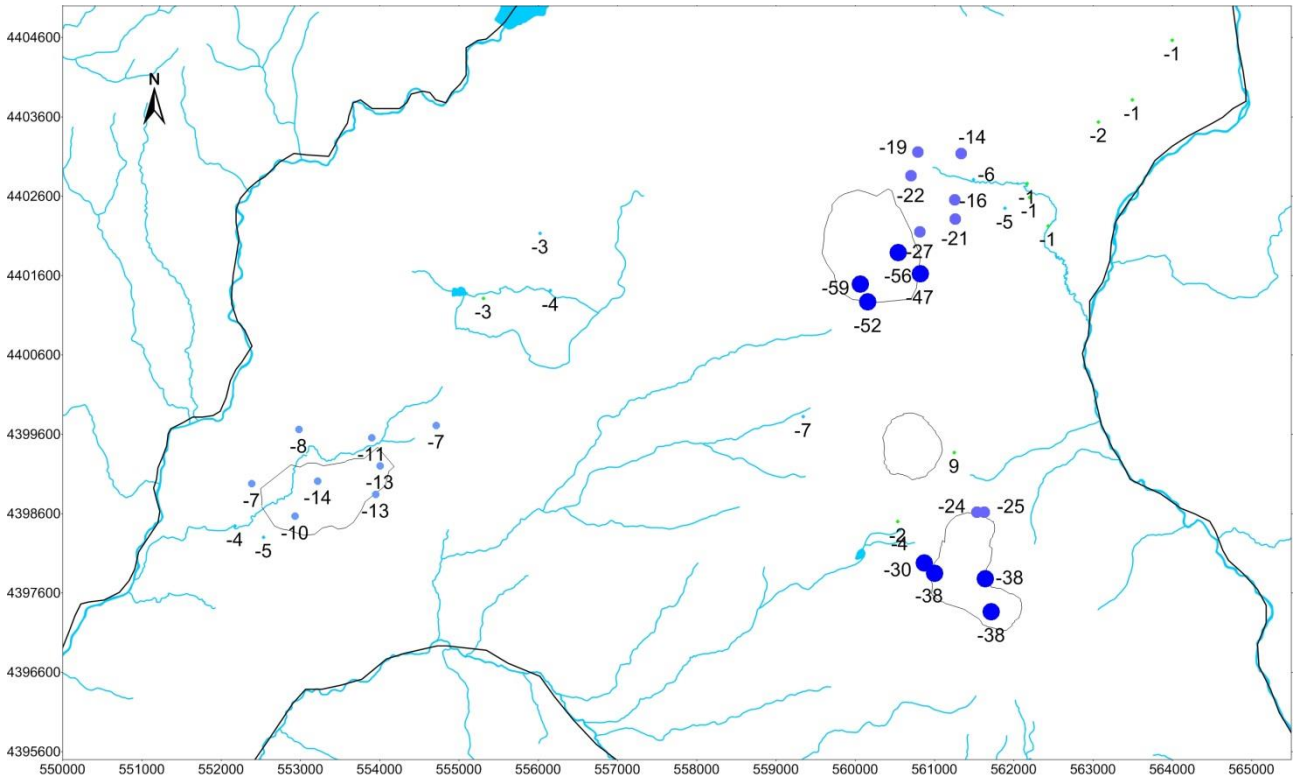

Figure B21: Change in Groundwater Elevation at Observation Points in Comparison to Base Case, Post Closure S1

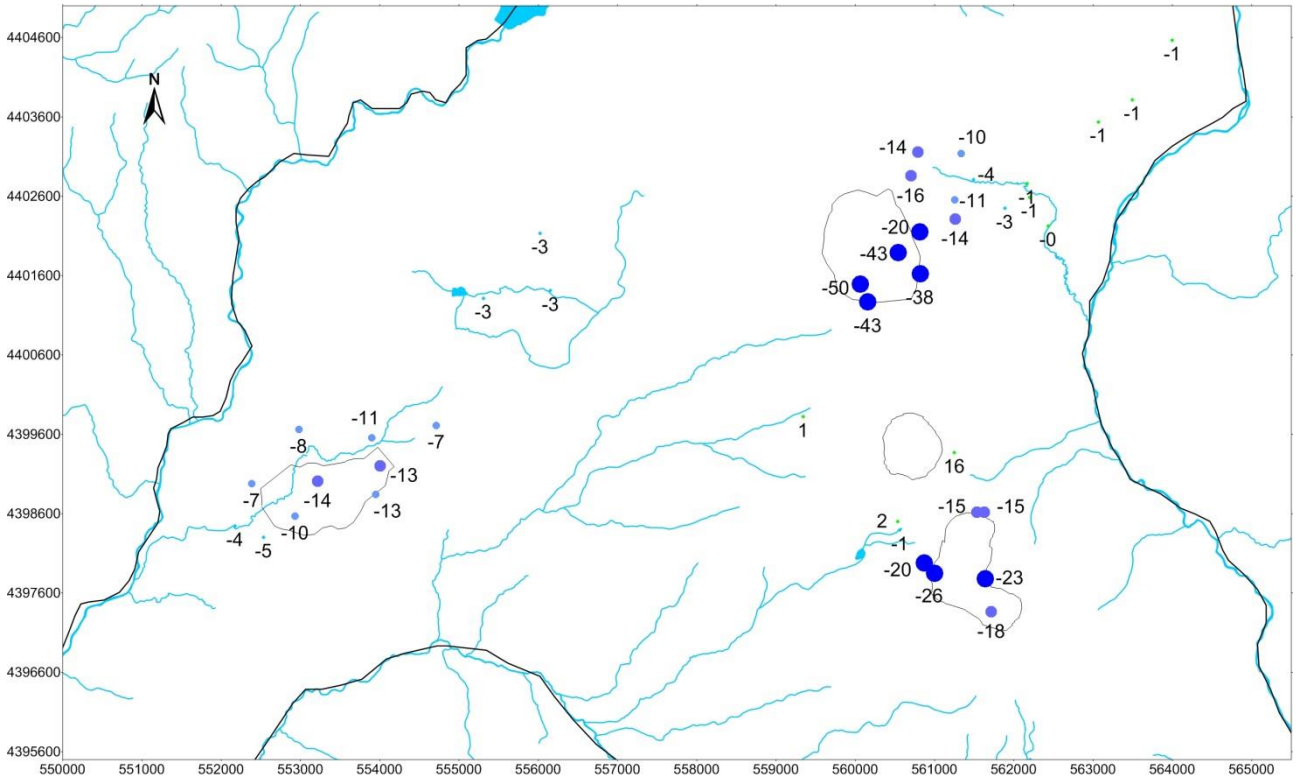

Figure 22: Change in Groundwater Elevation at Observation Points in Comparison to Base Case, Post Closure S2

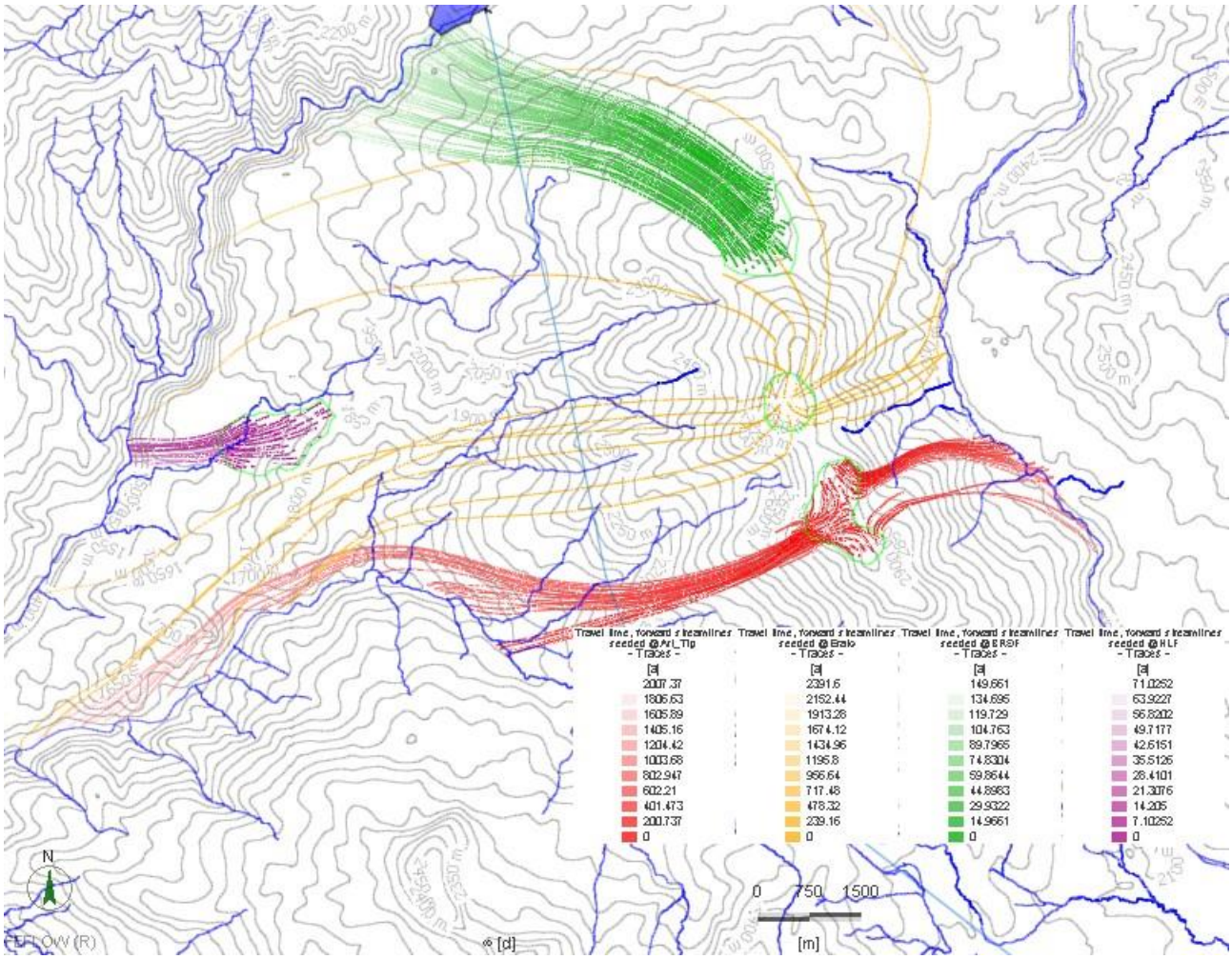

Figure B23: Groundwater Flow Pathlines, Post Closure Scenario

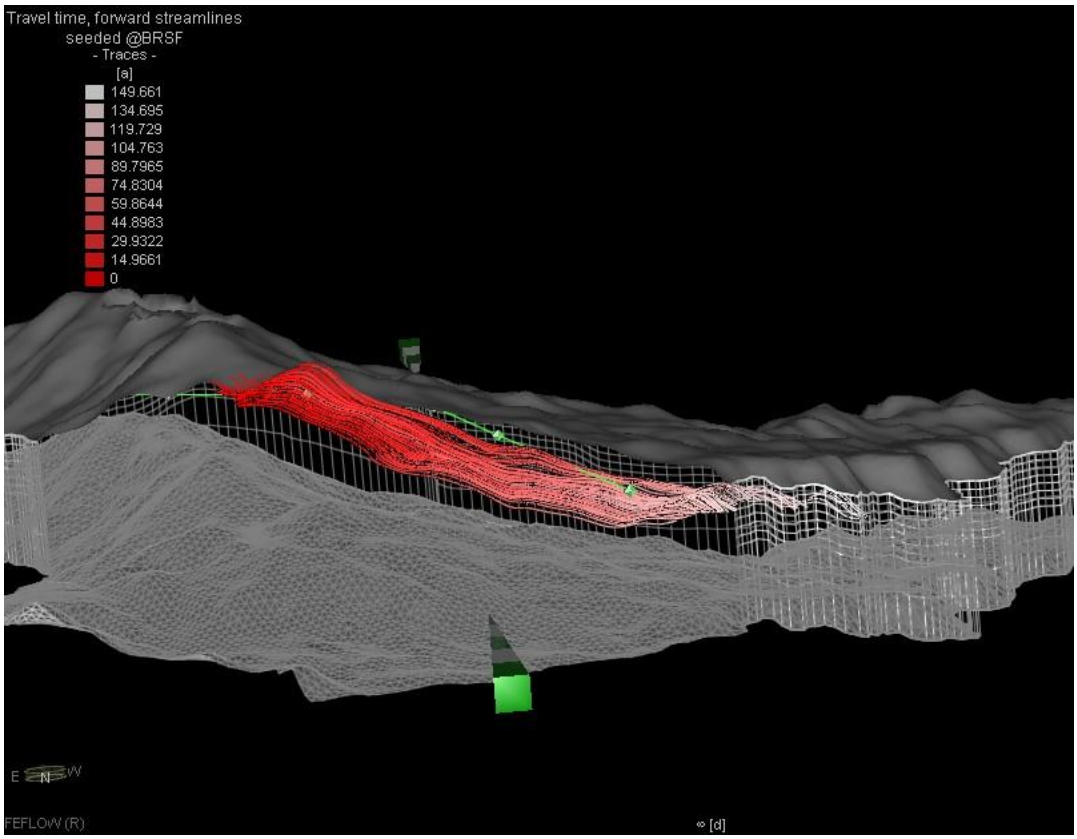

Figure B24: Pathlines, BRSF, Post Closure

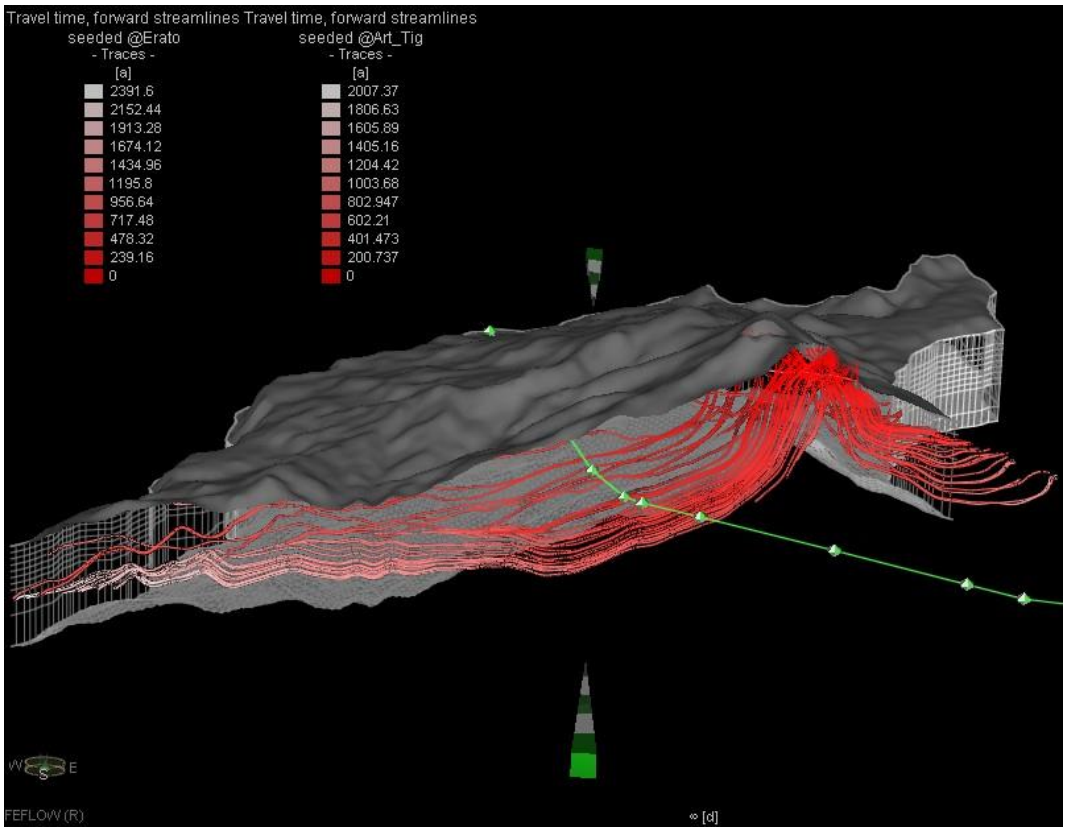

Figure B25: Pathlines, Pit Area, Post Closure

APPENDIX C

Sensitivity Analysis Results

Difference between the baseline model calculated hydraulic head at observation wells and the calculated value in sensitivity analyses SA1 to SA6 is presented in Table C1.

Table C1: Sensitivity Analysis, Change in Calculated Head from Baseline

Lydian ID	Easting	Northing	SA1	SA2	SA3	SA4	SA5	SA6
DDAGLP267	561252	4402552	133	-130	26	-47	-152	73
DDAGLP268	561886	4402447	130	-78	8	-25	-83	39
DDAGLP269	562201	4402587	46	-39	-4	-6	-53	15
DDAW002	562169	4402759	40	-37	-1	-5	-52	18
DDAW003	561490	4402807	91	-78	6	-18	-94	37
DDAW004	560814	4402150	121	-147	36	-56	-178	100
DDAW005	560159	4401267	178	-217	85	-117	-247	150
DDAW007	561249	4399368	175	-311	201	-207	-304	247
DDAW012	560817	4401622	189	-215	76	-112	-226	124
DDGW005	563068	4403536	8	-20	4	-9	-55	47
DDGW006	563496	4403815	6	-13	2	-6	-47	42
DDGW007	564001	4404566	4	-7	0	-3	-40	37
GGDW002	555309	4401314	9	-41	0	1	-111	91
GGDW003A	556155	4401409	9	-46	2	1	-117	94
GGDW005	556024	4402134	8	-41	5	-1	-108	86
GGDW007	552536	4398302	6	-17	-2	0	-44	34
GGDW008	552932	4398566	10	-24	-1	0	-60	45
GGDW009	552978	4399660	6	-20	-2	0	-61	50
GGDW010B	553898	4399557	13	-42	-2	1	-85	72
GGDW011	554714	4399713	18	-63	-3	1	-104	89
GGDW012	553947	4398843	14	-43	-2	1	-78	66
GGDW013	553220	4399010	11	-29	-2	0	-69	55
GGDW014	552385	4398975	5	-6	-1	0	-58	33
GGDW015	554003	4399203	14	-46	-3	1	-85	72
GGDW016	552174	4398443	6	-10	-1	0	-47	28
GGSC037	560790	4403154	100	-111	40	-45	-164	106
GGSC049	560063	4401493	90	-177	76	-91	-230	127
GGSC050	560542	4401892	121	-178	52	-86	-213	97
RCAW288	560562	4398393	134	-264	42	-147	-255	105
RCAW289	560537	4398497	161	-271	64	-156	-261	118
RCAW399	560702	4402856	129	-128	39	-47	-171	100
RCAW400	561263	4402314	148	-152	36	-62	-168	86
RCAW401	561336	4403139	109	-112	36	-43	-149	91
RCAW403	562432	4402226	14	-19	-1	-5	-38	9
RCAW286	561533	4398618	167	-325	198	-217	-313	263

Lydian ID	Easting	Northing	SA1	SA2	SA3	SA4	SA5	SA6
RCAW287	561003	4397849	166	-332	204	-223	-321	265
RCAW404	561717	4397364	157	-333	210	-226	-324	279
RCAW405a	561640	4397780	160	-330	204	-222	-320	274
RCAW407	561625	4398616	165	-323	197	-215	-311	262
RCAW408	560871	4397975	170	-325	183	-215	-314	250
DDAW009	559342	4399820	95	-216	240	-132	-274	209
Root mean square difference (m)			**106**	**173**	**95**	**105**	**184**	**134**

At Golder Associates we strive to be the most respected global company providing consulting, design, and construction services in earth, environment, and related areas of energy. Employee owned since our formation in 1960, our focus, unique culture and operating environment offer opportunities and the freedom to excel, which attracts the leading specialists in our fields. Golder professionals take the time to build an understanding of client needs and of the specific environments in which they operate. We continue to expand our technical capabilities and have experienced steady growth with employees who operate from offices located throughout Africa, Asia, Australasia, Europe, North America, and South America.

Africa	+ 27 11 254 4800
Asia	+ 86 21 6258 5522
Australasia	+ 61 3 8862 3500
Europe	+ 356 21 42 30 20
North America	+ 1 800 275 3281
South America	+ 55 21 3095 9500

solutions@golder.com
www.golder.com

Golder Associates (UK) Ltd
Attenborough House
Browns Lane Business Park
Stanton-on-the-Wolds
Nottinghamshire
NG12 5BL
UK
T: [+44] 0115 937 1111

Golder Associates